NUREG-1263

Hydrologic Design for Riprap On Embankment Slopes

U.S. Nuclear Regulatory Commission

Office of Nuclear Material Safety and Safeguards
Technical Review Branch

R. B. Codell

SEPTEMBER 1988

HYDROLOGIC DESIGN FOR RIPRAP ON EMBANKMENT SLOPES

NUREG-1263

NOTICE

Availability of Reference Materials Cited in NRC Publications

Most documents cited in NRC publications will be available from one of the following sources:

1. The NRC Public Document Room, 1717 H Street, N.W.
   Washington, DC 20555
2. The Superintendent of Documents, U.S. Government Printing Office, Post Office Box 37082,
   Washington, DC 20013-7082
3. The National Technical Information Service, Springfield, VA 22161

Although the listing that follows represents the majority of documents cited in NRC publications, it is not intended to be exhaustive.

Referenced documents available for inspection and copying for a fee from the NRC Public Document Room include NRC correspondence and internal NRC memoranda; NRC Office of Inspection and Enforcement bulletins, circulars, information notices, inspection and investigation notices; Licensee Event Reports; vendor reports and correspondence; Commission papers; and applicant and licensee documents and correspondence.

The following documents in the NUREG series are available for purchase from the GPO Sales Program: formal NRC staff and contractor reports, NRC-sponsored conference proceedings, and NRC booklets and brochures. Also available are Regulatory Guides, NRC regulations in the *Code of Federal Regulations*, and *Nuclear Regulatory Commission Issuances*.

Documents available from the National Technical Information Service include NUREG series reports and technical reports prepared by other federal agencies and reports prepared by the Atomic Energy Commission, forerunner agency to the Nuclear Regulatory Commission.

Documents available from public and special technical libraries include all open literature items, such as books, journal and periodical articles, and transactions. *Federal Register* notices, federal and state legislation, and congressional reports can usually be obtained from these libraries.

Documents such as theses, dissertations, foreign reports and translations, and non-NRC conference proceedings are available for purchase from the organization sponsoring the publication cited.

Single copies of NRC draft reports are available free, to the extent of supply, upon written request to the Division of Information Support Services, Distribution Section, U.S. Nuclear Regulatory Commission, Washington, DC 20555.

Copies of industry codes and standards used in a substantive manner in the NRC regulatory process are maintained at the NRC Library, 7920 Norfolk Avenue, Bethesda, Maryland, and are available there for reference use by the public. Codes and standards are usually copyrighted and may be purchased from the originating organization or, if they are American National Standards, from the American National Standards Institute, 1430 Broadway, New York, NY 10018.

NUREG-1263

Hydrologic Design for Riprap On Embankment Slopes

Manuscript Completed: May 1988
Date Published: September 1988

R. B. Codell

Office of Nuclear Material Safety and Safeguards
U.S. Nuclear Regulatory Commission
Washington, DC 20555

ABSTRACT

Waste impoundments for uranium tailings and other hazardous substances are often protected by compacted earth and clay, covered with a layer of loose rock (riprap). The report outlines procedures that could be followed to design riprap to withstand forces caused by runoff resulting from extreme rainfall directly on the embankment. The Probable Maximum Precipitation for very small areas is developed from considerations of severe storms of short duration at mid-latitudes. A two-dimensional finite difference model is then used to calculate the runoff from severe rainfall events. The procedure takes into account flow both beneath and above the rock layer and approximates the concentration in flow which could be caused by a non-level or slumped embankment. The sensitivity to various assumptions, such as the shape and size of the rock, the thickness of the layer, and the shape of the embankment, suggests that peak runoff from an armored slope could be attenuated with proper design. Frictional relationships for complex flow regimes are developed on the basis of flow through rock-filled dams and in mountain streams. These relationships are tested against experimental data collected in laboratory flumes; the tests provide excellent results. The resulting runoff is then used in either the Stephenson or safety factor method to find the stable rock diameter. The rock sizes determined by this procedure for a given flow have been compared with data on the failure of rock layers in experimental flumes, again with excellent results. Computer programs are included for implementing the method.

TABLE OF CONTENTS

TABLE OF CONTENTS (Continued)

FIGURES

TABLE OF CONTENTS (Continued)

FIGURES (Continued)

TABLES

HYDROLOGIC DESIGN FOR RIPRAP ON EMBANKMENT SLOPES

1 INTRODUCTION

1.1 Need for Protection of Mill Tailings Embankments

The long-term storage of hazardous waste, radioactive waste, and uranium mill tailings presents a unique challenge to engineers. Unprotected impoundments can pose a significant long-term risk to nearby inhabitants and the environment. The engineering designs should provide overall site stability with little or no maintenance, and should not place an undue burden on future generations (EPA, 1985).

One means of providing long-term stabilization of a waste impoundment is to place a protective filter blanket and a layer of loose rock (riprap) over a thick earth cover. Typical embankments for uranium mill tailings have surface areas of a few acres, with gentle top slopes (0-2% grade) and steep side slopes (10-20% grade). The tailings are generally covered with a 6- to 8-foot layer of silt and clay, topped with about 1 to 2 feet of rock armor. The riprap design must be conservative enough to ensure cover stabilization, yet be economically attractive. Rock armor is often the most suitable protection for large embankments, especially in arid climates where other means of slope stabilization such as vegetation may be impractical.

1.2 Hydrologic Design

The rock armor must, among other things, withstand the runoff caused by intense rainfall directly on the embankments. Design procedures have been established for stabilizing embankment toes and side slopes of channels from erosive forces; little attention, however, has been devoted to situations in which the direct runoff from intense rainfall flows through and/or overtops the riprap. Models exist for calculating overland flow on hillsides (e.g., Morris 1980), but no models have been found that deal explicitly with the routing of runoff water on armored embankments. Overland flow models for runoff would not be very useful for computing velocity and depth on armored embankments, because the rock layer has a large capacity to store rainfall temporarily in its void space. In addition, runoff on armored embankments differs from typical overland flow, because substantial turbulent flow can occur beneath the surface of the rock layer at low runoff, and can also occur both above and below the surface at high runoff. Furthermore, other than work on rubble and rock-filled dams (e.g., Stephenson 1979, Olivier, 1967), relatively little attention has been paid to the stability of rock armor for overtopping conditions with flow down an embankment.

A methodology to design riprap for embankments depends on the relationship of the forces exerted by the water on the rock (e.g., traction, uplift, overturning, buoyancy) and the resistance to movement of the rock (e.g., gravity). Flume tests can measure directly the stability of a particular rock armor layer to a range of flows for relatively simple geometries. The fundamental relation-

ships of the forces at play must be understood, however, to extrapolate laboratory measurements to other more complicated configurations of armor with different rock sizes and properties. An understanding of the frictional and conveyance relationships for flow through and over the riprap is a prerequisite of a complete routing model capable of simulating the velocity and depth of water on armored embankments of complex geometry resulting from intense rainfall.

This report outlines procedures that could be followed to design riprap for the protection of uranium mill tailings. The principles of runoff calculations for armored embankments will be derived. Methods will then be presented that can solve the equations for flow on the armored embankments. These principles are formalized into a computer program that solves the finite difference equations for flow. The proper choice of the Probable Maximum Precipitation onto the embankment will be covered. These techniques will allow the computation of the maximum credible flow over the embankment. As the last step, procedures will be described that allow the characteristics of the riprap to be chosen on the basis of rates calculated. Procedures are supported with experimental results wherever possible.

Relationships for flow resistance are based on previously published studies for flow through rock layers and in gravel beds and mountain rivers, and are compared with data collected in experimental flumes at the Colorado State University (CSU). Similarly, the CSU flume data on the stability of rock armor are compared with published methods used for designing riprap.

2 RUNOFF MODEL

This chapter details the basic relationships for runoff from armored embankments. The constitutive relationships for flow will be developed first, followed by a development for flow resistance on armored embankments and a model for severe precipitation. The flow resistance model is compared with data collected in experimental flumes at Colorado State University (Abt et al., 1987).

2.1 Flow Equations

Rain falling on an armored embankment will flow downhill, except for the fraction infiltrating the ground, which, for the present case, can be neglected. Referring to Figure 2-1, the flow of water on the embankment may be described for a two-dimensional case by a macroscopic mass balance and the kinematic approximation of the energy balance (Overton, 1976). The kinematic approximation neglects acceleration, which can be shown to be small, and balances friction versus hydraulic gradient only. The kinematic equations for runoff are stated:

$$\frac{\partial(\xi U)}{\partial x} + \frac{\partial(\xi V)}{\partial y} + \frac{\partial \xi}{\partial t} = R \qquad (2\text{-}1)$$

$$\theta\frac{\partial \xi}{\partial x} + \frac{KU\sqrt{U^2 + V^2}}{gn^2\langle d\rangle} - S_x = 0 \qquad (2\text{-}2)$$

$$\theta\frac{\partial \xi}{\partial y} + \frac{KV\sqrt{U^2 + V^2}}{gn^2\langle d\rangle} - S_y = 0 \qquad (2\text{-}3)$$

where ξ = water depth above an impermeable layer
U = flux of water across the embankment
V = flux of water down the embankment
n = rock void porosity
t = time
R = rainfall rate
θ = a factor used to adjust the surface gradient (see Section 2.2.3)
g = acceleration of gravity
K = friction factor
$\langle d\rangle$ = representative rock diameter
S_x = the slopes across the embankment
S_y = the slope down the embankment

The upper end of the top slope is assummed to be a no-flow boundary:

$$V = 0 \text{ where } \frac{\partial V}{\partial y} = 0 \qquad (2\text{-}4)$$

cut 1

Figure 2-1 Tailings embankment in profile

The water level is continuous across the break between the top and side slopes. Free slip and no flow are assumed at the lateral boundaries. The flow boundary condition at the base of the lower slope considers that the depth of the water layer is determined only by the balance between friction and gravity:

$$\xi = \frac{q_b}{n}\left(\frac{K}{g\langle d\rangle S_y}\right)^{\frac{1}{2}} \qquad (2\text{-}5)$$

where q_b = the discharge across the downstream boundary

2.2 Resistance to Flow

Most armored embankments employ a filter layer beneath the riprap layer. Run-off from the slope could be conveyed in the filter layer, riprap layer, and over the top of the rock. The filter generally will be a shallow layer of relatively small, well-graded rock. Criteria for filter design are covered in Sherard (1963). Flow through the filter will be significantly smaller than flow in the riprap layer, but not necessarily negligible. Increased conveyance in the rock layers is a generally favorable condition as far as the stability of the riprap layer to overtopping flow is concerned, so neglecting the conveyance in the filter layer will be a conservative assumption.

2.2.1 Flow Confined to Riprap Layer

Typical embankments are covered by one or more rock layers as illustrated in Figure 2-2, e.g., a filter layer and a riprap layer. Stephenson (1979) has proposed an empirical formula for flux V through each rock layer:

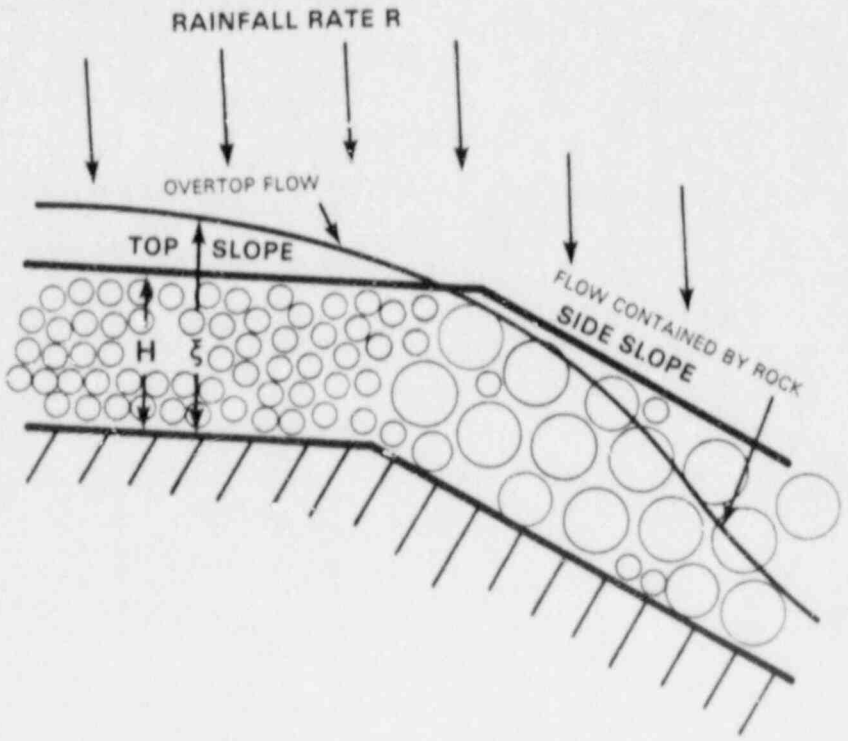
RAINFALL RATE R
OVERTOP FLOW
TOP
SLOPE
H
ξ
FLOW CONTAINED BY ROCK
SIDE SLOPE

cut 1

$$V = \left(\frac{Sgn^2 \langle d \rangle}{K'} \right)^{\frac{1}{2}} \qquad (2\text{-}6)$$

where S = slope
$g = 9.8\ m/sec^2$

The dimensionless friction factor K' for the riprap or filter layer is defined (Stephenson, 1979):

$$K' = k + \frac{800}{Re} \qquad (2\text{-}7)$$

where $k = 1$ for smooth marbles
$k = 2$ for rounded gravel
$k = 4$ for crushed rock

Re = Reynolds number = $\frac{\langle d \rangle V}{\nu n}$

ν = kinematic viscosity

The estimated values of k for rock used in the present study are given in Table 2-1.

cut 2

Figure 2-2 Cross section of embankment

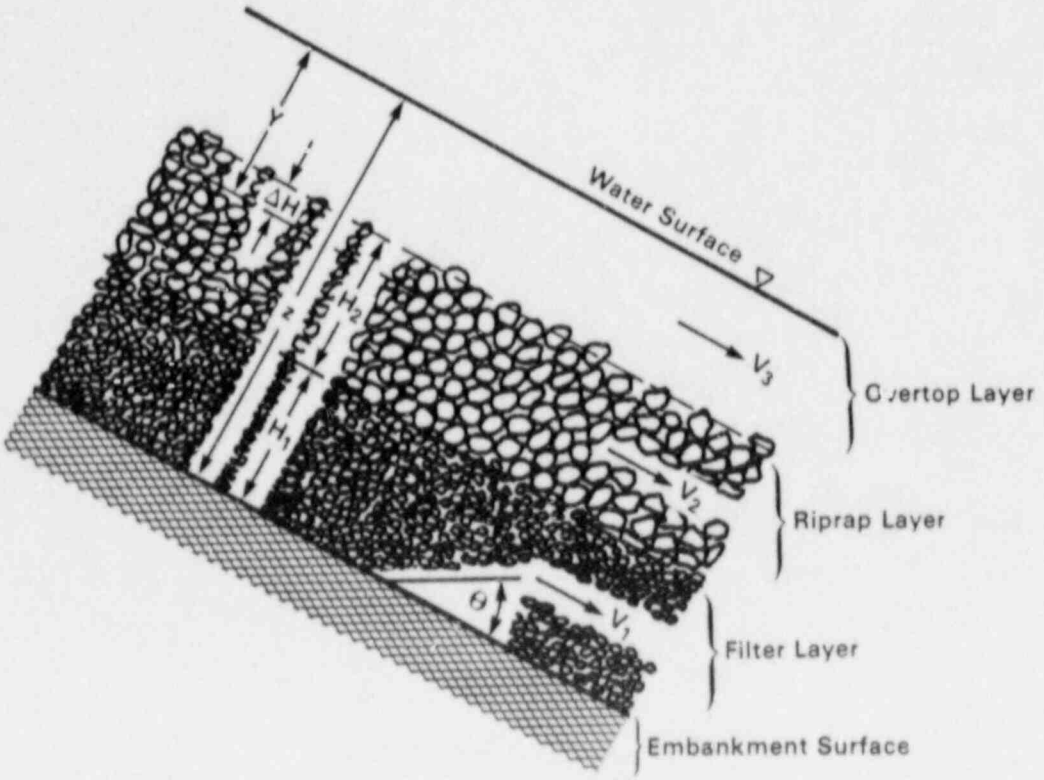
Water Surface
Y
ΔH
H2
H1
V3
V2
V1
θ
Overtop Layer
Riprap Layer
Filter Layer
Embankment Surface

cut 2

Table 2-1 Properties of riprap and filter rock

d_{50}, mm	d_{84}, mm	d_h, mm	C_u (1)	C_z (2)	n	$H^{(3)}$ mm	$H^{(4)}$ mm	Shape	k
26 (5)	30	23	1.7	1.3	0.44	76	152	Sub-angular	3
56 (6)	74	50	2.1	1.3	0.45	152	-	Angular	4
104	135	89	2.2	1.1	0.44	305	-	Angular	4
130	178	125	1.6	1	0.46	305	-	Angular	4
157	203	144	1.7	1.1	0.46	305	-	Angular	4
3.4 (7)	5.8	2.7	2.9	1.2	0.3 (8)	-	152	Rounded	2
6.1 (9)	14.5	4.5	3.8	0.9	0.3 (8)	-	152	Rounded	2

(1) Coefficient of uniformity = d_{60}/d_{10}.

(2) Coefficient of gradation = $\frac{d_{30}^2}{d_{10}d_{60}}$.

(3) Thickness of layer when used as riprap.
(4) Thickness of layer when used as filter.
(5) This rock is also used for filter in 157-mm riprap experiments.
(6) This rock is also used for filter in 104- and 130-mm riprap experiments.
(7) Filter for 26-mm riprap.
(8) Estimated.
(9) Filter layer for 56-mm riprap.

Stephenson suggests that the representative rock diameter <d> should be the harmonic mean diameter:

$$\langle d \rangle = d_h = \frac{1}{\sum_{i=1}^{N} \frac{p_i}{d_i}} \qquad (2\text{-}8)$$

where p_i = the fraction of rocks of diameter d_i by mass

N = the number of size classifications

Stephenson (1979) based his correlations of friction almost exclusively on the median rock diameter d_{50}, however, because the true gradations of the rock were usually not available. In the present study, the harmonic mean diameters determined from Equation 2-8 with N = 10 and p_i = 0.1 will be used. It is important to note that the flux predicted by Stephenson's formula is independent of stage. The veracity of this assumption will be questioned later in Section 2.2.5.1 by comparison to the data collected for the present study.

2.2.2 Flow Over Top of Rock

The Darcy-Weisbach friction factor f is used to express the flux for flows that overtop the rock layer:

$$V_3 = \left(\frac{8gSY}{f}\right)^{1/2} \tag{2-9}$$

where Y is the water depth normal to the flow above the effective top-of-rock datum as shown in Figure 2-2. The flux V_3 is the average flow per unit cross-sectional area [i.e. $(m^3/sec)/m^2$]. It is useful to regard V_3 as a flux rather than the average velocity in the layer, in order to be consistent with the fluxes through the rock layers.

The conveyance of the embankment increases sharply as the stage exceeds the top of the rock layer. Flow resistance is a function of depth above the rock surface. Individual rocks protrude above the water surface at low flows, and the relative roughness of the rock layer surface is large. At greater flow rates, the rocks become increasingly submerged, and the relative roughness decreases. There does not appear to be a unified theoretical approach to quantifying flow resistance at sites over wide ranges of relative roughness caused by changing discharges (Bathurst, 1985).

Hey (1979) developed an expression for the Darcy-Weisbach friction factor f in gravel bed streams:

$$\frac{1}{\sqrt{f}} = 2.03 \log\left(\frac{\alpha Y}{3.5 d_{84}}\right) \tag{2-10}$$

Where d_{84} is the 84th-percentile finer diameter of the riprap determined from a grid and number sampling procedure. The factor α ranges from about 11.08 to 13.46, and depends on channel geometry. A value of $\alpha = 11.08$ is appropriate for wide, flat channels and is used in the present study. This equation, although not meant to represent flow resistance where rocks are only slightly submerged, has been shown to perform well in this situation (Thorne, 1985).

Bathurst (1985) developed an empirical relationship for the Darcy-Weisbach friction factor from data on mountain rivers of 0.4% to 4% slope, and for a wide range of relative roughness:

$$\frac{1}{\sqrt{f}} = \frac{\log\left(\frac{Y}{d_{84}}\right) + 4}{\sqrt{8}} \tag{2-11}$$

The Bathurst form of the Darcy-Weisbach friction factor has been adopted for the present model, although the Hey relationship, equation 2-10, gives nearly identical results.

2.2.3 Definition of the Effective Top-of-Rock Datum

In the present series of flume experiments, the rock layers were dump-placed and leveled to give the appearance of a uniform surface. The physical top-of-rock

datum, $z = H_1 + H_2$, where z is the distance above the bottom of the filter layer normal to the slope, was measured to the approximate height of the top of the rock determined by a flat plate parallel to the slope. The transition between flow through the rock layer and overtopping flow is indistinct. It is clear, however, that the relationships for flux above the rock layer implicitly assume some flow within the rock layers. The effective datum for overtopping flow therefore must be beneath the physical top-of-rock datum, as illustrated in Figure 2-2. For the present model, the effective top-of-rock datum, $Y = 0$, is defined at a point below the physical top-of-rock datum so that the flux in the riprap layer V_2 defined by equation 2-6 equals the flux in the overtopping layer V_3 defined by equation 2-9 at the physical top-of-rock datum $z = H_1 + H_2$, where H_1 and H_2 are the thicknesses of the filter and riprap layers, respectively. The intent of this definition is to assure that the runoff is a monotonically increasing function of stage. The stage $Y = \Delta H$ of the physical top-of-rock datum is calculated by setting V_2 from equations 2-6 and 2-7 equal to V_3 from equations 2-9 and 2-11 and solving iteratively for Y:

$$\log\left(\frac{\Delta H}{d_{84}}\right) = \frac{1}{5.62}\left(\frac{n^2 d_{h2}}{\Delta H K_2'} - 4\right)^{\frac{1}{2}} \qquad (2\text{-}12)$$

where K_2' = the dimensionless friction factor of the riprap layer
d_{h2} = the harmonic mean diameter of the riprap layer

The stage Y used in equations 2-9 and 2-11 is defined therefore in terms of the measured stage z:

$$Y = z - (H_1 + H_2 - \Delta H) \qquad (2\text{-}13)$$

2.2.4 Rating Curve

A depth-discharge rating curve can be expressed by following the algorithm:

$$q = V_1 z \text{ where } z \leq H_1 \qquad (2\text{-}14)$$

$$q = V_1 H_1 + V_2(z - H_1) \text{ where } H_1 \leq z < (H_1 + H_2) \qquad (2\text{-}15)$$

$$q = V_1 H_1 + V_2 H_2 + V_3(z - H_1 - H_2) \text{ where } z \geq (H_1 + H_2) \qquad (2\text{-}16)$$

where q = flow rate per unit width
V_1 = flux in filter layer from equation 2-6
V_2 = flux in riprap layer from equation 2-6
V_3 = flux in flow in the overtopping layer from equation 2-9

Equations 2-14 through 2-16 (hereafter referred to as "Model 1") are a rigorous representation for conveyance on the embankment slopes. The simulation model, however, employs a slightly different arrangement for flow, in terms of a modified friction factor K^*, hereafter called "Model 2," and conservatively neglects the conveyance of the filter layer.

For flow over the top of the rock layer, the depth ξ becomes a virtual depth; that is, the depth that the water would have to assume if the riprap layer were

water surface for flows that overtop the rock layer. It is equal to unity if flow is below the level of the rock layer and equal to the porosity n if flow is above the rock layer surface.

Consider, for the time being, only the flow down a slope that is covered by a uniform layer of rock. The total flow q past a point on the slope is the sum of the flows through the rock layer (q_2) and over the rock layer (q_3):

$$q = q_2 + q_3 = V_2 H_2 + V_3(\xi - H_2)n \tag{2-17}$$

where V_2 = flux in the rock layer
V_3 = flux over-top of rock
H_2 = thickness of riprap layer

The flux over the top of the rock layer is calculated using the Darcy-Weisbach equation for flow resistance in open channels:

$$V_3 = \left[\frac{8gR_h\left(S_y - n\frac{\partial \xi}{\partial y}\right)}{f}\right]^{\frac{1}{2}} \tag{2-18}$$

where R_h = the hydraulic radius
f = the Darcy-Weisbach friction factor

The hydraulic radius is approximated as the water depth over the top of rock:

$$R_h = n(\xi - H_2) \tag{2-19}$$

An effective resistance factor K* for the total flow in and over the rock layer can be derived:

$$K^* = \frac{\langle d\rangle \xi^2}{\left\{H_2(\langle d\rangle/K')^{\frac{1}{2}} + \left[\frac{\xi - H_2}{n}\right]\left[\frac{8(\xi - H_2)}{f}\right]^{\frac{1}{2}}\right\}^2} \tag{2-20}$$

Equations 2-1, 2-2, and 2-3 are solved with the effective value K* substituted for K' when ξ is greater than the rock layer thickness H_2.

Rating curves for flowrate versus water depth at steady state for the example are shown in Figure 2-3. The much higher carrying ability of the over-top layer is evident from this figure.

2.2.5 Comparison of Model and Data

Recognizing a lack of basic information, the Nuclear Regulatory Commission sponsored research at Colorado State University (CSU) to collect data on flow resistance and failure of rock armor. The experiments were conducted in flumes for a variety of rock sizes, layer thicknesses, and slopes, both with and without a filter layer. They are described in detail in Abt et al. (1987).

A large concrete outdoor flume, shown in Figure 2-4, was used to simulate a steep (20%) embankment; a smaller indoor flume with a tiltable bed, shown in Figure 2-5, was used to simulate the flatter (1% to 10%) top slopes.

cut 3

Figure 2-3 Rating curve example

Nominal median stone sizes (d_{50}) tested were 26, 56, 104, 130, and 157 mm (1, 2, 4, 5, and 6 inches) in diameter. Riprap was obtained from a limestone quarry near Denver, Colorado, except for the smallest rock, which was crushed alluvial gravel. The 26-mm riprap was also used for filter material for the 157-mm riprap; the 56-mm rock was used as the filter material for the 104- and 130-mm riprap. Filter rock for the 26-mm and 157-mm riprap was gravel with d_{50} of 3.4 and 6.1 mm, respectively.

Armor and riprap were dump-placed in the flumes, and leveled manually to form a level surface. The thicknesses of the rock layers were measured by means of a flat plate to approximately the top of the largest rocks in the layer. Riprap and filter layer properties are summarized in Table 2-1. The porosity values of the filter rock for the 26- and 56-mm riprap have not been measured, but were estimated to be 30%, because of their wide gradations.

The flow resistance formulas proposed for the present simulation models are compared in the following sections with the data collected from the CSU flumes. Data from the CSU studies are summarized in Tables 2-2 and 2-3.

2.2.5.1 Flow Below the Top of Rock

Flows above the surface of the armor layer were shown by means of model experiments to occur only when the conveyance of the rock layer was exceeded. The

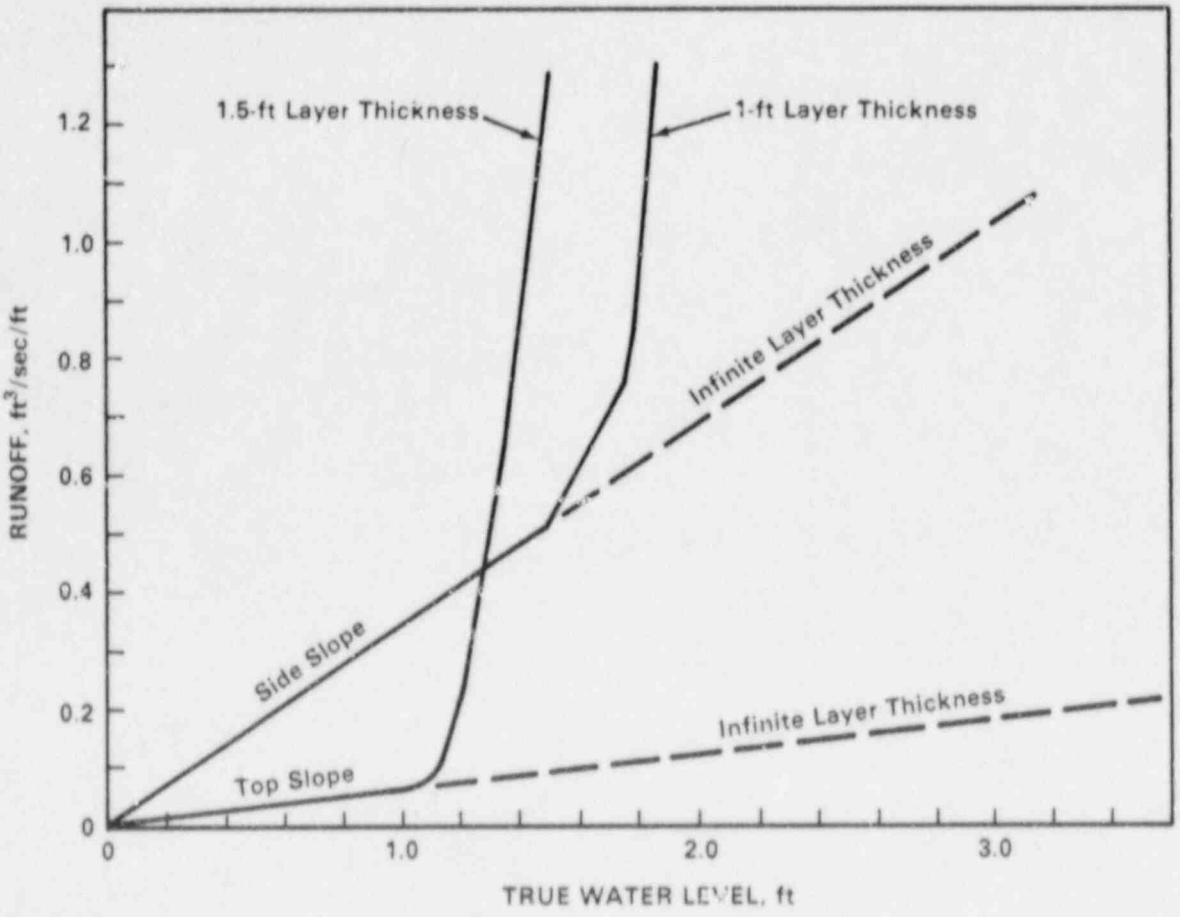
1.5-ft Layer Thickness
1-ft Layer Thickness
Infinite Layer Thickness
Side Slope
Infinite Layer Thickness
Top Slope
RUNOFF, ft³/sec/ft
TRUE WATER LEVEL, ft
0
0.2
0.4
0.6
0.8
1.0
1.2
1.0
2.0
3.0

Cut 3

cut 4

Figure 2-4 Diagram of outdoor flume

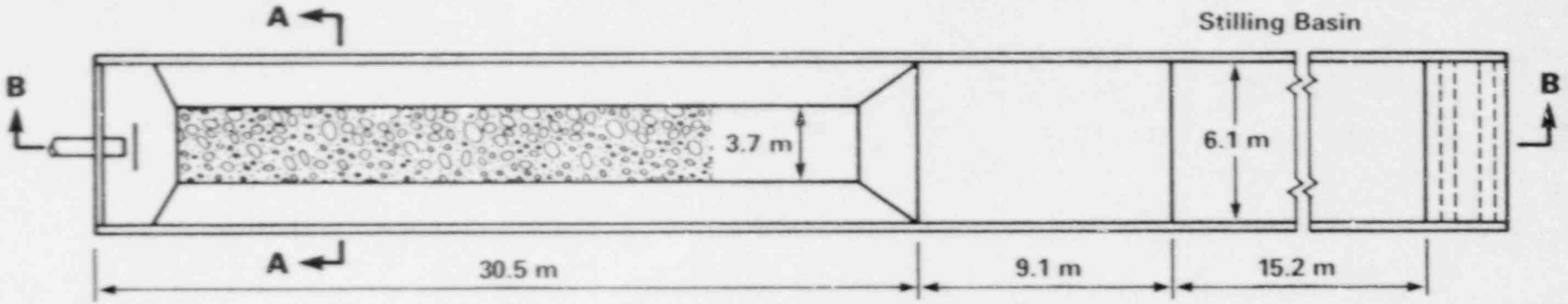

PLAN

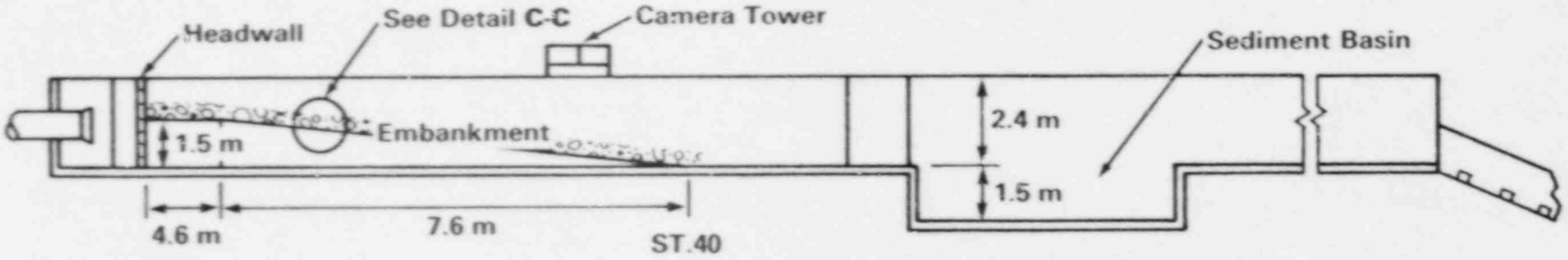

SECTION B-B

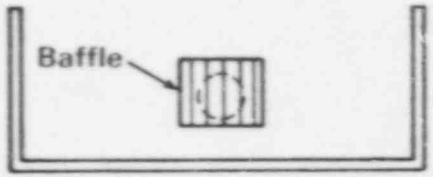

SECTION A-A

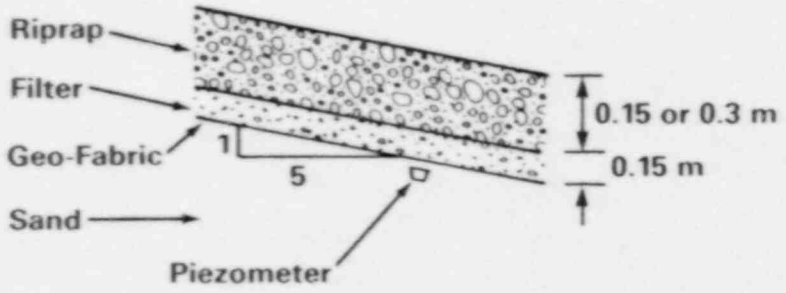

DETAIL C-C

cut 5

Figure 2-5 Diagram of indoor flume

velocities of water estimated from the model and the occurrence of flow concentrations were strongly dependent on the conveyance below the surface of the rock.

The stage-discharge relationship represented by equations 2-14, 2-15, and 2-16 (Model 1) are compared in Figure 2-6 to the measured values for those cases in which the stage is below the top surface of the riprap, in terms of the dimensionless flowrate

$$q' = \frac{q}{W(H_1 + H_2)(gSd_2)^{\frac{1}{2}}}$$

as is the flow rate where W is the width of the flume. This comparison demonstrates that Model 1 generally overestimates flow for a given stage, especially for the smaller rock sizes. The lack of agreement is not necessarily surprising, since there was considerable scatter in the correlations performed by Stephenson (1979).

Discussion

Direct measurements of interstitial velocity in the riprap layer by the tracer injection technique have been analyzed in order to understand the frictional relationships more thoroughly. Friction depends approximately on the square of the velocity through the tortuous paths around the rocks. Stephenson suggests that the interstitial velocity of water through the rock layer should be based on the flux divided by the porosity V/n. Direct measurements of the movement of the salt water tracer down the flume however, indicate that the water is moving faster than V/n.

Measurement of tracer velocity is analogous to the situation commonly encountered in the transport of dissolved tracers in groundwater. The speed at which an inert tracer is transported through a porous medium is related to the flux divided by an "effective porosity" n_e, which takes into account the fact that not all of the voids that can be measured in the medium are likely to carry flow. Table 2-4 shows the values of porosity determined as the ratio of rock volume to total volume and effective porosity (back-calculated from measurements of tracer

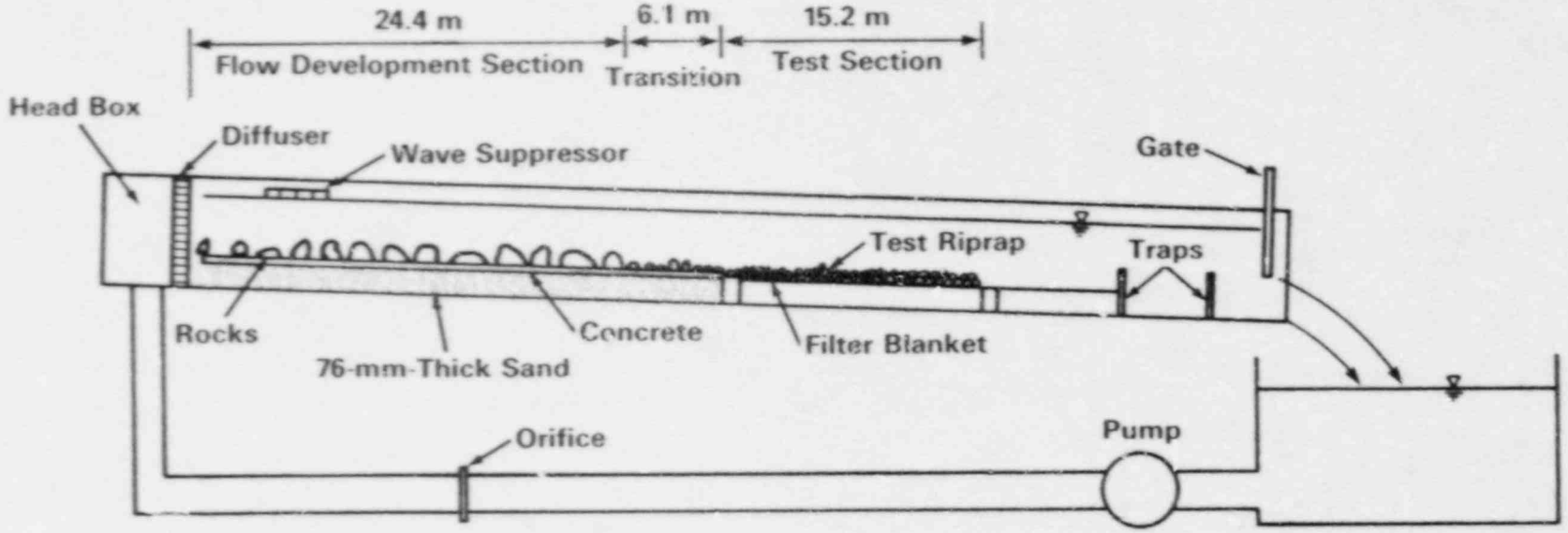
24.4 m
6.1 m
15.2 m
Flow Development Section
Transition
Test Section
Head Box
Diffuser
Wave Suppressor
Gate
Test Riprap
Traps
Rocks
Concrete
Filter Blanket
76-mm-Thick Sand
Orifice
Pump

Table 2-2 Data summary for outdoor flume

Run number	d_{50}, mm	Slope	q, liters/sec	Stage[1], mm	Av. velocity[2], mm/sec	Station[3]
3W	104	0.2	122.9	0	219	22-24
3W	104	0.2	145.8	18	221	22-24
3W	104	0.2	226.5	41	235	22-24
3W	104	0.2	75.9	-117	129	22-24
4W	104	0.2	120.1	0	296	35-37
4W	104	0.2	150.4	41	280	35-37
4W	104	0.2	229.9	72	351	35-37
4W	104	0.2	73.1	-99	238	35-37
6W	104	0.2	291.4	27		35-37
6W	104	0.2	368.1	37		35-37
6W	104	0.2	455.9	46		35-37
6W	104	0.2	496.1	55		35-37
7W	104	0.2	399.3	34		35-37
7W	104	0.2	531.5	56		35-37
7W	104	0.2	584.4	55		35-37
7W	104	0.2	616.7	51		35-37
8W	130	0.2	161.4	0	317	22-24
8W	130	0.2	171.9	18	320	22-24
8W	130	0.2	247.8	51	327	22-24
8W	130	0.2	323.1	76	376	22-24
8W	130	0.2	82.1	-152	381	22-24
8W	130	0.2	168.8	0	263	35-37
8W	130	0.2	204.4	25	268	35-37
8W	130	0.2	275.8	64	564	35-37
8W	130	0.2	86.6	-152	256	35-37
8W	130	0.2	247.8	29		10-12
8W	130	0.2	323.1	49		10-12
9W	130	0.2	290.5	35		35-37
9W	130	0.2	356.5	41		35-37
9W	130	0.2	411.4	51		35-37
9W	130	0.2	497.2	60		35-37
9W	130	0.2	547.1	64		35-37
9W	130	0.2	583.6	62		35-37
9W	130	0.2	677.6	72		35-37
9W	130	0.2	741.6	79		35-37
11W	157	0.2	222.8	13		22-24
11W	157	0.2	385.1	51		22-24
11W	157	0.2	551.1	80		22-24
12W	157	0.2	353.9	46		22-24
12W	157	0.2	560.7	70		22-24
13W	157	0.2	750.4	100		22-24
13W	157	0.2	795.7	110		22-24
13W	157	0.2	880.6	107		22-24
14W	157	0.2	129.7	-18	343	35-37
14W	157	0.2	176.1	0	460	35-37
14W	157	0.2	246.6	36	464	35-37
14W	157	0.2	304.4	53	483	35-37
14W	157	0.2	376.0	66	564	35-37
17W	56	0.2	114	17		35-37
17W	56	0.2	133	22		35-37
17W	56	0.2	151	28		35-37
17W	56	0.2	158	30		35-37
18W	56	0.2	76.6	12		22-24
18W	56	0.2	108	19		22-24
18W	56	0.2	126	24		22-24
18W	56	0.2	171	34		22-24

(1) Stage measured above apparent top of rock.
(2) Average of available velocities measured 38 mm, 114 mm, and 190 mm below riprap surface.
(3) Station = feet downstream from end of diffuser or headwall.

Table 2-3 Data summary for indoor flume

Run number	d_{50}, mm	Slope	q, liters/sec	Stage[1], mm	Av. velocity[2], mm/sec	Station[3]
3I[4]	56	0.02	3.4	-7.6	58	120
3I	56	0.02	9.3		72	120
3I	56	0.02	17.8	2[illegible]	7[illegible]	120
3I	56	0.02	134	76	78	120
3I	56	0.02	445	150	140	120
4I	56	0.01	2.0	-71	27	120
4I	56	0.01	6.5	0	46	120
4I	56	0.01	17.8	25	49	120
4I	56	0.01	106	76	75	120
4I	56	0.01	351	152	126	120
6I	26	0.01	1.4	-20	30	120
6I	26	0.01	3.1	0	30	120
6I	26	0.01	18.7	25	27	120
6I	26	0.01	134	76	-	120
7I	26	0.02	1.1	-36	34	120
7I	26	0.02	3.1	0	40	120
7I	26	0.02	177	76	-	120
7I	26	0.02	385	122	-	120
8I	26	0.02	0.6	-36	27	120
8I	26	0.02	2.3	0	34	120
8I	26	0.02	18.7	25	27	120
8I	26	0.02	134	71	-	120
8I	26	0.02	268	102	-	120
8I	26	0.02	283	96	-	120
9I	26	0.1	2.8	-44	52	120
9I	26	0.1	5.9	0	73	120
9I	26	0.1	11.3	24	73	120
9I	26	0.1	19.0	33	95	120
9I	26	0.1	47.3	42	52	120
10I	56	0.1	8.2	-74	101	140-142
10I	56	0.1	15.9	0	110	140-142
10I	56	0.1	19.3	4.4	113	140-142
10I	56	0.1	60.0	32	113	140-142
10I	56	0.1	142	54	102	140-142
11I	56	0.1	283	7.9	-	148-150
11I	56	0.1	8.2	-6.1	98	148-150
11I	56	0.1	15.9	0	101	148-150
11I	56	0.1	19	10.2	114	148-150
11I	56	0.1	60	26.7	114	148-150
11I	56	0.1	142	54.6	108	148-150
1	56	0.02	697	175	-	120
2	56	0.02	1376	255	-	120
3	56	0.02	1235	247	-	120
4	56	0.02	1328	260	-	120
5	56	0.02	1492	283	-	120

See footnotes at end of table.

Table 2-3 (Continued)

Run number	d_{50}, mm	Slope	q, liters/sec	Stage[1], mm	Av. velocity[2], mm/sec	Station[3]
5	56	0.02	1602	305	-	120
6	56	0.02	1007	225	-	120
9	56	0.02	430	126	-	120
10	26	0.02	518	142		120
11	26	0.02	251	93		120
12	26	0.02	241	94		120
13	26	0.02	340	117		120
14	26	0.02	425	132		120
15	26	0.02	504	126		120
16	26	0.02	340	102		120
17	26	0.02	425	121		120
18	26	0.02	507	130		120
19	26	0.01	283	123		120
20	26	0.01	340	142		120
21	26	0.01	898	244		120
22	26	0.01	977	261		120
23	26	0.01	1133	285		120
24	26	0.01	1218	304		120
26	26	0.1	76	24		140-142
27	26	0.1	70	34		140-142
28	26	0.1	95	43		140-142
29	56	0.1	255	7.0		148-150
30	56	0.1	283	7.4		148-150
31	56	0.1	283	7.9		148-150
32	56	0.08	411	10.4		140-142

(1) Stage measured above apparent top of rock.
(2) Average of available velocities measured 38 mm, 114 mm, and 190 mm below physical top-of-rock surface.
(3) Station = feet downstream from end of diffuser or headwall.
(4) The suffix I indicates that the run was set up to measure interstitial velocity. These runs should not be confused with those without the suffix.

velocity in the flumes), and the measured stage-discharge relationship for flows beneath the surface of the rock. The effective porosity is defined:

$$n_e = \frac{q_2}{WH_2V_2}$$

where q_2 = flow through riprap layer
V_2 = average measured velocity of the tracer in the riprap layer

cut 6

Figure 2-6 Correlation of calculated and measured discharge for flow below surface of riprap

Table 2-4 Effective porosities back-calculated from measured interstitial velocities

Run	d_{50}, mm	S	H_2, m	q, m^3/sec	W, m	F(1)	V_2, m/s	n(2)	n_e(3)
6I	26	0.01	0.076	0.0031	2.4	0.079	0.03	0.44	0.52
7I	26	0.02	0.076	0.0031	2.4	0.103	0.04	0.44	0.38
4I	56	0.01	0.152	0.0065	2.4	0.045	0.046	0.45	0.37
3I	56	0.02	0.152	0.0093	2.4	0.059	0.072	0.45	0.33
9I	26	0.1	0.076	0.0059	2.4	0.182	0.073	0.44	0.36
10I	56	0.1	0.152	0.0159	2.4	0.096	0.11	0.45	0.36
11I	56	0.1	0.152	0.159	2.4	0.096	0.101	0.45	0.36
3W	104	0.2	0.305	0.123	3.7	0.201	0.219	0.44	0.4
4W	104	0.2	0.305	0.12	3.7	0.201	0.296	0.44	0.29
8W	130	0.2	0.305	0.161	3.7	0.171	0.317	0.46	0.37
8W	130	0.2	0.305	0.169	3.7	0.171	0.263	0.46	0.47
14W	157	0.2	0.305	0.176	3.7	0.11	0.460	0.46	0.30
Average									0.38

(1) F = estimated fraction of flow in filter layer.
(2) Measure directly from pore volumes.
(3) $n_e = \frac{q^2}{WH_2V_2}$

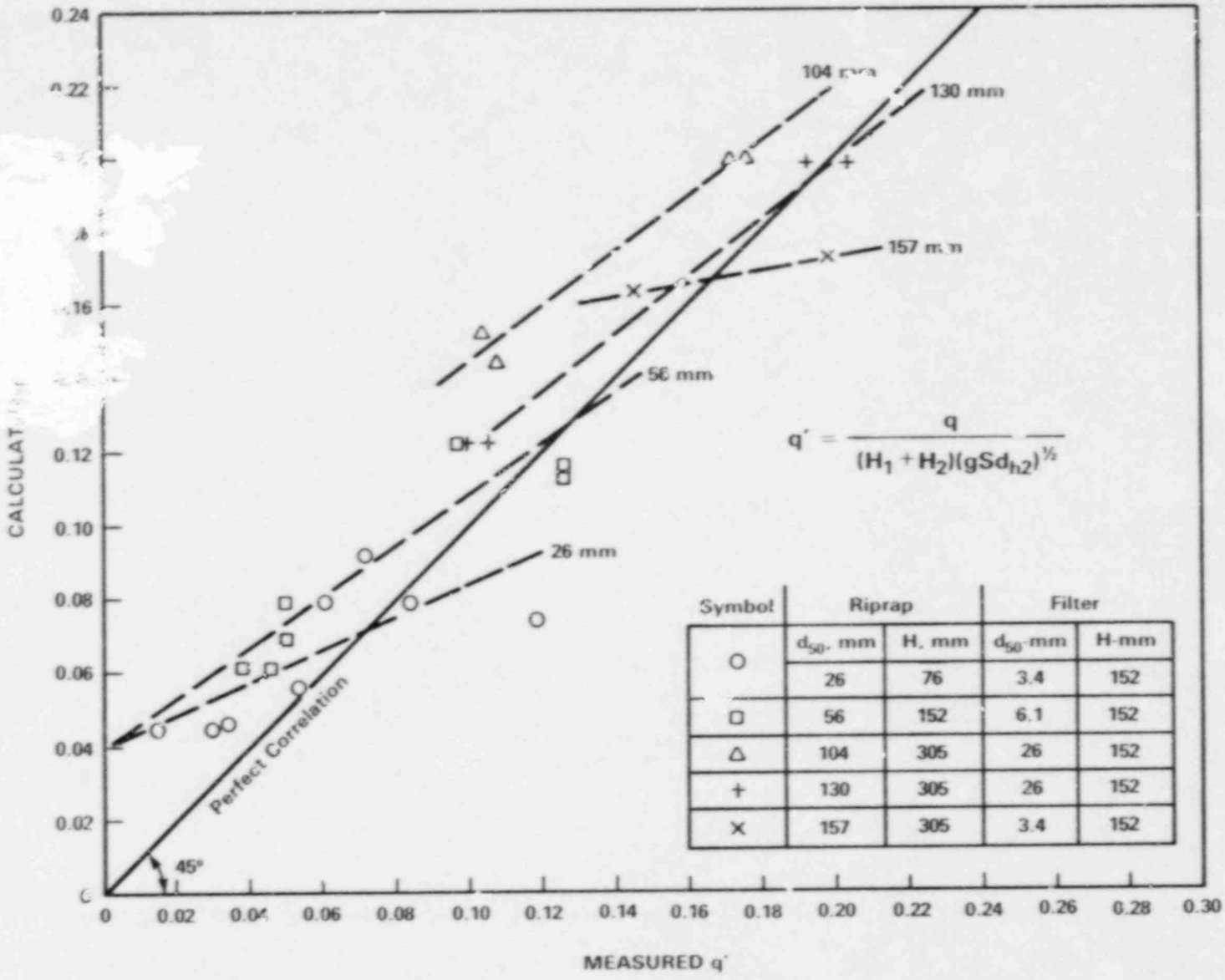
0.24
0.22
0.16
0.12
0.10
0.08
0.06
0.04
0.02
0
0.02
0.04
0.06
0.08
0.10
0.12
0.14
0.16
0.18
0.20
0.22
0.24
0.26
0.28
0.30
CALCULAT
MEASURED q'
104 mm
130 mm
157 mm
56 mm
26 mm
Perfect Correlation
45°
$q' = \frac{q}{(H_1 + H_2)(gSd_{h2})^{1/2}}$
Symbol
Riprap
Filter
d_{50}, mm
H, mm
d_{50} mm
H mm
○ 26 76 3.4 152
□ 56 152 6.1 152
△ 104 305 26 152
+ 130 305 26 152
× 157 305 3.4 152

The flowrate q_2 in the riprap layer is estimated from the fraction of flow in each layer calculated by equations 2-14, 2-15, and 2-16, because flow in the filter layer was not measured directly. The fraction of flow through the filter layer is estimated to be up to a third of the total, and generally cannot be neglected. This estimated correction inserts a possible source of error. Results of the calculation indicate that the effective porosity is significantly smaller than the measured porosity. The average value of n_e is 0.38, as compared to measured values of n ranging from 0.44 to 0.46.

Measurements within the rock layer indicate that velocity may be correlated to stage. Figure 2-7 demonstrates this apparent relationship between stage and the velocity measured at two levels and stages, for the 56-mm riprap in the indoor flume. Neither the Stephenson (1979) nor Leps (1973) formulations for interstitial friction indicate that flows confined below the surface of the rock would be dependent on stage. This phenomenon is a possible explanation for the deviation demonstrated in Figure 2-6 of measured and predicted runoff as stage approaches the surface of the rock layer. It appears that there may be a vertical velocity gradient established within the rock layer, with the lowest velocities near the bottom and the highest velocities near the surface.

In overtopping flows, velocities above the top of the rock are appreciably greater than the interstitial velocities, and are also highly sensitive to stage. This high velocity boundary condition seems to influence the velocity closer to the surface (38 mm below the surface) than the velocity closer to the bottom (114 mm below surface). The influence of stage on interstitial velocity is not as evident for flows that do not overtop the riprap. The conveyance of the rock layer relative to the total flow decreases for increasing stage once the rock is overtopped however, reducing the significance of this potential error on the total conveyance.

2.2.5.2 Combined Flow Relationships

The stage-discharge relationships calculated from Model 1 for the complete range of flows are shown in Figures 2-8 through 2-12 for the range of rock sizes studied. Agreement between the model and data is generally excellent. The results of Model 2 are not shown, but demonstrate higher stage for a given flowrate, especially at low flow and for cases in which flow through the filter layer is appreciable, notably the experiments with the 4- and 5-inch-diameter rock.

2.3 Numerical Solution

The numerical solution of the two-dimensional model as presently implemented employs the "leapfrog" explicit algorithm (Roach, 1972). This method was chosen because it was easily programmed, and appeared to give acceptable results. The staggered finite difference grid employed for the two-dimensional model is illustrated in Figure 2-13. The finite difference grid blocks are square, and of equal size throughout. The variables in the finite difference equations are defined on the corners of the grid blocks as shown in Figure 2-13.

cut 1

Figure 2-7 Velocity in 56-mm riprap layer vs. stage

The continuity equation, equation 2-1, is represented in finite difference form:

$$\xi_{i,j}^{n+1} = \xi_{i,j}^{n} + \frac{R\Delta t}{n} \left(\xi_{i-1,j}^{n} + \xi_{i,j}^{n}\right) U_{i,j}^{n} \frac{\Delta t}{2n\Delta x} - \left(\xi_{i+1,j}^{n} + \xi_{i,j}^{n}\right) U_{i,j}^{n} \frac{\Delta t}{2n\Delta x} + \left(\xi_{i,j-1}^{n} + \xi_{i,j}^{n}\right) V_{i,j-1}^{n} \frac{\Delta t}{2n\Delta x} - \left(\xi_{1,j-1} + \xi_{i,j}\right) V_{i,j} \frac{\Delta t}{2n\Delta x} \quad (2\text{-}21)$$

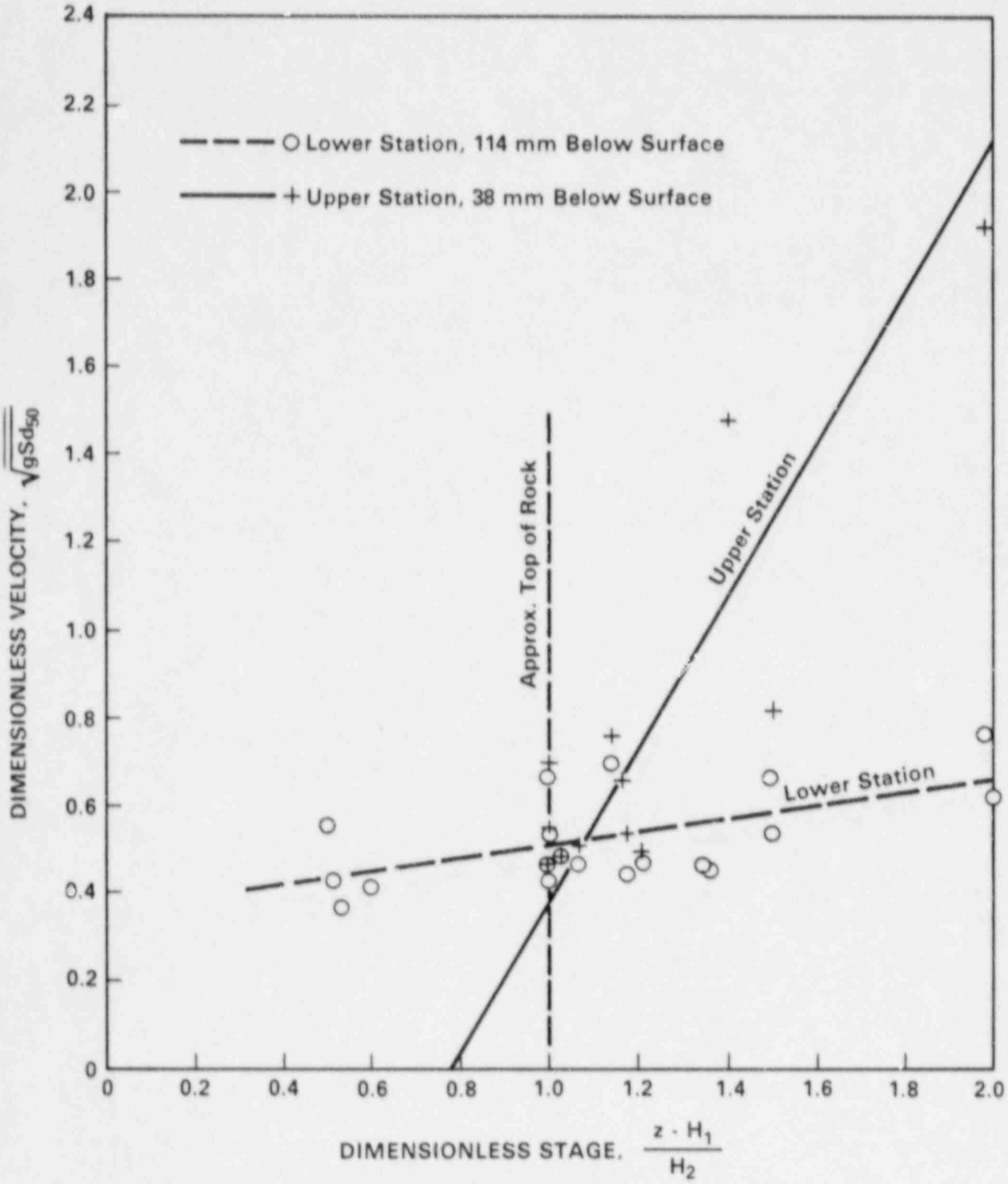
Lower Station, 114 mm Below Surface
Upper Station, 38 mm Below Surface
Approx. Top of Rock
Upper Station
Lower Station
DIMENSIONLESS VELOCITY, $\sqrt{gSd_{50}}$
DIMENSIONLESS STAGE, $\frac{z - H_1}{H_2}$
0
0.2
0.4
0.6
0.8
1.0
1.2
1.4
1.6
1.8
2.0
2.2
2.4

cut 7

cut 8

Figure 2-8 Stage vs. discharge for 26-mm riprap

The subscripts i and j refer to the locations on the finite-difference grid, Figure 2-13. The superscripts n and n+1 refer to the time level, either $n\Delta t$ or $(n+1)\Delta t$.

The relationships for velocity, equations 2-2 and 2-3, are coupled through the absolute flux term $(U^2 + V^2)^{\frac{1}{2}}$. Since the gradient down the embankment is greater than that across the embankment, the flux in the y direction (V) will be larger than the flux in the x direction (U) in these runoff calculations.

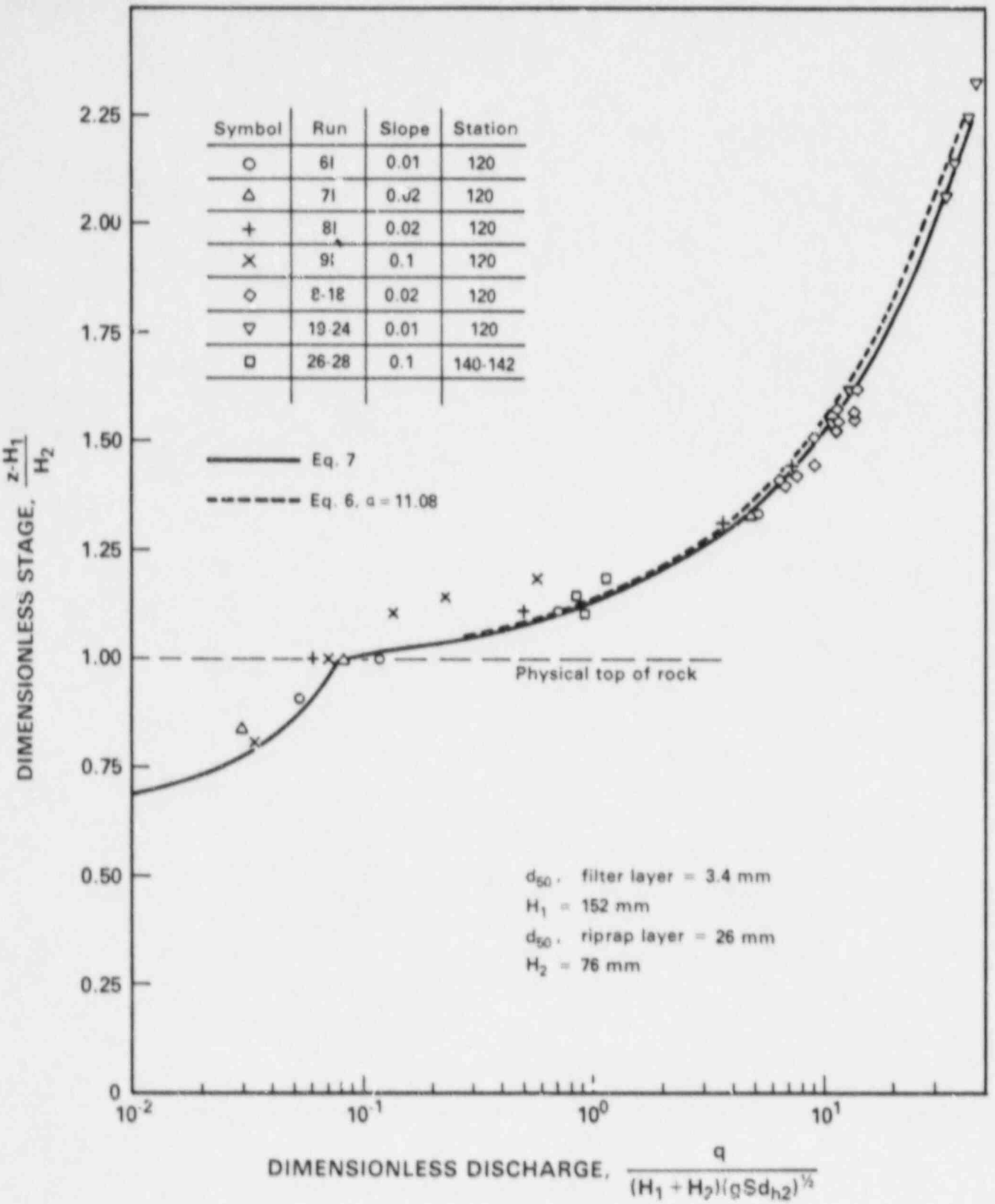
Symbol | Run | Slope | Station
○ | 6I | 0.01 | 120
△ | 7I | 0.02 | 120
+ | 8I | 0.02 | 120
× | 9I | 0.1 | 120
◇ | 8-18 | 0.02 | 120
▽ | 19-24 | 0.01 | 120
□ | 26-28 | 0.1 | 140-142
Eq. 7
Eq. 6, a = 11.08
Physical top of rock
d_{50}, filter layer = 3.4 mm
H_1 = 152 mm
d_{50}, riprap layer = 26 mm
H_2 = 76 mm
DIMENSIONLESS STAGE, $\frac{z-H_1}{H_2}$
DIMENSIONLESS DISCHARGE, $\frac{q}{(H_1+H_2)(gSd_{h2})^{1/2}}$
2.25
2.00
1.75
1.50
1.25
1.00
0.75
0.50
0.25
0
10^{-2}
10^{-1}
10^{0}
10^{1}

cut B

cut 9

Figure 2-9 Stage vs. discharge for 56-mm riprap

Therefore, equation 2-2 is solved for V, using the U and V fluxes from the previous timestep in a correction factor:

$$V_i = \left(\frac{gn^2}{R^{\frac{1}{3}}C^2}\right)^{\frac{1}{2}} SGN(S) \qquad (2\text{-}22)$$

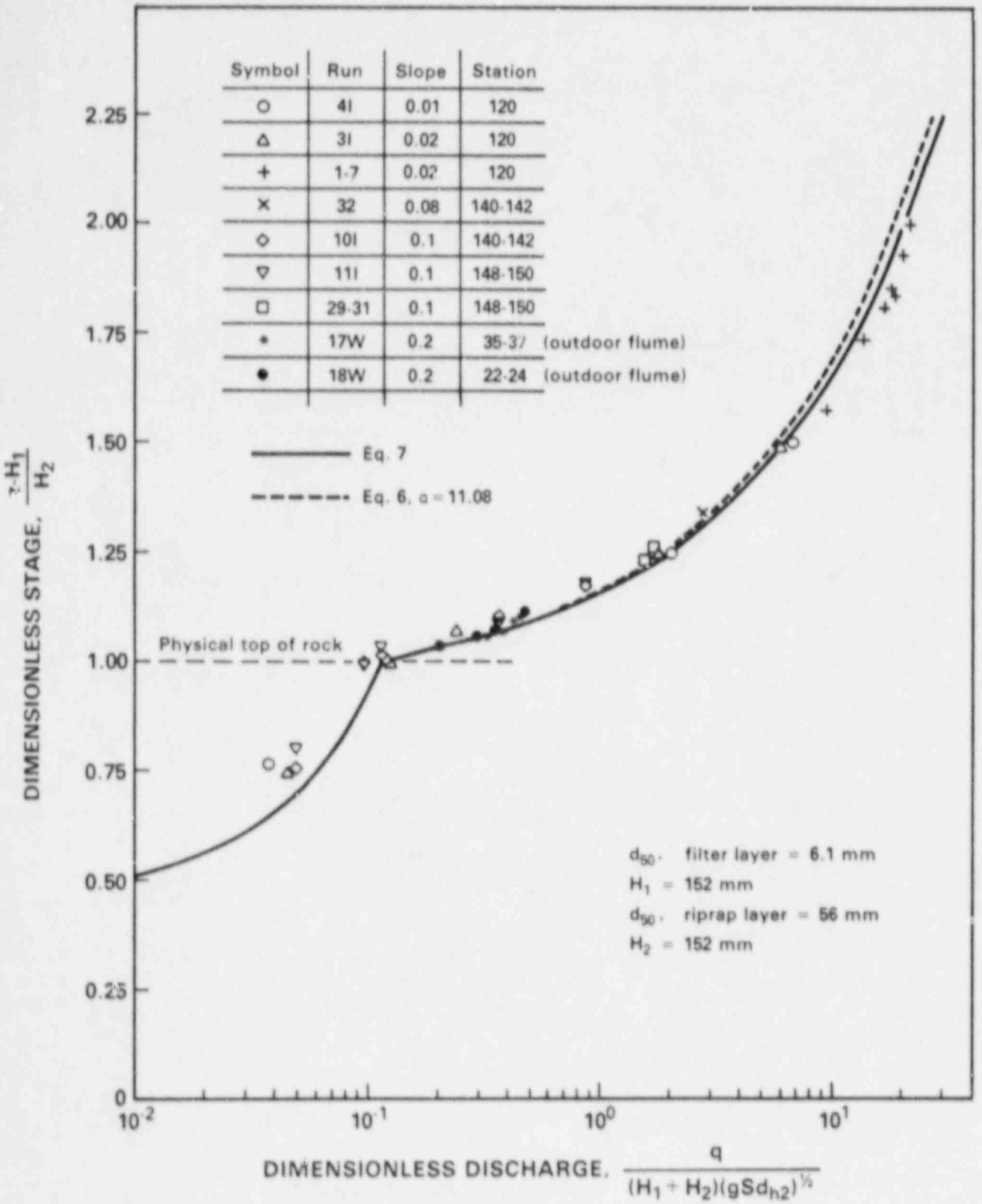
Symbol | Run | Slope | Station
○ | 4I | 0.01 | 120
△ | 3I | 0.02 | 120
+ | 1-7 | 0.02 | 120
× | 32 | 0.08 | 140-142
◇ | 10I | 0.1 | 140-142
▽ | 11I | 0.1 | 148-150
□ | 29-31 | 0.1 | 148-150
* | 17W | 0.2 | 35-37 (outdoor flume)
● | 18W | 0.2 | 22-24 (outdoor flume)
Eq. 7
Eq. 6, a = 11.08
Physical top of rock
d_{50}, filter layer = 6.1 mm
H_1 = 152 mm
d_{50}, riprap layer = 56 mm
H_2 = 152 mm
DIMENSIONLESS STAGE, $\frac{\tau - H_1}{H_2}$
DIMENSIONLESS DISCHARGE, $\frac{q}{(H_1 + H_2)(gSd_{h2})^{1/2}}$
2.25
2.00
1.75
1.50
1.25
1.00
0.75
0.50
0.25
0
10^{-2}
10^{-1}
10^{0}
10^{1}

cut 10

Figure 2-10 Stage vs. discharge for ¾-mm riprap

where $C' = \left[1 + \frac{(U^{xy})^2}{V}\right]^{\frac{1}{2}}$ (2-23)

SGN = the sign of S

$$U^{xy} = \frac{U^n_{1,j} + U^n_{i-1,j} + U^n_{i,j-1} + U^n_{i-1,j-1}}{4} \quad (2\text{-}24)$$

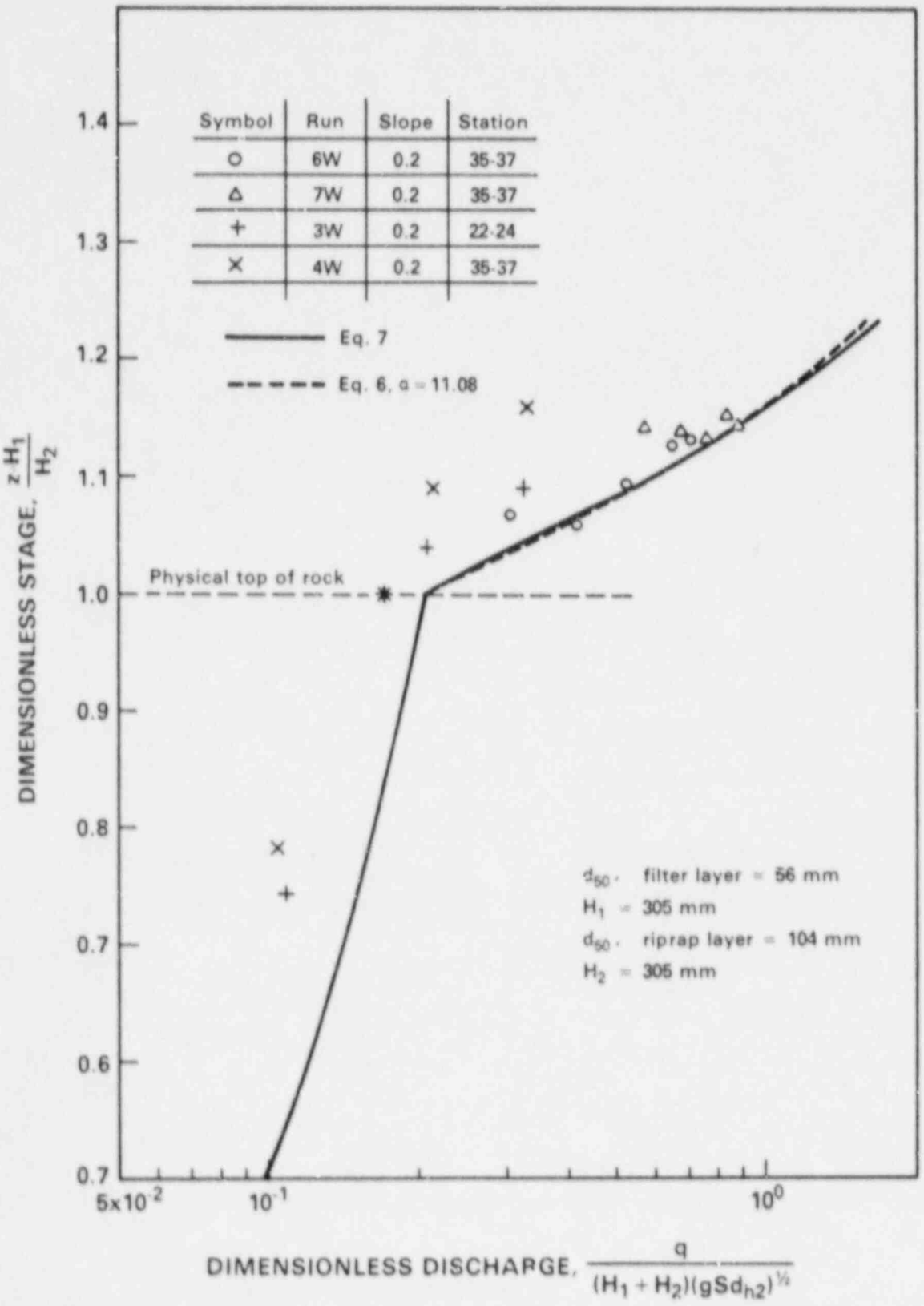
Symbol | Run | Slope | Station
○ | 6W | 0.2 | 35-37
△ | 7W | 0.2 | 35-37
+ | 3W | 0.2 | 22-24
× | 4W | 0.2 | 35-37
Eq. 7
Eq. 6, a = 11.08
Physical top of rock
d_{50} - filter layer = 56 mm
H_1 = 305 mm
d_{50} - riprap layer = 104 mm
H_2 = 305 mm
DIMENSIONLESS STAGE, $\frac{z-H_1}{H_2}$
DIMENSIONLESS DISCHARGE, $\frac{q}{(H_1+H_2)(gSd_{h2})^{1/2}}$
1.4
1.3
1.2
1.1
1.0
0.9
0.8
0.7
0.6
0.7
$5x10^{-2}$
10^{-1}
10^{0}

Cut 10

cut 11

Figure 2-11 Stage vs. discharge for 130-mm riprap

$$V^{xy} = \left\{ \left(U^{xy} \right)^2 + \left(V^n_{i,j} \right)^2 \right\}^{\frac{1}{2}} \tag{2-25}$$

$$S = S_{y,j} - \frac{\xi^{n+1}_{i,j+1} + \xi^{n+1}_{i,j}}{\Delta x} \tag{2-26}$$

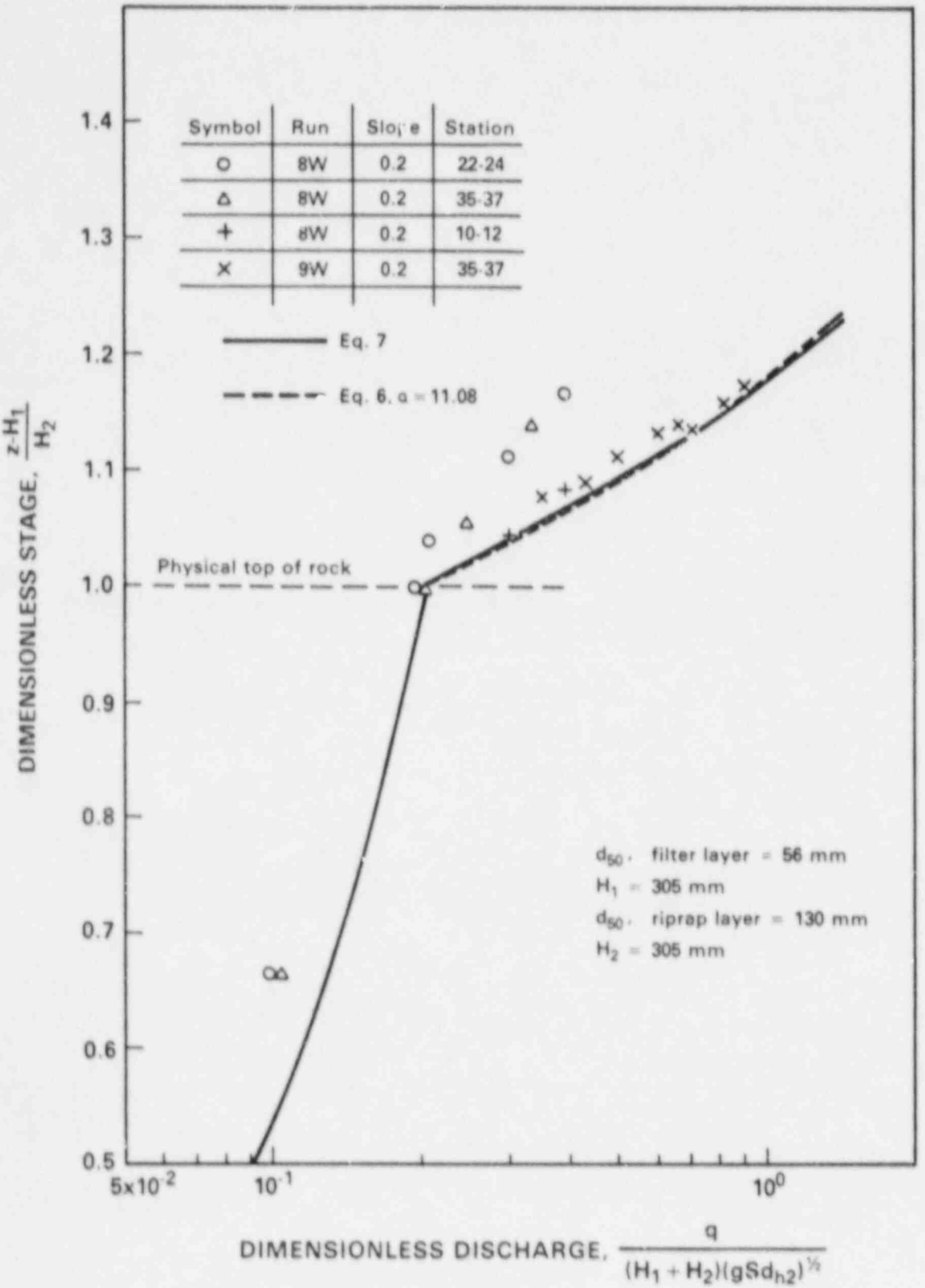
Symbol | Run | Slope | Station
○ | 8W | 0.2 | 22-24
△ | 8W | 0.2 | 35-37
+ | 8W | 0.2 | 10-12
× | 9W | 0.2 | 35-37
Eq. 7
Eq. 6, a = 11.08
Physical top of rock
d_{50}, filter layer = 56 mm
H_1 = 305 mm
d_{50}, riprap layer = 130 mm
H_2 = 305 mm
DIMENSIONLESS STAGE, $\frac{z-H_1}{H_2}$
DIMENSIONLESS DISCHARGE, $\frac{q}{(H_1+H_2)(gSd_{h2})^{1/2}}$
1.4
1.3
1.2
1.1
1.0
0.9
0.8
0.7
0.6
0.5
5×10^{-2}
10^{-1}
10^{0}

cut 12

Figure 2-12 Stage vs. discharge for 157-mm riprap

The U fluxes are then solved once all of the V values have been generated:

$$U_{i,j}^{n+1} = S_x - \frac{\xi_{i+1,j} - \xi_{i,j}}{\Delta x} \frac{gn^2V}{K^2\langle d\rangle_j} \qquad (2\text{-}27)$$

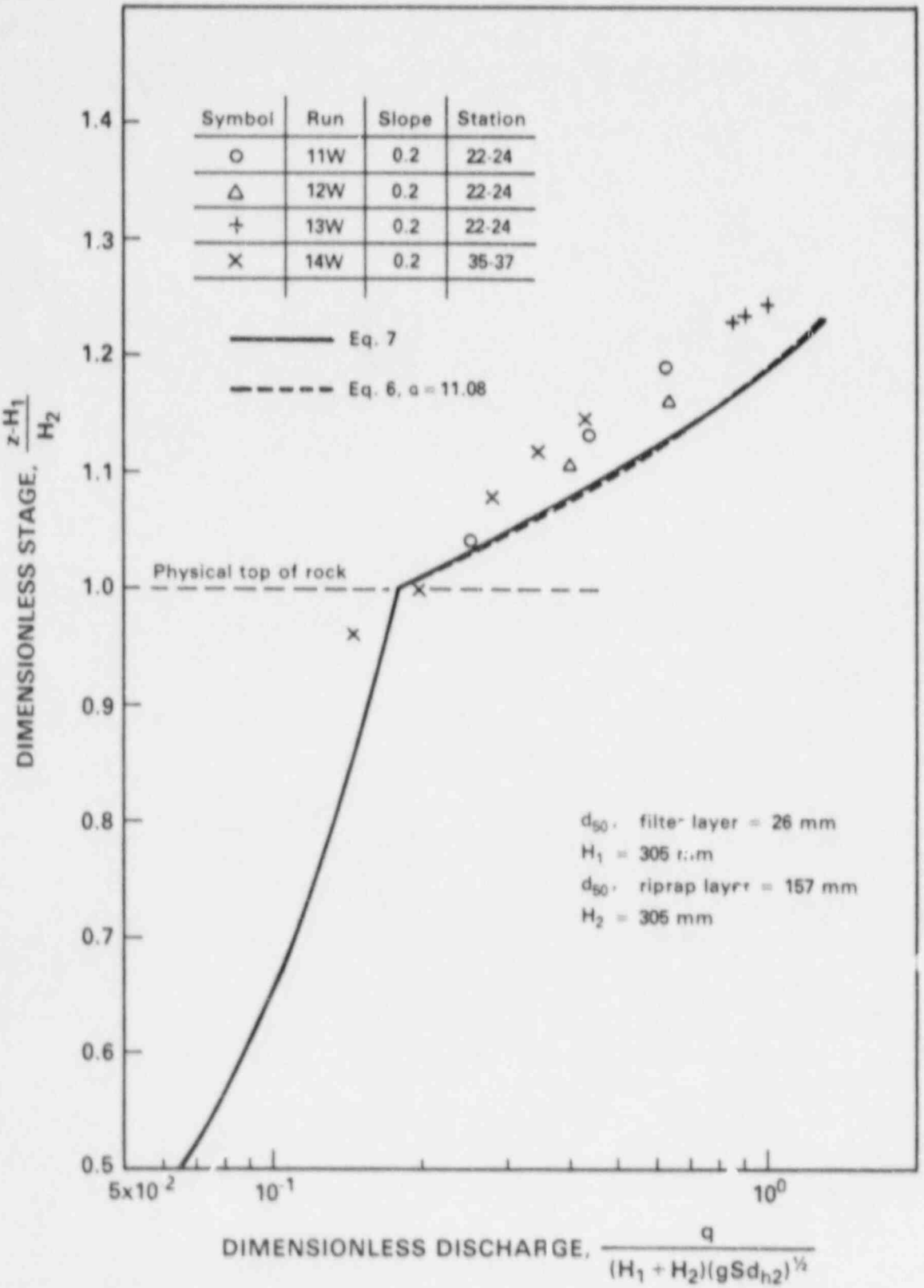
Symbol | Run | Slope | Station
○ | 11W | 0.2 | 22-24
△ | 12W | 0.2 | 22-24
+ | 13W | 0.2 | 22-24
× | 14W | 0.2 | 35-37
Eq. 7
Eq. 6, a = 11.08
Physical top of rock
d_{50}, filter layer = 26 mm
H_1 = 305 mm
d_{50}, riprap layer = 157 mm
H_2 = 305 mm
DIMENSIONLESS STAGE, $\frac{z-H_1}{H_2}$
1.4
1.3
1.2
1.1
1.0
0.9
0.8
0.7
0.6
0.5
5×10^{-2}
10^{-1}
10^{0}
DIMENSIONLESS DISCHARGE, $\frac{q}{(H_1+H_2)(gSd_{h2})^{1/2}}$

cut 13

Figure 2-13 Finite-difference grid

$$\text{where } V = \left[\left(U^n_{i,j}\right)^2 + \left(V^{xy}\right)^2\right]^{1/2} \tag{2-28}$$

$$V^{xy} = \frac{V^{n+1}_{i,j} + V^{n+1}_{i+1,j} + V^{n+1}_{i,j-1} + V^{n+1}_{i-1,j-1}}{4} \tag{2-29}$$

Fluxes normal to all borders except the downstream boundary are defined as zero. The gradient $\partial\xi/\partial x$ is zero at the ends of each row vector. The gradient $\partial\xi/\partial y$ is zero at the end of each column vector. Normal flow (i.e., gravitational forces exactly balance frictional forces) in the +y direction is assumed at the downstream end of each column vector, and is implemented in the finite difference solution as:

$$\xi^{n+1}_{i,N} + \frac{R\Delta t}{n} + \frac{\Delta t}{2n\Delta x}\left[\left(\xi^n_{i-1,N} + \xi^n_{i,N}\right) U^n_{i-1,N} - \left(\xi^n_{i+1,N} + \xi^n_{i,N}\right)U^n_{i,N}\right.$$

$$\left. + \left(\xi^n_{i,N-1} + \xi^n_{i,N}\right) V^n_{i,N-1}\right] = \frac{\Delta t}{n\Delta x}\, \xi^n_{i,N}\, \frac{g\, d_N\, n^2 S^{1/2}_{y,N}}{K'} \tag{2-30}$$

The maximum flow will occur along the centerline of the embankment. The vertical velocity and stage are not calculated explicitly along the centerline, since it is a boundary. The nearest points at which vertical velocity and stage are calculated are $\Delta x/2$ away. The centerline flowrate is estimated by assuming the symmetry boundary conditions, $\partial V/\partial x = 0$ and $\partial\xi/\partial x = 0$ apply, and fitting a

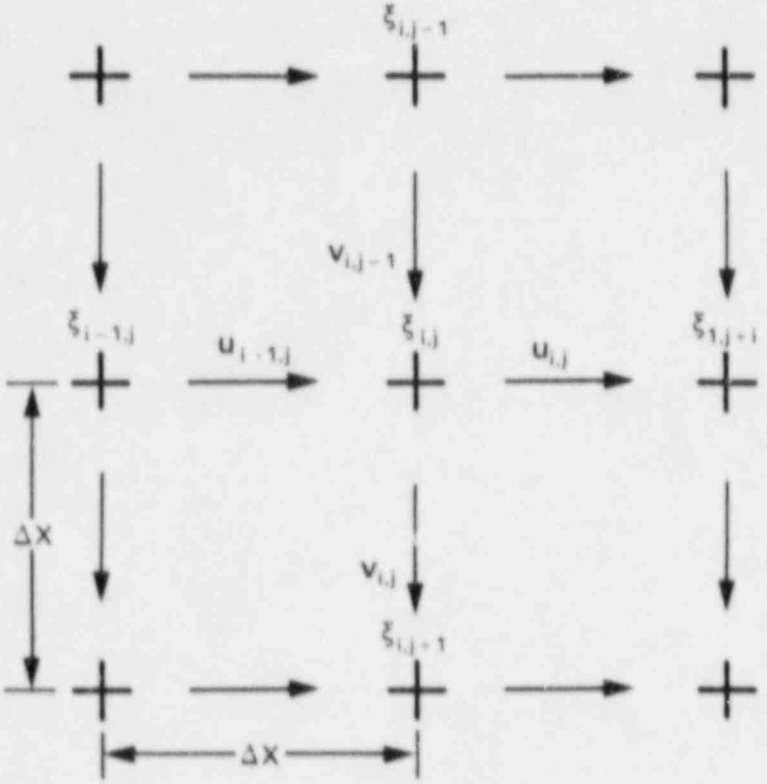
$\xi_{i,j-1}$
$v_{i,j-1}$
$\xi_{i-1,j}$
$u_{i-1,j}$
$\xi_{i,j}$
$u_{i,j}$
$\xi_{1,j-i}$
Δx
$v_{i,j}$
$\xi_{i,j-1}$
Δx

cut 13

parabola to the first two points on its right. For an equally spaced grid, the relationship for the centerline variables (e.g., q) is:

$$q_{1,j} = (1 + \beta)q_{2,j} - \beta q_{3,j} \qquad (2\text{-}31)$$

where β = a factor equal to 0.125

2.4 Precipitation Model

The rate and duration of precipitation onto the embankment is one of the most important factors determining the runoff, which in turn, determines the design requirements of the armor. The Probable Maximum Precipitation (PMP) is the most severe precipitation event that can reasonably be expected to occur at the site, and it is this precipitation that is suggested for the design criterion. It is axiomatic that precipitation events that cover a small area of land can be very intense, but short lived. Conversely, precipitation events covering larger areas may be less intense, but ultimately produce greater amounts of rainfall over longer periods of time. The PMP chosen for a particular site depends on the characteristic time at which the drainage basin responds to a precipitation event. That is, a large drainage basin would respond much more slowly than would the drainage basin for a small tributary stream. The PMP for the former would be a storm of long duration, with only moderate rates of rainfall. The PMP for the small tributary, however, would be a storm of short duration but of intense rates of precipitation. This time constant is generally called the "time of concentration." The time of concentration for large rivers could be weeks or even months; that of small tributary streams would be hours or fractions of hours. Typical tabulations for the PMP give rainfall intensities for periods no shorter than 15 minutes.

The drainage area for typical embankments is generally not more than a few tens of acres. The time of concentration would be measured in minutes. There are no widespread estimates for the PMP which are tabulated for cases in which the times of concentration are so small. Therefore, the rainfall-duration relationships for the model have been developed from estimates made by the staff of the U.S. National Weather Service (NWS) for durations less than 15 minutes (Hansen, 1985). The NWS estimated that the 5-minute duration PMP for the area covered by Hydrometerological Report 49 (HR-49) (NOAA, 1977) was 45 ± 5% of the 1-hour PMP. For durations shorter than 5 minutes, NWS advised that the maximum rainfall rates could be estimated from record rainfall amounts measured at mid-latitudes on the globe. NRC therefore used the U.S. record for 1 minute of 1.23 inches, measured at Unionville, Md, on July 4, 1956. The rainfall-duration curve for durations of 15 minutes to 2 hours was estimated from HR-49. This report is most suited to the Colorado and Great Basin drainages of the western United States, but rainfall-duration relationships for other regions of the United States could be developed along similar lines. The above estimates have been interpolated by means of a cubic spline. The spline equation and coefficients are given in Table 2-5.

Standard practice in performing flood estimates dictates that rainfall within the period of the PMP is not temporally correlated; i.e., the rainfall can be arranged any way within the time period of the PMP, as long as the cumulative amounts over the period are the same. Recognizing that conditions that saturate

Table 2-5 Spline curve for rainfall intensity vs. duration

i	t_i, min	$Range_i$ min	$C_{i,1}$	$C_{i,2}$	$C_{i,3}$	F_i
1	0.0	0.0 - 1.0	0.1616205E+00	0.0	-0.7820493E-0	2 0.0
2	1.0	1.0 - 5.0	0.1381590E+00	-0.2346148E-01	-0.7820493E-02	0.1538
3	5.0	5.0 - 15.0	0.3967789E+01	-0.1158800E-02	-0.7820493E-02	0.45
4	15.0	15.0 - 30.0	0.1923221E-01	-0.8857681E-03	-0.7820493E-02	0.74
5	30.0	30.0 - 45.0	0.4822097E-02	-0.7490628E-04	-0.7820493E-02	0.89
6	45.0	45.0 - 60.0	0.3749401E-02	-0.1460676E-04	-0.7820493E-02	0.95

Equation: $R' = \left[\left(C_{i,3} \times D + C_{i,2}\right) \times D + C_{i,1}\right] \times D + F_i$

where R' = fraction of 1-hour PMP accumulation
D = duration - t_i, min

Standard practice in performing flood estimates dictates that rainfall within the period of the PMP is not temporally correlated; i.e., the rainfall can be arranged any way within the time period of the PMP, as long as the cumulative amounts over the period are the same. Recognizing that conditions that saturate the rock layers are likely to produce the greatest runoffs, the design-basis rate of precipitation for embankments was formulated so that there would be an increasing intensity of precipitation, and that the last 2.5 minutes of the first hour would be the most intense. Total precipitation for the first hour was 203 mm (8 inches). Precipitation for the second hour was 1% of that for the first hour. A tabulation of rainfall intensities versus time is given in Table 2-6.

Table 2-6 Rainfall rate for Probable Maximum Precipitation

Time, sec	Multiplier for 1-hr rate(1)	Multiplier for 1-hr rate(2)
0 - 1800	0.22	0.22
1800 - 2700	0.6	0.6
2700 - 3000	1.43	1.43
3000 - 3300	2.05	2.05
3300 - 3450	3.25	5.4
3450 - 3600	7.55	5.4
3600 - 3750	1.06	0.753
3750 - 3900	0.445	0.753
3900 - 4200	0.286	0.286
4200 - 4500	0.2	0.2
4500 - 5400	0.084	0.084
5400 - 7200	0.031	0.031

(1) 2.5-minute minimum duration.
(2) 5-minute minimum duration.

The sensitivity of the maximum rate of runoff to the choice of the duration of the shortest, most intense segment will be demonstrated in Section 2.5.

2.5 Model Results and Sensitivity Experiments

An example is presented to demonstrate the use of the model for estimating peak runoffs. The modeled embankment is typical of those found at uranium mill tailings sites. The embankment is assumed to be of triangular shape and symmetrical around the vertical centerline, similar to that shown in Figure 2-14a. It is 213 m (700 feet) long from top to bottom, and 266 m (1200 feet) wide at the base. The top portion of the embankment is 134 m (440 feet) long, the slope is 2%, and the rock thickness of the layer is 1 foot. The lower portion of the embankment is 79 m (260 feet) long, the slope is 20%, and the rock layer is 0.46 m (1.5 feet) thick. The harmonic mean diameters of the rock are 0.305 to 0.1 m (0.1 foot), and 0.3 foot for the top and side slopes, respectively. The d_{84} diameters are 0.1 to 0.23 m (0.32 and 0.75 foot), respectively. The rock is crushed quarry material, and is assumed to have a friction factor for flow of K = 4.0. Other properties of the riprap and embankments are given in Table 2-7. Rainfall intensity for the design is given in Table 2-6.

Table 2-7 Inputs for sample design of stable rock

Parameter	Top slope	Side slope
Friction index, k	4	4
Diameter, d_h	49 mm (0.16 ft)	143 mm (0.47 ft)
d_{84}	73 mm (0.24 ft)	201 mm (0.66 ft)
H_1	305 mm (1.0 ft)	457 mm (1.5 ft)
n_1	0.35	0.35
S	0.02	0.2
q	22.91 liters/sec (0.81 ft^3/sec)	22.91 liters/sec (0.81 ft^3/sec)
C factor (0.22 for smooth rock, 0.27 for crushed, eq. 3-4)	0.27	0.27
Angle of repose, 0	40°	41.5°
Specific gravity of rock	2.65 gm/cc	2.65 gm/cc
Safety factor	1.5	1.5
d_{50}, safety factor method	43.6 mm (0.143 ft)	488 mm (1.6 ft)
d_{50}, Stephenson method	12.5 mm (0.041 ft) (after multiplying by factor of 1.5)	72.8 mm (0.239 ft)

2.5.1 Benchmark Case

Runoff per unit width from the toes of the top and side slopes of the sample embankment is shown in Figure 2-15. These and subsequent results are also summarized in Table 2-8. In the present case, the top and side slopes are assumed to be unfailed. Peak flow from the top slope is nearly coincident with the peak precipitation rate. Runoff from the side slope shows a small disturbance after its peak, which is caused by the routing of the peak flow from the top slope.

The sensitivity of the maximum rate of runoff to the choice of the duration of the shortest, most intense segment will be demonstrated in Section 2.5.

2.5 Model Results and Sensitivity Experiments

An example is presented to demonstrate the use of the model for estimating peak runoffs. The modeled embankment is typical of those found at uranium mill tailings sites. The embankment is assumed to be of triangular shape and symmetrical around the vertical centerline, similar to that shown in Figure 2-14a. It is 213 m (700 feet) long from top to bottom, and 366 m (1200 feet) wide at the base. The top portion of the embankment is 134 m (440 feet) long, the slope is 2%, and the rock thickness of the layer is 1 foot. The lower portion of the embankment is 79 m (260 feet) long, the slope is 20%, and the rock layer is 0.46 m (1.5 feet) thick. The harmonic mean diameters of the rock are 0.305 to 0.1 m (0.1 foot), and 0.3 foot for the top and side slopes, respectively. The d_{84} diameters are 0.1 to 0.23 m (0.32 and 0.75 foot), respectively. The rock is crushed quarry material, and is assumed to have a friction factor for flow of K = 4.0. Other properties of the riprap and embankments are given in Table 2-7. Rainfall intensity for the design is given in Table 2-6.

Table 2-7 Inputs for sample design of stable rock

Parameter	Top slope	Side slope
Friction index, k	4	4
Diameter, d_h	49 mm (0.16 ft)	143 mm (0.47 ft)
d_{84}	73 mm (0.24 ft)	201 mm (0.66 ft)
H_1	305 mm (1.0 ft)	457 mm (1.5 ft)
n_1	0.35	0.35
S	0.02	0.2
q	22.91 liters/sec (0.81 ft^3/sec)	22.91 liters/sec (0.81 ft^3/sec)
C factor (0.22 for smooth rock, 0.27 for crushed, eq. 3-4)	0.27	0.27
Angle of repose, 0	40°	41.5°
Specific gravity of rock	2.65 gm/cc	2.65 gm/cc
Safety factor	1.5	1.5
d_{50}, safety factor method	43.6 mm (0.143 ft)	488 mm (1.6 ft)
d_{50}, Stephenson method	12.5 mm (0.041 ft) (after multiplying by factor of 1.5)	72.8 mm (0.239 ft)

2.5.1 Benchmark Case

Runoff per unit width from the toes of the top and side slopes of the sample embankment is shown in Figure 2-15. These and subsequent results are also summarized in Table 2-8. In the present case, the top and side slopes are assumed to be unfailed. Peak flow from the top slope is nearly coincident with the peak precipitation rate. Runoff from the side slope shows a small disturbance after its peak, which is caused by the routing of the peak flow from the top slope.

cut 14

Figure 2-14 Embankment failure scenarios

Table 2-8 Summary of model experiments

Scenario	Peak runoff, $ft^3/sec/ft$	
	Top slope	Side slope
Benchmark, 0% slump	0.27	0.31
Halved d_h	0.57	0.28
Doubled d_h	0.17	0.39
1/2 layer thickness	0.56	0.94
1/2% slump	0.81	0.44
1% slump	1.65	0.99
Infinite layer, 1% slump	0.19	0.42
Filled rock, 1/2 <d> layer thickness	0.52	0.85
5-min minimum duration, benchmark	0.25	0.31
5-min minimum duration, 1/2% slump	0.69	0.43

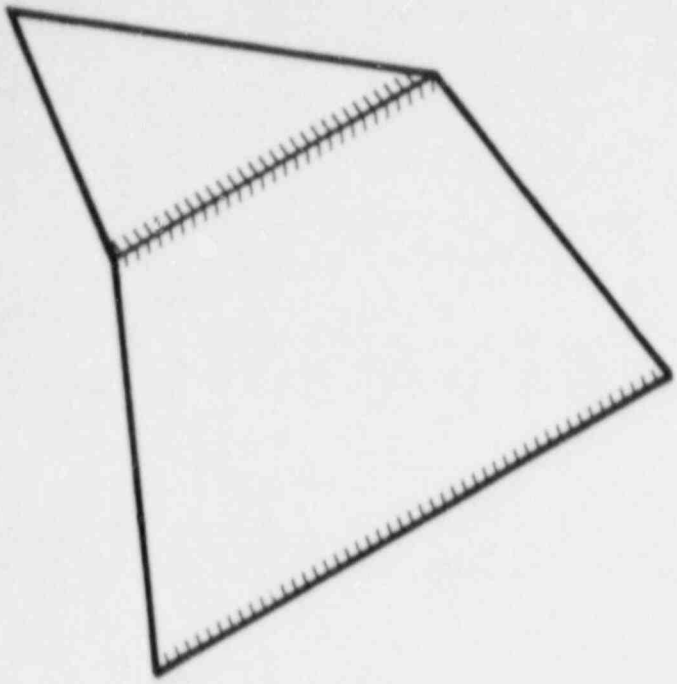

(a) Benchmark slope

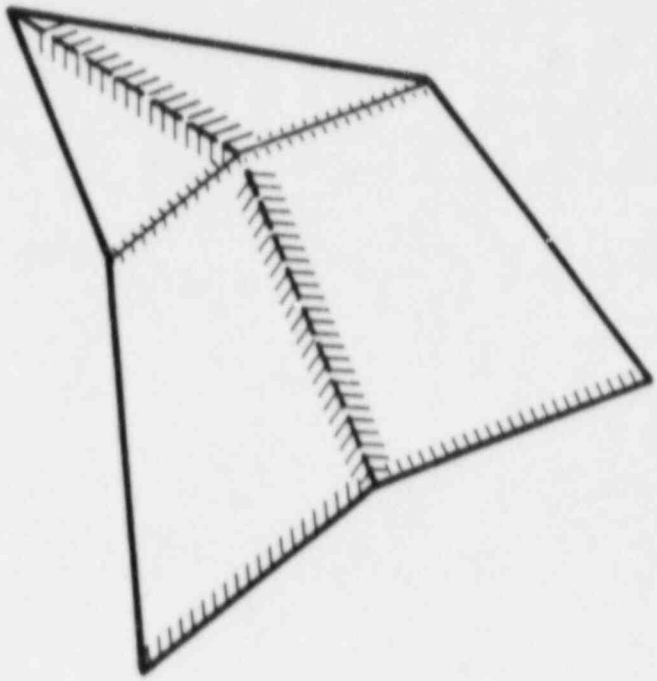

(b) Single failure

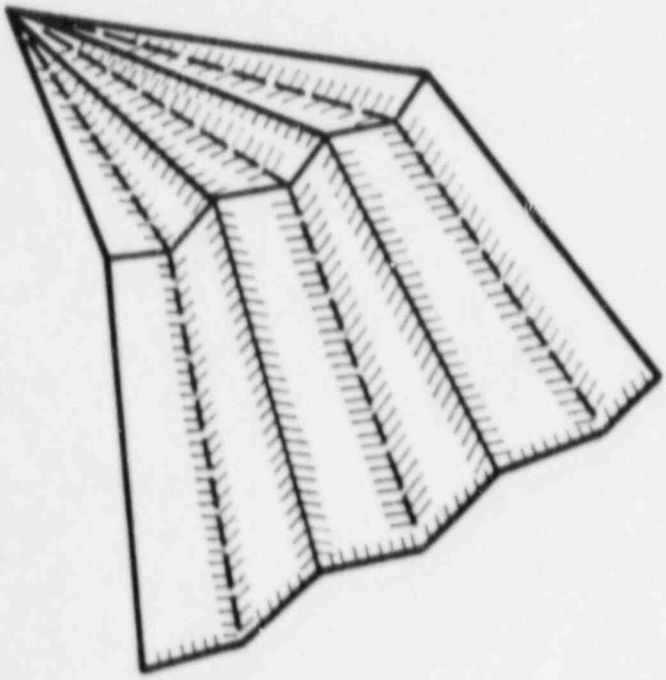

(c) Multiple failure

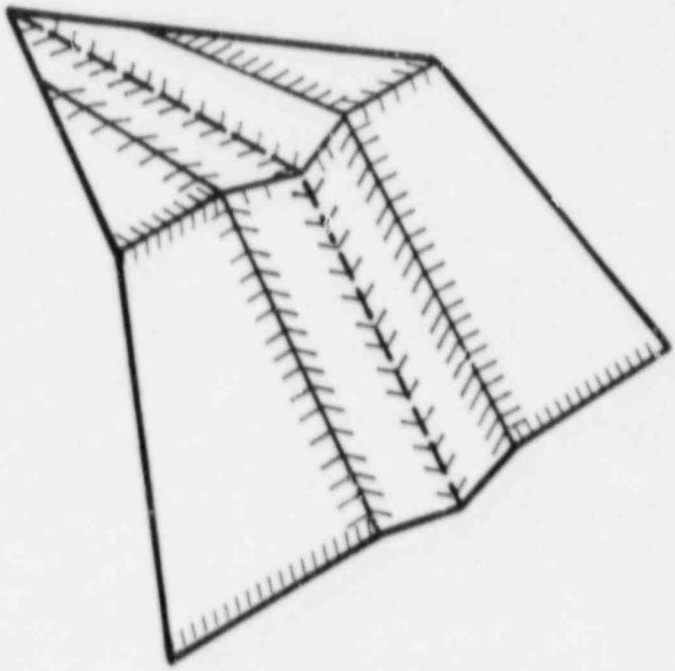

(d) Trench failure

Cut 14

cut 15

Figure 2-15 Transient runoff for benchmark case

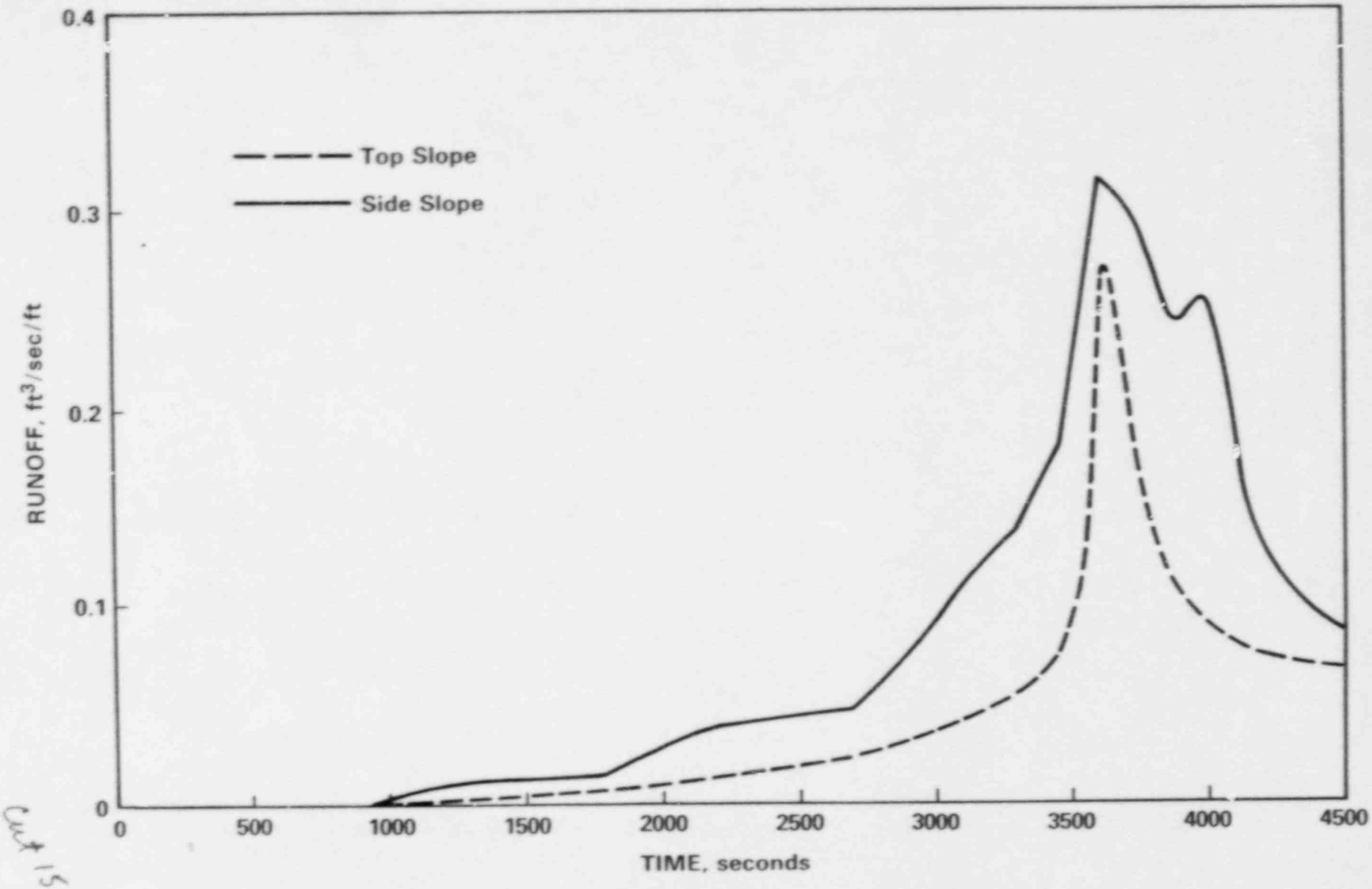
0.4
0.3
0.2
0.1
0
RUNOFF, ft³/sec/ft
Top Slope
Side Slope
0
500
1000
1500
2000
2500
3000
3500
4000
4500
TIME, seconds

2.5.2 Flow Concentration

Flow concentration is a term that describes the preferential flowpaths on the embankments caused by nonuniformities of the embankment profile. The analysis of runoff presented above is for flat surfaces with uniform slopes. Construction practices on the embankment earthworks will presumably strive to maintain flat or crowned surfaces and uniform placement of the rock layer. Nonuniformity of the embankments, however, could lead to concentration of runoff, causing higher flowrates than would otherwise be predicted. Conditions that could lead to flow concentration include:

(1) non-uniform slope grading
(2) uneven placement of rock
(3) gullying caused by erosion
(4) slumping of earthwork

There is evidence that natural slopes often erode when runoff through underground channels leads to collapse. Erosion of soil at the surface will be inhibited by the protection of the rock armor and filter layers. It is not clear at this time whether observations of erosion on natural unprotected slopes are relevant to erosion on armored, well-engineered embankments.

A likely cause of flow concentration, given that good grading and rock placement practices are followed, is a failure or differential settlement of the earthwork with subsequent subsidence or slumping. Such a failure could create a depression toward which water running off the embankment would collect. The nature of such a failure is highly speculative.

There are at least two compensating factors tending to resist flow concentration:

(1) If the rock layers are thick enough, water will flow beneath the rock layer surface, and the uniformity of the layer should be less important.

(2) Tailings embankments are often narrow at the top and wide at the bottom. This condition leads to a natural hydraulic gradient out from the centerline of the slope, tending to disperse rather than concentrate flow.

The smaller grade and lower water-carrying ability on the top slope would accentuate the effects of settlement on flow concentration, Settlement of from one to several feet might be possible (Wardwell, 1984). Good engineering and construction practice probably can reduce the effect of settlement.

Nevertheless, several scenarios of embankment failure have been postulated and studied with the numerical runoff model, as illustrated in Figure 2-14. Figure 2-14b shows the embankment as built. Figure 2-14b shows a uniform inward slumping of the embankment toward the centerline. Multiple failures as illustrated in Figure 2-14c probably would cause less severe flow concentration, because the drainage area for each sub-basin is smaller than the single-failure case. Other failures are possible, such as the opening of a trough by slumping and erosion of an otherwise-unfailed embankment (Figure 2-14d).

2.5.2.1 Embankment Slumping

Two cases of embankment slumping of the type illustrated in Figure 2-14b are presented in order to demonstrate flow concentration: (1) uniform inward slope of 1/2% toward centerline and (2) uniform inward slope of 1%.

Flow concentrations resulting from steady rainfall on the slumped embankments are presented in Figure 2-16 as the ratio of runoff at the embankment centerline to that runoff to the same embankment with no slumping.

cut 16

Figure 2-16 Flow concentration for steady rate of precipitation

Flow concentration for the 1/2% and 1% slump scenarios are all greater than unity and depend on the rainfall intensity. The high degree of flow concentration from the top slope is explained largely by the saturation and overtopping of the rock layer. Resistance to flow is greatly reduced once overtopping occurs. In addition, the inward slope in each case is a significant fraction of the 2% downward gradient of the original slope. There is significantly less flow concentration on the steep side slopes. Overtopping would occur only at points above the slope break. Peak flow rates are attenuated within the rock layer of the side slope.

Transient runoffs from the top and side slopes resulting from the local PMP are presented in Figure 2-17 for the 1/2% slump scenario. There is a considerable degree of flow concentration for the slumped case, particularly on the top slope. An interesting observation is that peak runoff may occur at the toe of the top slope rather than at the toe of the side slope. The design of the rock layer on the side slope may therefore be controlled by runoff from the top slope.

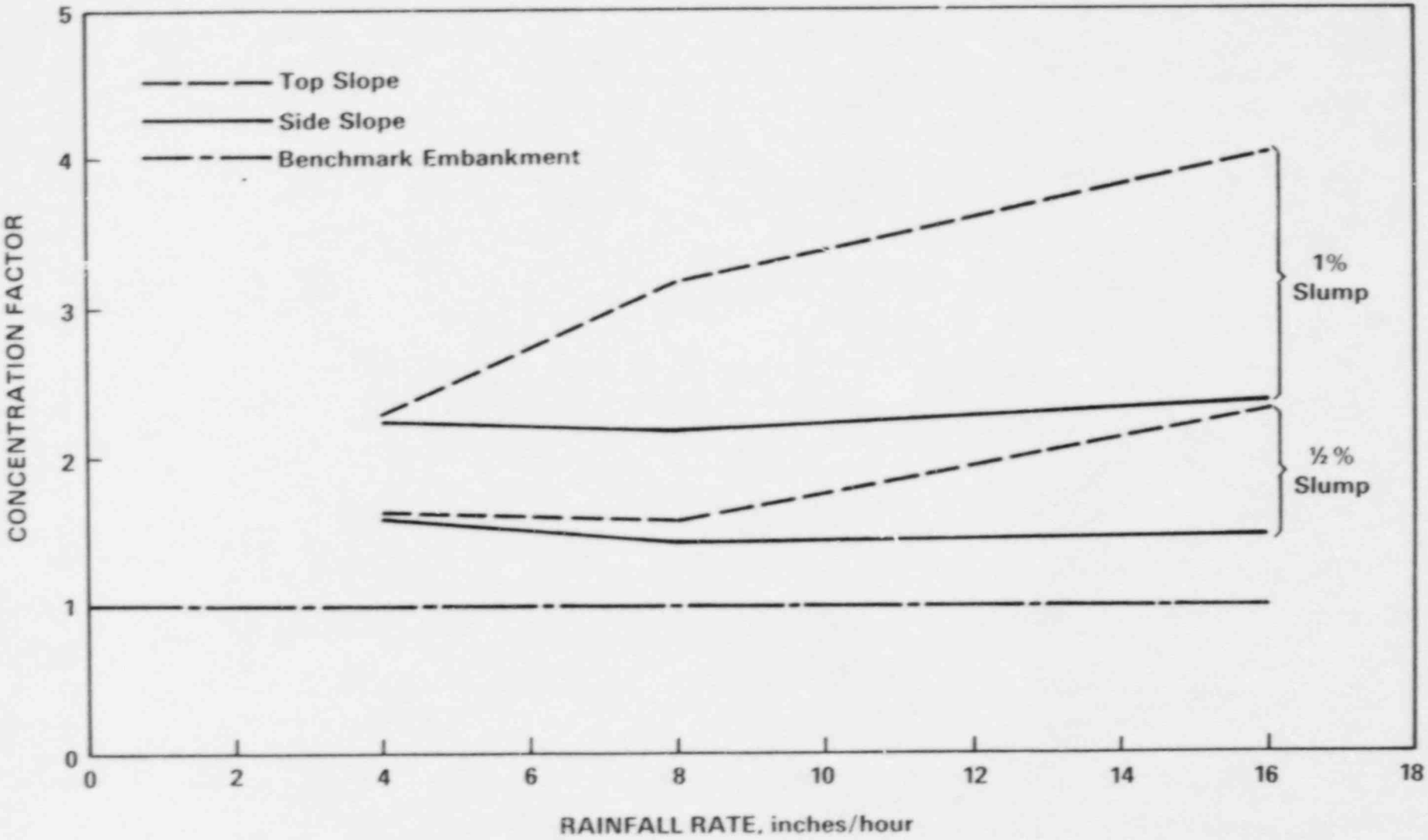
Top Slope
Side Slope
Benchmark Embankment
1% Slump
½% Slump
CONCENTRATION FACTOR
RAINFALL RATE, inches/hour
0
1
2
3
4
5
0
2
4
6
8
10
12
14
16
18

cut 17

Figure 2-17 Transient runoff for 1/2% inward slump

2.5.2.2 Reduced Conveyance

Peak runoff is sensitive to the ability of the flow to remain confined to the rock layer rather than overtop it. The ability of the rock layer to store and transport most of the runoff is a critical factor in the attenuation of peak flow from the slope. This effect will be diminished, however, if the rock layer is too thin, its friction too great, or its porosity too small.

The capacity of the rock layer to conduct flow is related to its thickness and flux. A convenient grouping of terms is the conveyance

$$q' = Hn\left(\frac{gSd_h}{K'}\right)^{\frac{1}{2}}$$

Reducing porosity n or increasing K would reduce the water-carrying ability of the rock layer. The flood peak will be attenuated as long as the flow remains confined below the surface of the rock. If overtopping should occur, however, the friction is decreased dramatically, and the conveyance of the slope increases. The net effect of friction on peak flood flow is highly nonlinear and cannot be expressed as a simple causal relationship.

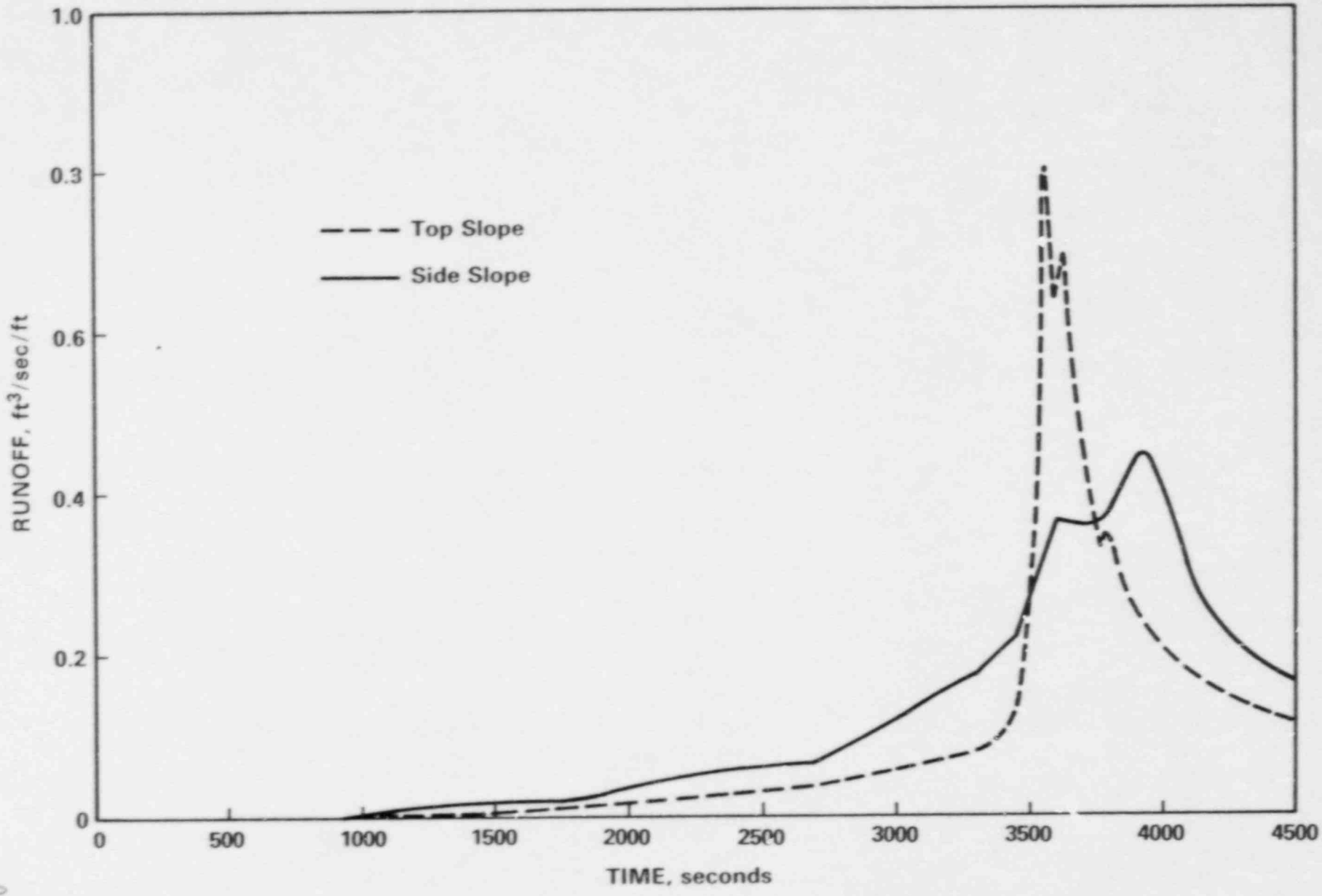
1.0
0.3
0.6
0.4
0.2
0
RUNOFF, ft³/sec/ft
Top Slope
Side Slope
0
500
1000
1500
2000
2500
3000
3500
4000
4500
TIME, seconds

L1 + cut 17

The effect of doubling and halving the estimate of d_h is given in Table 2-8. Doubling d_h lowers the internal friction, increasing the peak runoff. Interestingly, halving d_h increases friction, but causes the flow on the top slope to exceed the carrying capacity of the rock layer, resulting in an increase in the peak runoff at the toe of the top slope.

The transient case was rerun for the 1/2% slump scenario, but with an essentially infinite layer thickness which eliminates the possibility of overtopping. The results of this run are shown in Figure 2-18, along with the runoff for the normal thickness of the rock layer. Peak runoffs for this case are lowered dramatically. Furthermore, the peak runoff occurs at the toe of the side slope and is no longer controlled by runoff from the top slope. The maximum thickness of the rock layer necessary for the sample embankment to completely contain the peak flows are about 3.3 feet on the top slope and 1.4 feet on the side slope.

cut 18

Figure 2-18 Runoff reduction on thick armored embankment

2.5.2.3 Peak Intensity of Precipitation

The "time of concentration" (TOC) is a measure of the response time or frequency response of a flow system (Overton, 1976). The TOC for flow on an embankment in response to a precipitation event depends on length of the embankment and the speed at which disturbances propagate. The usefulness of the time of

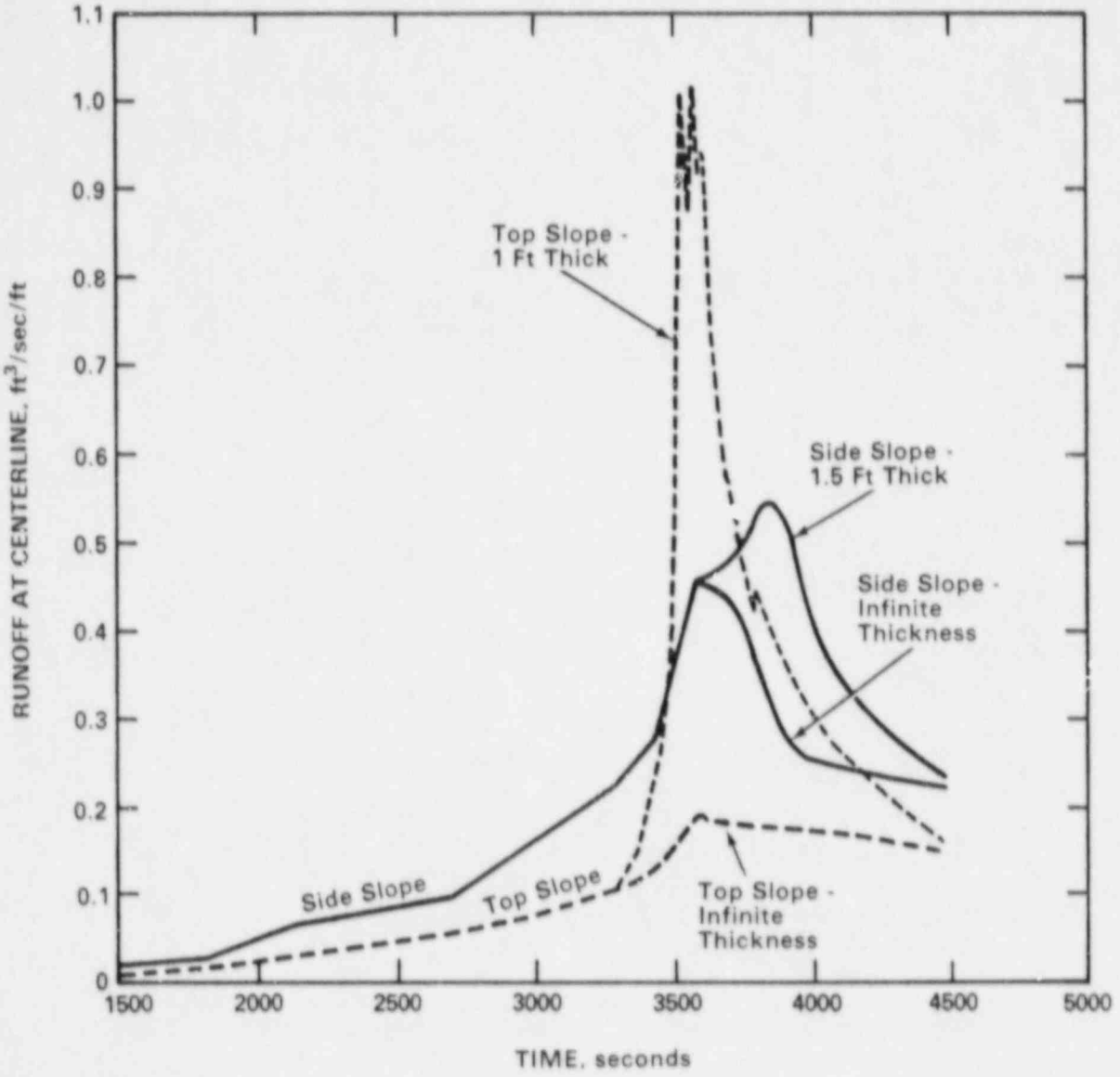
RUNOFF AT CENTERLINE, ft³/sec/ft
1.1
1.0
0.9
0.8
0.7
0.6
0.5
0.4
0.3
0.2
0.1
0
1500
2000
2500
3000
3500
4000
4500
5000
TIME, seconds
Top Slope - 1 Ft Thick
Side Slope - 1.5 Ft Thick
Side Slope - Infinite Thickness
Top Slope - Infinite Thickness
Side Slope
Top Slope

cut 18

concentration is that it sets a limit to the duration of the PMP that must be considered in the analysis; i.e., the peak flowrate should be relatively insensitive to the duration of disturbances shorter than the time of concentration. The shorter the time of concentration, the shorter, and therefore more intense, the periods of precipitation that must be considered. For example, a large embankment will be less sensitive than a small embankment to intense but short-lived precipitation.

The speed at which the disturbances propagate along the embankment is assumed to be the kinematic velocities of flow through and over the rock, determined by balancing the forces of gravity and friction. The kinematic velocity increases once the rock layer is overtopped. The time of concentration, therefore, should be smaller for higher rates of precipitation, or for conditions of the embankment that are likely to cause overtopping of the rock layer. Although there are a number of relationships for times of concentration (Overton, 1976), they were derived largely for impermeable plane surfaces, and require difficult-to-define parameters such as Manning's coefficient. Their adequacy for the present situation of flow on compound armored embankments has not been demonstrated.

The PMP used in the present analysis considers periods in the rainfall duration curve as short as 2.5 minutes. To test the sensitivity of the peak runoff to duration and intensity of the rainfall, the benchmark and 1/2% slump scenarios were rerun, but under the influence of the most intense 5-minute periods instead of the 2.5-minute periods. The revised rainfall-duration curve is presented in Table 2-6. The benchmark case shows modest sensitivity to the change. The case for the 1/2% slump shows a greater difference between the two rainfall-duration curves: the 5-minute duration case gives peak runoff values up to 15% lower than for the 2.5-minute case. This indicates that the time of concentration is shorter than 5 minutes for the slumped scenarios, and the 2.5-minute rainfall-duration curve would be more acceptable.

2.5.2.4 Infilling of Rock

Some embankment designs call for the interstices of the riprap to be filled with soil. Even where this is not being done deliberately, it is conceivable that natural processes such as rock weathering and windblown transport of soil may cause the interstices to clog. Much of the attenuation of the PMP is due to the capacity for flow beneath the surface of the rock layer, and this would be lost should the interstices become filled.

Two additional runs were made to demonstrate the effects on peak flow of a diminished thickness of rock layer on an unslumped slope. The first run diminishes the rock layer thickness by half. In the second run, the rock layer thickness is reduced to one-half of the <d> rock diameters. Peak runoffs increase for both cases, as presented in Table 2-8. Interestingly, the more significant runoff occurred for the former case where the rock layer thickness was diminished by half, rather than the later case where the thicknesses of the layers were much smaller. This phenomenon probably is caused by the timing of the rainfall onto the slope and the speed at which it runs off. In the later case, the higher speed of runoff allowed the water to drain off the top slope; in the former case, water accumulated and ran off coincidentally with the peak flow. This somewhat counterintuitive finding points to the complexity of runoff from armored slopes, and the need to study the designs carefully.

2.6 Conclusions

Runoff from armored compound slopes on tailings embankments resulting from intense precipitation has been studied by means of a mathematical model for kinematic flow. Several interesting conclusions can be drawn from the mathematical experiments with the model:

(1) The calculation of runoff must consider flow both through and over the top of the armor layer.

(2) Irregularities in the surface of the slopes may lead to large concentrations of flow along preferential paths.

(3) The peak runoff from the gentler top slope could be greater than the peak runoff from the steeper side slope, thereby controlling the design of the armor on both slopes. This condition may occur when the ability of the rock layer to carry the flow is inadequate, as illustrated in Section 2.5.2.2, forcing the flow to overtop the rock layer. The most severe hydrologic stresses on the armor are likely to occur at the break between the top and side slopes for this situation. This observation indicates that the larger armor used on the side slope should extend a distance above the break in the slope, onto the less steep slope.

(4) The use of larger diameter rock and thicker rock layers tends to diminish peak runoff from the top slope.

(5) The effects of flow concentration caused by geotechnical failure or slumping can be greatly diminished by having an adequate rock layer thickness.

(6) For typical embankments, the rainfall duration should consider durations as short as 2.5 minutes, especially when evaluating cases for slumped embankments. Experiments with a 5-minute minimum duration showed up to 15% lower results for peak runoff than produced for the same embankment with a 2.5-minute minimum duration. Results were less critical for unslumped embankments.

(7) Attenuation in the armor layer is lost if a soil-filled rock is used, leading to significantly higher flood peaks because of a shorter time of concentration.

3 DETERMINING THE SIZE OF THE RIPRAP

3.1 Introduction

This chapter deals with one possible method that could be used by the designer to determine the size of rock necessary to resist the forces generated by runoff from severe precipitation. It is presumed that standard design principles and good design practices will be followed for the overall design of the riprap and filter layers. Such specifications are outside the scope of this report. The present report provides only the necessary tools for the hydrologic stability analysis.

The demonstration of suitability presented in this chapter will be based on the following procedures:

(1) Select initial riprap layer specifications for the entire embankment. Using the methodology for runoff calculations discussed in Chapter 2, calculate the peak flowrate and stage at key points on the embankment for a given design.

(2) Utilize the safety factor method (Stevens, 1971) and Stephenson method (Stephenson, 1979) to determine the size of rock necessary to withstand the forces generated by the peak flows.

(3) Check to see that the given rock sizes meet or exceed the rock sizes calculated in step 2.

(4) If the given rock sizes are smaller than sizes needed, modify the design; e.g., decrease the slope, increase the rock size, increase the layer thicknesses. It may be necessary to recalculate peak flows from step 1, if it is suspected that they might increase under the new design.

The safety factor and Stephenson methods will be described in the sections that follow, and will be compared with the results of flume studies conducted at Colorado State University. Other methods for determining the rock size are reviewed in Abt et al. (1987). Finally, a brief computer program will be described, which will aid the investigator in applying the formulas presented in this chapter for determining the rock size.

3.2 Safety Factor Method

The safety factor method was developed to determine the stability of rock riprap in flowing water in the absence of wave and seepage forces (Stevens, 1971). The method relies primarily on the observation that rocks on side slopes tend to roll rather than slide. The stability of the rock is determined by summing the moments produced by gravity, buoyancy, drag force, and lift force around the axis of rotation.

For overtopping flows principally down the gradient of an embankment, the safety factor method can be simplified. For flowing water at steady state, the tractive force on the rock surface (τ_s), must just balance the force of gravity:

$$\tau_s = \gamma \xi S_y \tag{3-1}$$

where γ = density of water (62.4 lb/ft^3)
ξ = depth of water over the top of rock (ft)
S_y = slope of the embankment face

The depth of water ξ is determined either from a stage-discharge rating curve or from a simple formula for conveyance (such as Manning's equation).

The representative diameter of the stable rock d can be determined if the tractive force on the rock is balanced against the natural tendency of the rock to remain in place:

$$d = \frac{21\tau_s}{(S_s - 1)\gamma\eta} \tag{3-2}$$

where $$\eta = \cos\alpha \frac{1}{SF} - \frac{\tan\alpha}{\tan\phi} \tag{3-3}$$

S_s = specific gravity of rock
α = angle of grade = $\tan^{-1} S_y$
ϕ = angle of repose for dumped rock
SF = safety factor

A safety factor of unity theoretically means that the rock is just on the verge of stability. A typical safety factor for the design of riprap is SF = 1.5.

The angle of repose is an empirical relationship shown in Figure 3-1, and is the measure of the maximum stable angle for a slope without external forces acting on it. It is a function of the median rock diameter d_{50} and rock angularity (i.e., crushed, angular, or very round).

3.3 Stephenson's Method

Stephenson's method was developed for calculating the stability of rock-fill dams in rivers (Stephenson, 1979). One of the main differences between the Stephenson and safety factors methods is that the former considers the stability of the rock layer as a whole but the latter considers the stability of individual rocks. It has been observed empirically that the stability of rock layers is greater than the stability of individual rocks in the layer treated in isolation. Consequently, the Stephenson method generally is less conservative than the safety factor method.

Using the Stephenson method, the rock diameter that would just begin to move under the influence of flowing water has been empirically determined to be:

cut 19

Figure 3-1 Angle of repose for typical rock armor

$$d = \left\{ \frac{qS^{7/6} n^{1/6}}{Cg^{1/2}[(1 - n)(S_s - 1)\cos \alpha(\tan \phi - S_y)]^{5/3}} \right\}^{2/3} \qquad (3\text{-}4)$$

where q = flowrate on the embankment
n = rock space fraction (i.e., porosity)
C = a factor that accounts for the angularity of the rock (determined to range from 0.22 for gravel to 0.27 for crushed granite)
g = acceleration of gravity
S_s = specific gravity of rock
ϕ = angle of repose of the rock

The diameter determined from equation 3-4 is for the "threshold" flowrate, which is the flowrate at which the rock will just start to move. At flowrates just above the threshold, the rock will rearrange to a more stable configuration. At much higher velocities, the structure will collapse. Olivier (1967) reports that the flowrate for collapse is from 120% of threshold flow for gravel to 180% of threshold flow for crushed ledge rock (the computer program ROCKSIZE, presented in Appendix B calculates the diameter for threshold flowrate, not failure).

3.4 Discussion

Both the safety factor and Stephenson methods are presented in terms of a "representative rock diameter <d>", rather than a typical measure such as the median d_{50}. Richardson et al. (1975) report that the representative diameter for riprap is larger than the median. Experimental data on scour of submerged rock armor using rock materials of widely different gradations showed that the larger rocks had a dominant effect on the determination of stability, and therefore should be more heavily weighted in determining the representative rock diameter. The ratio of representative diameter <d> to d_{50} ranged from 1.06 to 2.25 in several experiments performed by Stevens (1971). Richardson et al. (1975) recommend that the riprap be thick enough to permit the loss of fines without uncovering the protected material or filter. The above discussion suggests that the use of d_{50} for the representative diameter in the safety factor and Stephenson methods is probably conservative. The possibility of loss of fines reducing the thickness of the riprap should be borne in mind, however, especially for those cases in which the riprap layers would be constructed from material with a large coefficient of gradation; i.e., with a significant fraction of fines.

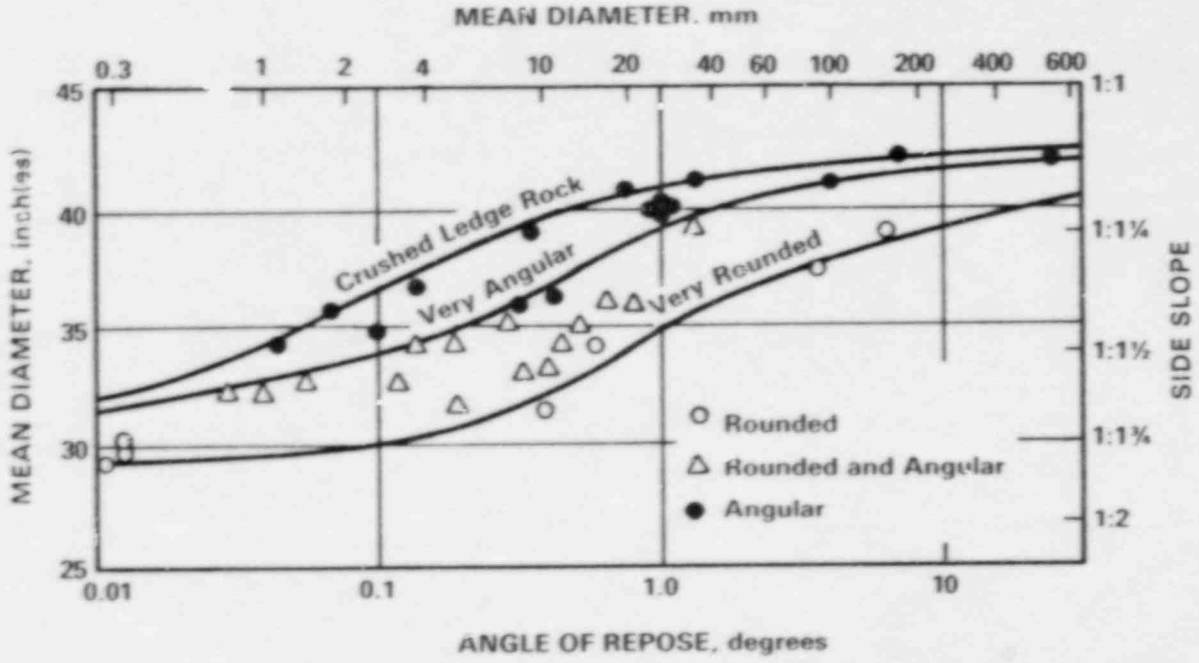
MEAN DIAMETER, mm
0.3
1
2
4
10
20
40
60
100
200
400
600
45
40
35
30
25
MEAN DIAMETER, inches
1:1
1:1¼
1:1½
1:1¾
1:2
SIDE SLOPE
Crushed Ledge Rock
Very Angular
Very Rounded
Rounded
Rounded and Angular
Angular
0.01
0.1
1.0
10
ANGLE OF REPOSE, degrees

The reliability of the safety factor and Stephenson methods to determine the stability of riprap layers is demonstrated using the experimental data collected in the Colorado State University flumes, and presented in Table 3-1. The representative diameters for failure for the safety factor method have been calculated using a safety factor of unity, and the computed stage-discharge relationship (Model 1) for the flowrate at which actual failure was observed. Similarly, the representative diameters are calculated from the Stephenson formula, assuming that the observed flowrate q at failure in equation 3-4 represents 120% of the flowrate for incipient movement. Also presented in Table 3-1 are the rock diameters d_{50}, which would have been chosen using typical design factors. A safety factor of 1.5 was chosen for the safety factor method; a 50% increase in diameter was used in the case of the Stephenson method.

Table 3-1 Modeled and measured flowrates for riprap failure

Slope	d_{50}[(1)], in.	Q_f, $ft^3/sec/ft$	Stage[(2)], ft	Stage[(3)], ft	d[(4)], in.	d[(5)], in.	d[(6)], in.	d[(7)], in.
0.01	1.02	1.5	0.467	0.503	0.75	1.13	0.34	0.51
0.02	1.02	1.1	0.353	0.304	1.06	1.61	0.48	0.72
0.10	1.02	0.36	0.129	-	2.16	3.47	0.90	1.35
0.02	2.2	4.5	0.89	0.74	2.67	4.05	1.21	1.82
0.08	2.2	1.81	0.386	0.338	5.0	7.9	2.12	3.18
0.1	2.2	1.25	0.303	0.259	5.04	8.1	2.02	3.03
0.2	2.2	0.5	0.161	-	6.25	11.0	2.24	3.36
0.2	4.1	1.81	0.355	0.167	14.2	24.9	5.1	7.7
0.2	5.1	3.55	0.543	-	21.7	38.1	8.43	12.6
0.2	6.2	4.43	0.632	-	25.3	44.3	9.8	14.7

(1) Riprap actually used.
(2) Calculated from Model 1.
(3) Measured where available.
(4) Safety factor method, SF = 1.
(5) Safety factor method, SF = 1.5.
(6) Stephenson method for incipient motion (not slope failure).
(7) 1.5 times the Stephenson method for incipient motion.

The water level necessary for the calculations by the safety factor method originated from the stage-discharge rating curves derived from equations 2-14 through 2-16 (Model 1). Measured values of stage are presented where they are available. There is often a significant difference between the predicted and measured stage, since the observed water level over the top of the rock in several of the runs was small. This error may be compounded because the datum for measuring stage is unclear. The computational model defines the datum for "top of rock" as the depth at which the frictional forces for flow through the rock just equal the frictional forces over the top of the rock (see Section 2.2.3). The difference between the measured top of rock and apparent datum is about 30 to 40% of d_{50} for the present data.

The safety factor method proved to be best suited at the lower slope angles (less than 10%), but overestimated the rock size on the steeper slopes. Some

of the rock sizes were underestimated with a safety factor of unity, but a safety factor of 1.5 always produced acceptably conservative results. Some of the rock sizes predicted for the steep slopes were greatly overestimated, however.

The Stephenson method was more suited to steep slopes, and did not overestimate the necessary rock size by as large a margin as did the safety factor method. The Stephenson method seriously underestimated the rock size needed on the gentler slopes, even when the predicted rock size was increased by 50%.

3.5 Example Calculations for Rock Armor

The Stephenson and safety factor methods are formalized into a BASIC language computer program ROCKSIZE, described in Appendix B. The interactive run with this program will be illustrated below.

Assume for the example that an independent geotechnical analysis has determined that the 1/2% inward slope scenario with the local Probable Maximum Precipitation would be the design-basis event. Other properties of the embankment are those given in Table 3-1. Determine the adequacy of the rock to resist the calculated runoff.

The interactive sessions with program ROCKSIZE are shown in Figures 3-2 and 3-3 for the side and top slopes, respectively. The calculations indicate that for the safety factor method on the top slope and the Stephenson method on the side slope (in accordance with the discussion of Section 3.4), the chosen rock sizes would be adequate to protect the embankment.

```
     PROGRAM ROCKSIZE
     DETERMINE THE STABLE DIAMETER FOR RIPRAP ON ARMORED SLOPES
     BY STEPHENSON AND SAFETY FACTOR METHOD
     U.S. NUCLEAR REGULATORY COMMISSION, WASHINGTON D.C.
INPUT FRICTION INDEX, K  ? 4
ENTER DBAR, D84, FT  ? 0.47,0.66
ENTER LAYER THICKNESS, FT  ? 1.5
ENTER SLOPE  ? 0.2
ENTER EFFECTIVE POROSITY  ? 0.35
CORRECTION TO LAYER THICKNESS =  .1915754  FEET
ENTER PEAK RUNOFF, CFS/FT  ? 1.13

STAGE ABOVE ROCK SURFACE =  .3224664  FT
ENTER ANGLE OF REPOSE, DEGREES? 41.5
ENTER SPECIFIC GRAVITY OF ROCK, GM/CC  ? 2.65
ENTER SAFETY FACTOR ? 1.0


STABLE ROCK DIAMETER BY SAFETY FACTOR METHOD =  1.081614  FEET

ENTER SMOOTHNESS FACTOR, C IN STEPHENSON FORMULA
(0.22 FOR SMOOTH ROCK AND 0.27 FOR ANGULAR CRUSHED ROCK)
? 0.27


STABLE ROCK DIAMETER BY STEPHENSON METHOD =  .1993453  FEET
```

Figure 3-2 Sample problem - interactive session for rocksize on side slope with program ROCKSIZE

```
      PROGRAM ROCKSIZE
      DETERMINE THE STABLE DIAMETER FOR RIPRAP ON ARMORED SLOPES
      BY STEPHENSON AND SAFETY FACTOR METHOD
      U.S. NUCLEAR REGULATORY COMMISSION, WASHINGTON D.C.
INPUT FRICTION INDEX, F  ? 4
ENTER DBAR, D84, FT  ? 0.16,0.24
ENTER LAYER THICKNESS, FT  ? 1.0
ENTER SLOPE  ? 0.02
ENTER EFFECTIVE POROSITY  ? 0.35
CORRECTION TO LAYER THICKNESS =  6.942815E-02  FEET
ENTER PEAK RUNOFF, CFS/FT  ? 1.13

STAGE ABOVE ROCK SURFACE =  .4278018  FT
ENTER ANGLE OF REPOSE, DEGREES? 40
ENTER SPECIFIC GRAVITY OF ROCK, GM/CC  ? 2.65
ENTER SAFETY FACTOR ? 1.0


STABLE ROCK DIAMETER BY SAFETY FACTOR METHOD =  .1115765  FEET

ENTER SMOOTHNESS FACTOR, C IN STEPHENSON FORMULA
(0.22 FOR SMOOTH ROCK AND 0.27 FOR ANGULAR CRUSHED ROCK)
? 0.27


STABLE ROCK DIAMETER BY STEPHENSON METHOD =  3.451491E-02  FEET
```

Figure 3-3 Sample problem - interactive session for rock size on top slope with program ROCKSIZE

4 CONCLUSIONS

The design of rock armor for embankments to resist the local Probable Maximum Precipitation (PMP) involves the calculation of runoff and the determination of the properties that help the rock resist movement by the calculated runoff. The staff has developed a set of mathematical models and associated computer programs to calculate runoff from armored embankments. The models take into account the resistance to flow both through and over top of the armor layer. The techniques developed here can be used to study the effects of various designs of the embankments on the runoff caused by intense precipitation. Runoffs calculated from the models are employed with empirical techniques to determine if the embankment slopes will be stable under the design-basis precipitation events.

Some of the conclusions that can be drawn from the experimentation with the runoff models are listed below:

(1) The calculation of runoff must consider the flow both through and over the top of the armor layer, unless the rock is filled with soil or otherwise impervious.

(2) Irregularities in the surface of the embankments may lead to large concentrations of flow along preferential paths; such concentrations of flow would place more severe loads on the rock armor.

(3) The peak runoff from the gentler top slope can be more severe than the peak runoff from the steeper side slope, thereby controlling the design of the armor on both slopes. This condition may occur when the capacity of the rock layer to carry the flow is inadequate, forcing the flow over the top of the rock layer. The most severe hydraulic stresses on the armor are likely to occur at the break between the top and side slopes for this situation.

(4) Design factors that tend to diminish the peak runoff from the top slope include larger rock diameter and thicker layers. Degradation of the rock over the design lifetime of the embankments should be taken into consideration, and the size of the rock should be adjusted accordingly. The effects of flow concentration caused by geotechnical failure can be eliminated almost entirely by having a large thick rock layer.

(5) The characteristic time for runoff on a typical embankment appears to be on the order of minutes. Therefore, short periods of very intense rainfall must be included in the design-basis PMP. For the embankments studied in the present report, periods as short as 2.5 minutes were required.

(6) Friction of flow on armored embankments is expressed adequately by a compound resistance curve, using a square law for flow beneath the surface of the rock layer and a Darcy-Weisbach law for flow that overtops the rock layer.

(7) Flume tests with crushed rock indicate that the safety factor method adequately describes the stability of the rock for slopes of less than 10%. The Stephenson method is suited for slopes greater than 10%.

Several shortcomings of the procedures presented in this report must be mentioned. The peak runoff to which the embankment is likely to be subjected is strongly dependent on the shape of the surface. One of the largest uncertainties in the application of the design principles presented in this report is the prediction of possible future states of the embankment. The scenarios studied in this report for various failure states were offered for illustrative purposes only and are highly speculative. Evidence of failure modes for embankments, other than those caused by hydrologic forces, should be compiled and analyzed. Measures that tend to offset the concentration of flow should be used to reduce the sensitivity of the peak runoff to future, unknown states of embankment shape.

Peak values of runoff were difficult to predict for cases of slumping and combinations of other factors that tend to diminish the capacity for flow within the rock layer. Severe oscillations of flowrate tended to occur for high rates of flow. These oscillations are probably computational artifacts, but real oscillation might occur also. Experimentation with other forms of solutions to the differential equations (such as implicit methods) and sensitivity to parameter values (such as time step and grid spacing) should be pursued.

The future development of model tests to demonstrate the phenomena of flow concentration should be considered. Such experiments could consider the irrigation of a scale model of a typical embankment for various shapes and parameter values. Results of this scale model experiment could serve to validate the mathematical models presented in this report.

5 REFERENCES

Abt, S. R., J. F. Ruff, M. S. Khattak, R. J. Wittler, A. Shaikh, J. D. Nelson, D. W. Lee, and N. E. Hinkle, "Development of Riprap Design Criteria by Riprap Testing in Flumes: Phase 1," NUREG/CR-4651, U.S. Nuclear Regulatory Commission, Washington, D.C., May 1987.

Environmental Protection Agency, Title 40, Code of Federal Regulations, Part 192, Washington, D.C., 1985.

Hey, R. D., "Flow Resistance in Gravel Bed Rivers," J. Hydraulics Division, ASCE, no. HY4 pp. 365-379, 1979.

Leps, T. M., "Flow Through Rockfill," in Embankment Dam Engineer, Casagrande Volume, R. C. Hirshfeld and S. J. Poulos, Editors, John Wiley and Sons, New York, pp. 87-108, 1973.

Morris, E. M., and D. A. Woolhiser, "Unsteady One Dimensional Flow Over a Plane," Water Resources Research, Vol. 16, no. 2; pp. 355-360, 1980.

National Oceanic and Atmospheric Administration, Hydrometeorological Report No. 49, "Probable Maximum Precipitation Estimates, Colorado River and Great Basin Drainages," Silver Spring, Maryland, U.S. Dept. of Commerce, 1977.

Olivier, H., "Through and Overflow Rockfill Dams--New Design Techniques," Proceedings, Institute of Civil Engineers, pp. 433-471, March 1967.

Overton, D. E., and M. E. Meadows, Stormwater Modeling, Academic Press, New York, 1976.

Richardson, E. V., D. B. Simons, S. Krek, K. Mahmood, and M. A. Stevens, "Highways in the River Environment--Hydraulics and Environmental Design Considerations," U.S. Dept. of Transportation, Available from Publications Office, Engineering Research Center, Colorado State University, Fort Collins, Colorado, 1975.

Roache, P. J., Computational Fluid Mechanics, Hermosa Publishers, Albuquerque N.M., 1972.

Sherard, J. L., J. W. Richard, W. Stanley, and A. C. Williams, Earth and Earth Rock Dams, John Wiley and Sons, New York, 1963.

Simons, D. B., and F. Senturk, Sediment Transport Technology, Water Resources Publications, Fort Collins, Colorado, 1977.

Stephenson, D., Rockfill in Hydraulic Engineering, Elsevier, Amsterdam, 1979.

Stevens, M. A., and D. B. Simons, "Stability Analysis for Coarse Granular Material on Slopes," Chapter 17 in River Mechanics, Edited and published by H. W. Shen, P.O. Box 606, Fort Collins, Colorado, 1971.

Wardwell, R. E., J. D. Nelson, S. R. Abt, and W. P. Staub, "Design Considerations for Long-Term Stabilization of Uranium Mill Tailings," in Management of Uranium Mill Tailings, Colorado State University, Fort Collins, Colorado, 1984.

APPENDIX A

USER'S GUIDE FOR SLOPE2D

Program SLOPE2D is a finite-difference computer code that computes the time-dependent runoff along the centerline of an armor-covered embankment according to the mathematical relationships presented in Chapter 2. The embankment consists of four subareas or quadrants, and is assumed to be symmetrical around the centerline, as illustrated in Figure A-1.

Rainfall rates are specified in a tabular fashion. The output of the program is the runoff rate per unit width along the centerline of the embankment at the base of the embankment and also at the break point between the upper and lower slopes. Peak runoff rates may then be used to design suitable rock armor covers.

The program is written in FORTRAN77. It is set up to run on an IBM-compatible personal computer. The program disk contains the source code (file SLOPE2D.FOR) and a compiled version for computers with the 8087 mathematics coprocesser (file SLOPE2D.EXE). A sample data file is also included on the disk (file SAMP.DAT), as well as program ROCKSIZE.BAS, described in Appendix B.

Program SLOPE2D can be used on a mainframe computer with minor revisions. Limitations on speed make the use of program SLOPE2D on a typical personal computer somewhat tedious, making the use of a high-speed microcomputer or mainframe computer desirable.

When run on a personal computer, the default input and output files are the keyboard and screen, respectively. The input file, however is generally a disk file created with a text editor such as EDLIN. The name of the input file is specified at run time using the standard DOS redirection method. For example, if the data were specified in file SAMP.DAT, the execution step would be:

```
SLOPE2D<SAMP.DAT
```

Output from the program is directed to the screen, but can be listed on the printer using the "Control" and "Printscreen" keys on the keyboard.

Data inputs to and outputs from the program are presented below. All data are input in a free format fashion. Individual data points are separated by commas for each line. Decimal points are optional.

Data Inputs

The following data are read by program SLOPE2D:

Line 1	Title line - up to 80 characters for run title
Line 2	Number of entries in rainfall table, NRAIN
Next NRAIN lines	Rainfall table. FR(I) = multiplier for the average 1-hour rainfall rate R8

cut 20

Figure A-1 Four quadrants of armored embankment

TR(I) = time, seconds, at which FR(I) becomes effective

Next line
DX = grid spacing, ft
N1 = effective porosity of riprap
D51 = median rock diameter for top slope, ft
D52 = median rock diameter for side slope, ft
THICK1 = thickness of riprap layer on top slope, ft
THICK2 = thickness of riprap layer on side slope, ft
SX1 = slope in the +x direction for quadrants 1 and 3
SX2 = slope in the +x direction for quadrants 2 and 4
SY1 = slope in the +y direction for quadrants 1 and 2
SY2 = slope in the +y direction for quadrants 3 and 4
A1 = index of the bottommost grid block in quadrants 2 and 4
B1 = index of the rightmost grid block in quadrants 1 and 3

Next line
DT = initial timestep for model, seconds
NT = number of iterations of model
KP = iterations between printouts
TSTART = time in rainfall table corresponding to commencement of simulation, seconds

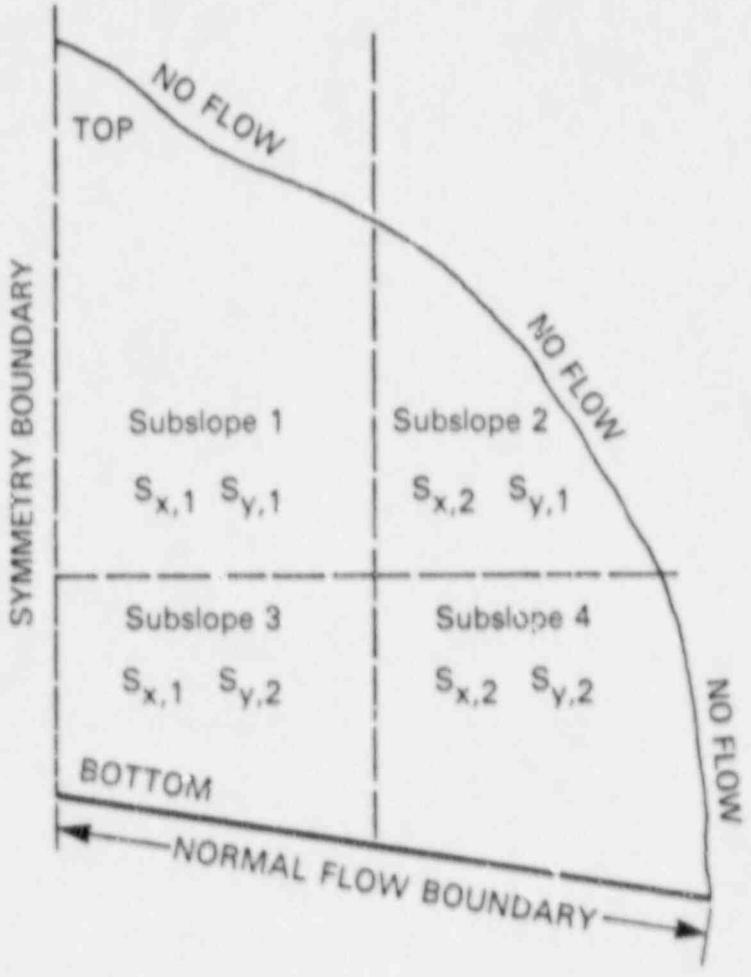
NO FLOW
TOP
NO FLOW
SYMMETRY BOUNDARY
Subslope 1
$S_{x,1}$ $S_{y,1}$
Subslope 2
$S_{x,2}$ $S_{y,1}$
Subslope 3
$S_{x,1}$ $S_{y,2}$
Subslope 4
$S_{x,2}$ $S_{y,2}$
NO FLOW
BOTTOM
NORMAL FLOW BOUNDARY

Next line	TCH = time at which timestep is changed, seconds
	DTCH = new timestep, seconds
Next line	K = roughness index k for riprap, i.e., 1 = smooth marbles
	2 = smooth rock, 4 = angular rock
	R8 = rainfall in 1-hour PMP, inches (typ. 8 in./hr)
	D81 = d_{84} diameter for rock on top slope, ft
	D82 = d_{84} diameter for rock on side slope, ft
Next line	NCOL = number of columns in grid
	NROW = number of rows in grid
Next (NCOL-1) lines	JSTART(I) = topmost grid block for the i^{th} column (greater than or equal to 2)
	JEND(I) = bottommost grid block for the i^{th} column (less than or equal to 40)
Next (NROW-1) lines	ISTART(J) = leftmost grid block for the j^{th} row (greater than or equal to 2)
	IEND(J) = rightmost grid block for the j^{th} row (less than or equal to 35)

Program Outputs

All of the data input to the program are specified at the start of the output listing. The flowrates along the centerline (i.e., x = 0) at the slope break (QBRK) and the bottom of the side slope (QCCENT) are then output as a function of time. Finally, the highest values of QBRK and QCCENT are given.

SETTING UP THE GRID

The embankment is assumed to be symmetrical around the vertical axis, and to be represented by four quadrants. The slope in the x and y directions can be specified in each quadrant, as illustrated in Figure A-1.

The finite difference grid for an embankment in the example is represented by 6 rows and 5 columns. The finite difference grid has cells of dimension DX (ft) on a side. Only the righthand side of the embankment is represented, because of the assumption of symmetry. Column and row indexes start with number 2, as illustrated in Figure A-2; also illustrated is the specification of the downslope and horizontal slope breaks, A-1 and R-1, respectively. The maximum row dimension is 35; the maximum column dimension is 40.

Determining Starting and Ending Times

The object of program SLOPE2D is generally to determine the peak runoff rates from the embankment. The PMP used in the calculations optimizes the rainfall rate so that the most intense rainfall occurs at the end of the first hour. Generally, the runoff from the top slope will peak right after one hour. The peak runoff from the foot of the side slope will peak at a somewhat later time. In order to reduce the computational burden, it is desirable to determine the shortest period that the simulation needs to be run in order to ensure that the peak runoffs will result. For a typical embankment, a starting time of 900 seconds into the PMP lasting until 4000 seconds appears to be adequate to allow maximum buildup of the flow and passage of the flood peaks. Some experimentation may be necessary to ensure that the proper time bounds are chosen.

cut 21

Figure A-2 Finite-difference grid for example problem

Determining Timestep Size

The finite-difference equations are solved by an explicit algorithm. The stability limit for a linear system states that the velocity times the timestep should be less than the spatial distance between grid points. Velocities over or through the riprap are not expected to exceed 3 ft/sec under any likely conditions. For a 20-foot grid spacing, a timestep of DT = 7 seconds would probably satisfy the linear stability criterion. In practice, however, the equations are not linear, especially when the rock is overtopped. For the example problem presented later, a 5-second DT was used for the first 3100 seconds of the PMP. After 3100 seconds, a 2-second DT was found to be suitable for the unfailed slope; a 0.5-second DT was used for the failed scenarios. These timesteps were determined by experimentation. If there is a question about the size of the timestep, a smaller timestep should be chosen and the results should be compared.

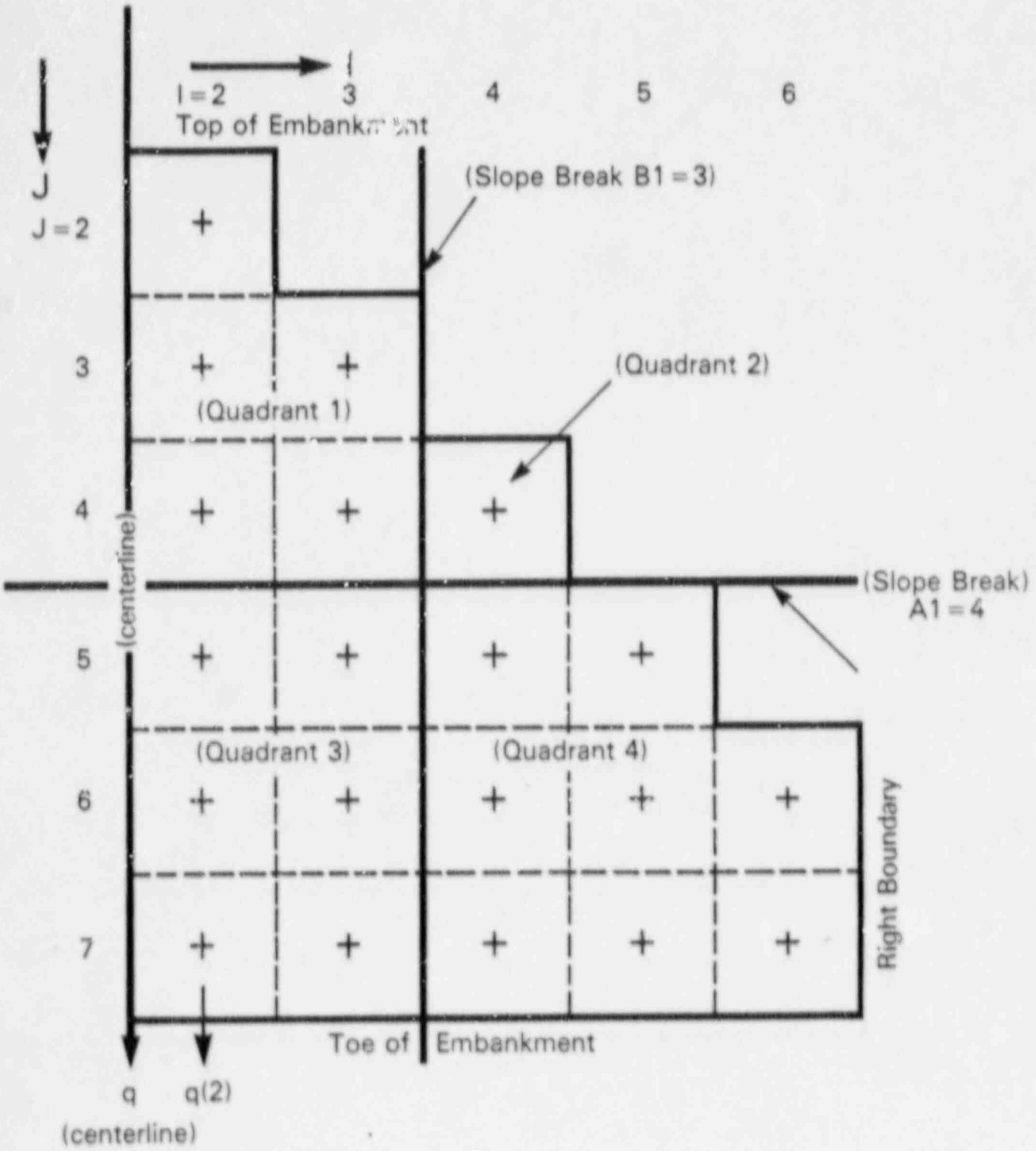
I
I = 2
3
4
5
6
Top of Embankment
J
J = 2
3
4
5
6
7
(Slope Break B1 = 3)
(Quadrant 2)
(Quadrant 1)
(centerline)
(Slope Break)
A1 = 4
(Quadrant 3)
(Quadrant 4)
Right Boundary
Toe of Embankment
q
q(2)
(centerline)

cut 21

SAMPLE PROBLEMS

Consider the triangular embankment as illustrated in Figure 2-14a. The upper section is 440 feet long, has a 2% grade, and is covered with a 1-foot-thick layer of riprap, consisting of crushed rock. The side slope is 260 feet long, has a 20% grade, and is covered by a 1.5-foot-thick layer of riprap, also of crushed rock. The effective porosity of the rock is estimated to be 0.35. The gradations for the rocks are given in Figure A-3. Calculate the peak runoff at the bottom of the top slope and the bottom of the side slope for the case of an unfailed embankment and the design-basis PMP. Repeat the calculations for the case of a uniform slump of 1/2% toward the centerline, and the case of a 200-foot-wide trench in an otherwise unfailed embankment, with a slump of 1%.

cut 22

Figure A-3 Gradation of rock armor for example problem

Benchmark Embankment

The grid size DX was chosen to be 20 feet. The downhill slope break occurs at A1 = 22. The horizontal slope break is immaterial in this case, but is set at B1 = 6.

The rainfall table has 14 lines (NRAIN = 14) and is based on the design-basis PMP presented in Table 2-6. The 1-hour PMP of 8 inches (R8 = 8) is assumed.

A friction index of k = 4 is chosen because the riprap is crushed rock, and therefore angular. The slopes SX1 and SX2 are zero for the benchmark slope. The slopes in the downhill direction are SY1 = 0.02 and SY2 = 0.2. The d_{84}

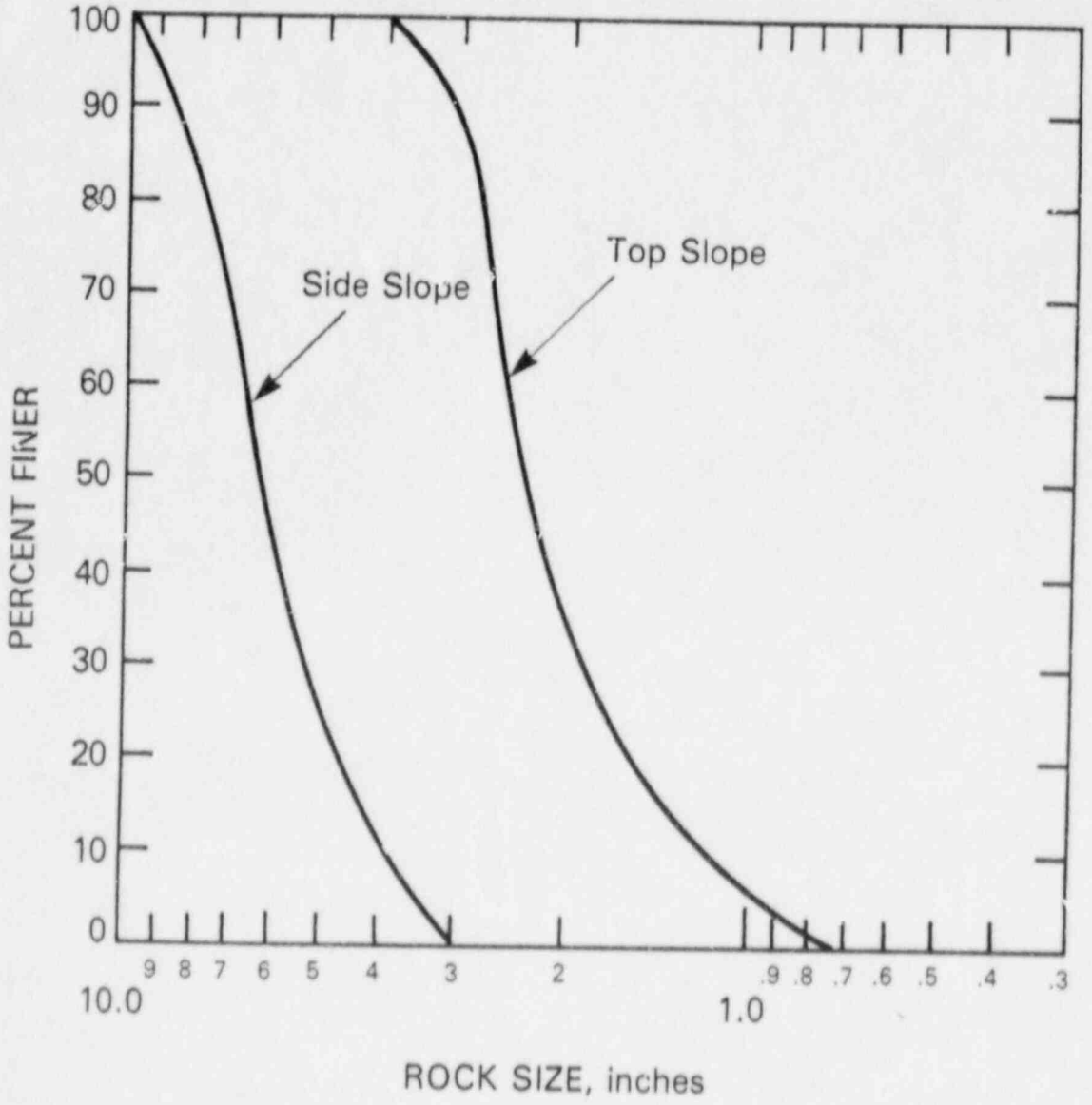
100
90
80
70
60
50
40
30
20
10
0
PERCENT FINER
Side Slope
Top Slope
9 8 7 6 5 4 3 2
10.0
.9 .8 .7 .6 .5 .4 .3
1.0
ROCK SIZE, inches

cut 22

rock diameters are read directly from the gradation curves presented in Figure A-3 to be 0.24 and 0.66 foot for the top and side slopes, respectively. The characteristic rock diameter <d> is represented by the harmonic mean d_h, as calculated by equation 2-8. The calculations for the harmonic mean are given in Table A-1. The harmonic means are 0.16 and 0.47 foot for the top and side slopes, respectively.

Table A-1 Calculation of harmonic mean rock diameters

Percentile range	d, in. (large rock)	1/d	d, in. (small rock)	1/d
90 - 100	9	0.111	3.3	0.303
80 - 90	8	0.125	2.9	0.345
70 - 80	7.2	0.139	2.7	0.37
60 - 70	6.6	0.152	2.5	0.4
50 - 60	6.2	0.161	2.3	0.435
40 - 50	6.0	0.167	2.1	0.476
30 - 40	5.6	0.179	1.95	0.513
20 - 30	5.0	0.2	1.7	0.588
10 - 20	4.2	0.238	1.5	0.667
0 - 10	3.4	0.294	0.99	1.01
Harmonic mean		5.66		1.96

The calculation commences at TSTART = 900 seconds into the PMP. An initial timestep of DT = 2.0 seconds is chosen, but is switched to DTCH = 0.5 second after TCH = 3100 seconds into the PMP. A total of NT = 4000 steps is used to cover the occurrence of the peak flows from the two slopes. A print interval of KP = 20 is chosen.

The input file is illustrated in Figure A-4. The output for the run is illustrated in Figure A-5. The peak runoff rates for the unfailed embankment are 0.27 and 0.31 $ft^3/sec/ft$ for the top and side slope, respectively. Results for this case are also plotted in Figure 2-18a.

1/2% Slump

The input file for this run differs from the benchmark embankment example because the horizontal slopes must now be specified as SX1 and SX2 = -.005. The horizontal breakpoint for the slope is immaterial for this case (as well as for the benchmark case), but is set to B1 = 6. The timestep DTCH = 0.5 second becomes effective at TCH = 3100 seconds. The revised input file is shown in Figure A-5(b) with the changes highlighted. The peak flows for this case were computed to be 0.81 $ft^3/sec/ft$ from the top slope and 0.44 $ft^3/sec/ft$ from the side slope. Results for this case are also plotted in Figure 2-17.

(a) Benchmark embankment

```
BENCHMARK CASE 2/27/87
14
-100,0.0
0,.22
1800,.6
2700,1.43
3000,2.05
3300,3.25
3450,7.55
3600,1.06
3750,.445
3900,.286
4200,.2
4500,.084
5400,.0308
7200,0
20,.35,.16,.43,1,1.5,0,0,0.02,0.2,22,22
2,4000,20,900
3100,0.5
4,8,.24,.66
31,36
2,36
2,36
3,36
4,36
6,36
7,36
8,36
9,36
11,36
12,36
13,36
14,36
15,36
17,36
18,36
19,36
20,36
21,36
23,36
24,36
25,36
26,36
27,36
29,36
30,36
31,36
32,36
33,36
```

Figure A-4 Inputs to computer program SLOPE2D

```
34,36
35,36
2,3
2,4
2,5
2,5
2,6
2,7
2,8
2,9
2,9
2,10
2,11
2,12
2,13
2,14
2,14
2,15
2,16
2,17
2,18
2,19
2,20
2,20
2,21
2,22
2,23
2,24
2,25
2,25
2,26
2,27
2,28
2,29
2,30
2,31
2,31
```

(b) Changes for 1/2% slump (in box)

```
   0.005 inward slump case 2/27/87
14
-100,0.0
0,.22
1800,.6
2700,1.43
3000,2.05
3300,3.25
3450,7.55
3600,1.06
3750,.445
```

Figure A-4 (Continued)

```
3900,.286
4200,.2
4500,.084
5400,.0308
7200,0
```

```
20,.35,.16,.43,1,1.5,-.005,-.005,.02,.2,22,22
```

```
2,4000,20,900
3100,0.5
4,8,.24,.66
31,36
2,36
```

(c) Changes for trench case (in box)

```
 200 FT WIDE 1% TRENCH SECENARIO
14
-100,0.0
0,.22
1800,.6
2700,1.43
3000,2.05
3300,3.25
3450,7.55
3600,1.06
3750,.445
3900,.286
4200,.2
4500,.084
5400,.0308
7200,0
```

```
20,.35,.16,.43,1,1.5,-.01,0,.02,.2,22,6
```

```
2,4000,20,900
3100,0.5
4,8,.24,.66
31,36
2,36
```

Figure A-4 (Continued)

(a) Benchmark case

```
PROGRAM SLOPE2D - RUNOFF FROM SLOPES
BENCHMARK CASE 2/27/87
GRID SIZE, DX =        20.0  FEET
EFFECTIVE POROSITY, N1 =        .350
D50 ROCK DIAMETER ON TOP, D51 =       .1600  FEET
D50 ROCK DIAMETER ON SIDE SLOPE, D52 =       .4300 FEET
THICKNESS OF TOP LAYER, THICK1 =        1.00  FEET
THICKNESS OF SIDE LAYER, THICK2 =        1.50  FEET
Y SLOPE ON TOP, SY1 =        .020
Y SLOPE ON SIDE, SY2 =        .200
X SLOPE ON TOP, SX1 =        .000
X SLOPE ON SIDE, SX2 =        .000
POSITION OF SLOPE BREAK DOWN SLOPE, A1 =         22
POSITION OF SLOPE BREAK IN Y DIRECTION, B1 =          22
DT =        2.00  SECONDS
NUMBER OF STEPS, NT =        4000
PRINT INTERVAL KP =          20
TIME AT WHICH COMPUTATIONS COMMENCE, TSTART =      900.00  SECONDS
TIME AT WHICH TIMESTEP CHANGES, TCH =     3100.0  SECONDS
NEW TIMESTEP, DTCH =        .500 SECONDS
FRICTION FACTOR INDEX, K =         4.0
1 HOUR RAINFALL AMOUNT, R8 =        8.00  INCHES
D84 DIAMETER FOR TOP SLOPE, D81 =        .240  FEET
D84 DIAMETER FOR SIDE SLOPE, D82 =        .660  FEET

TIME-SECONDS        QCCENT - CFS/FT          QBREAK - CFS/FT
 940.00                  .0012                    .0006
 980.00                  .0026                    .0009
1020.00                  .0039                    .0011
1060.00                  .0053                    .0014
1100.00                  .0066                    .0016
1140.00                  .0080                    .0018
1180.00                  .0093                    .0021
1220.00                  .0106                    .0023
1260.00                  .0117                    .0026
1300.00                  .0124                    .0028

(Output from 1340 to 3300 deleted from this listing)

3300.00                  .1385                    .0568
3310.00                  .1416                    .0585
3320.00                  .1446                    .0600
3330.00                  .1477                    .0614
3340.00                  .1506                    .0627
3350.00                  .1536                    .0639
3360.00                  .1564                    .0650
3370.00                  .1592                    .0661
3380.00                  .1619                    .0671
```

Figure A-5 Outputs from computer program SLOPE2D

```
      3390.00                .1646                .0681
      3400.00                .1672                .0691
      3410.00                .1698                .0702
      3420.00                .1723                .0712
      3430.00                .1748                .0722
      3440.00                .1772                .0732
      3450.00                .1797                .0742
      3460.00                .1684                .0792
      3470.00                .1974                .0836
      3480.00                .2064                .0876
      3490.00                .2154                .0912
      3500.00                .2244                .0948
      3510.00                .2334                .0986
      3520.00                .2424                .1033
      3530.00                .2514                .1090
      3540.00                .2604                .1157
      3550.00                .2694                .1296
      3560.00                .2784                .1515
      3570.00                .2874                .1778
      3580.00                .2963                .2052
      3590.00                .3052                .2328
      3600.00                .3141                .2576
      3610.00                .3133                .2686
      3620.00                .3121                .2715
      3630.00                .3107                .2686
      3640.00                .3093                .2618
      3650.00                .3078                .2527
      3660.00                .3061                .2418
      3670.00                .3044                .2303
      3680.00                .3025                .2188
      3690.00                .3005                .2076
      3700.00                .2983                .1972
      3710.00                .2960                .1877
      3720.00                .2936                .1797
      3730.00                .2910                .1728
      3740.00                .2883                .1666
      3750.00                .2854                .1608
      3760.00                .2816                .1548
      3770.00                .2775                .1489
      3780.00                .2734                .1433
      3790.00                .2693                .1378
      3800.00                .2652                .1325

      (Output from t = 3800 to 4500 deleted from this listing)

      4500.00                .0848                .0667
      4510.00                .0841                .0664
      4520.00                .0836                .0662
      4530.00                .0831                .0659
      4540.00                .0826                .0657
      4550.00                .0822                .0654
MAX FLOW AT BASE = .314494 CFS/FT
MAX FLOW, TOP SLOPE = .271536 CFS/FT
```

Figure A-5 (Continued)

(b) 1/2% inward slump case

```
     PROGRAM SLOPE2D - RUNOFF FROM SLOPES
0.005 inward slump case 2/27/87
     GRID SIZE, DX =        20.0  FEET
     EFFECTIVE POROSITY, N1 =        .350
     D50 ROCK DIAMETER ON TOP, D51 =       .1600  FEET
     D50 ROCK DIAMETER ON SIDE SLOPE, D52 =       .4300 FEET
     THICKNESS OF TOP LAYER, THICK1 =         1.00  FEET
     THICKNESS OF SIDE LAYER, THICK2 =        1.50  FEET
     Y SLOPE ON TOP, SY1 =        .020
     Y SLOPE ON SIDE, SY2 =        .200
     X SLOPE ON TOP, SX1 =       -.005
     X SLOPE ON SIDE, SX2 =       -.005
     POSITION OF SLOPE BREAK DOWN SLOPE, A1 =          22
     POSITION OF SLOPE BREAK IN Y DIRECTION, B1 =           22
     DT =        2.00  SECONDS
     NUMBER OF STEPS, NT =        4000
     PRINT INTERVAL KP =          20
     TIME AT WHICH COMPUTATIONS COMMENCE, TSTART =      900.00  SECONDS
     TIME AT WHICH TIMESTEP CHANGES, TCH =     3100.0  SECONDS
     NEW TIMESTEP, DTCH =        .500 SECONDS
     FRICTION FACTOR INDEX, K =         4.0
     1 HOUR RAINFALL AMOUNT, R8 =        8.00  INCHES
     D84 DIAMETER FOR TOP SLOPE, D81 =        .240  FEET
     D84 DIAMETER FOR SIDE SLOPE, D82 =        .660  FEET

     TIME-SECONDS         QCCENT - CFS/FT          QBREAK - CFS/FT
      940.00                    .0012                    .0006
      980.00                    .0027                    .0009
     1020.00                    .0042                    .0012
     1060.00                    .0058                    .0015
     1100.00                    .0074                    .0019
     1140.00                    .0091                    .0022
     1180.00                    .0109                    .0026
     1220.00                    .0126                    .0030
     1260.00                    .0141                    .0035
     1300.00                    .0151                    .0039

     (Output from t = 1310 to 3400 deleted from this listing)

     3400.00                    .2081                    .1047
     3410.00                    .2110                    .1090
     3420.00                    .2138                    .1125
     3430.00                    .2166                    .1182
     3440.00                    .2194                    .1263
     3450.00                    .2222                    .1372
     3460.00                    .2312                    .1564
     3470.00                    .2406                    .1804
     3480.00                    .2499                    .2090
```

Figure A-5 (Continued)

```
        3490.00                 .2593                   .2452
        3500.00                 .2688                   .2856
        3510.00                 .2782                   .3243
        3520.00                 .2877                   .3406
        3530.00                 .2973                   .5173
        3540.00                 .3068                   .6731
        3550.00                 .3164                   .7919
        3560.00                 .3260                   .7997
        3570.00                 .3356                   .7325
        3580.00                 .3451                   .6774
        3590.00                 .3547                   .6355
        3600.00                 .3643                   .6556
        3610.00                 .3643                   .6580
        3620.00                 .3638                   .6829
        3630.00                 .3632                   .6924
        3640.00                 .3625                   .6438
        3650.00                 .3618                   .5758
        3660.00                 .3611                   .5317
        3670.00                 .3603                   .5063
        3680.00                 .3596                   .4856
        3690.00                 .3589                   .4614
        3700.00                 .3583                   .4347
        3710.00                 .3579                   .4112
        3720.00                 .3578                   .3916
        3730.00                 .3580                   .3773
        3740.00                 .3587                   .3650
        3750.00                 .3600                   .3537
        3760.00                 .3610                   .3389
        3770.00                 .3629                   .3248
        3780.00                 .3656                   .3498
        3790.00                 .3693                   .3455
        3800.00                 .3739                   .3416

        (Output from t = 3810 to 4500 deleted from this listing)

        4500.00                 .1602                   .1111
        4510.00                 .1587                   .1105
        4520.00                 .1573                   .1098
        4530.00                 .1559                   .1091
        4540.00                 .1545                   .1084
        4550.00                 .1531                   .1077
MAX FLOW AT BASE = .443591 CFS/FT
MAX FLOW, TOP SLOPE = .811763 CFS/FT
```

(c) 200-ft-wide, 1% inward slump trench

```
     PROGRAM SLOPE2D - RUNOFF FROM SLOPES
200 FT WIDE 1% TRENCH SECENARIO
     GRID SIZE, DX =       20.0  FEET
     EFFECTIVE POROSITY, N1 =       .350
```

Figure A-5 (Continued)

```
D50 ROCK DIAMETER ON TOP, D51 =       .1600  FEET
D50 ROCK DIAMETER ON SIDE SLOPE, D52 =       .4300 FEET
THICKNESS OF TOP LAYER, THICK1 =       1.00  FEET
THICKNESS OF SIDE LAYER, THICK2 =       1.50  FEET
Y SLOPE ON TOP, SY1 =       .020
Y SLOPE ON SIDE, SY2 =       .200
X SLOPE ON TOP, SX1 =      -.010
X SLOPE ON SIDE, SX2 =       .000
POSITION OF SLOPE BREAK DOWN SLOPE, A1 =        22
POSITION OF SLOPE BREAK IN Y DIRECTION, B1 =         6
DT =       2.00  SECONDS
NUMBER OF STEPS, NT =       4000
PRINT INTERVAL KP =         20
TIME AT WHICH COMPUTATIONS COMMENCE, TSTART =     900.00  SECONDS
TIME AT WHICH TIMESTEP CHANGES, TCH =     3100.0  SECONDS
NEW TIMESTEP, DTCH =       .500 SECONDS
FRICTION FACTOR INDEX, K =        4.0
1 HOUR RAINFALL AMOUNT, R8 =       8.00  INCHES
D84 DIAMETER FOR TOP SLOPE, D81 =       .240  FEET
D84 DIAMETER FOR SIDE SLOPE, D82 =       .660  FEET

TIME-SECONDS        QCCENT - CFS/FT          QBREAK - CFS/FT
 940.00                  .0013                    .0006
 980.00                  .0028                    .0010
1020.00                  .0045                    .0013
1060.00                  .0063                    .0017
1100.00                  .0082                    .0021
1140.00                  .0103                    .0026
1180.00                  .0125                    .0031
1220.00                  .0148                    .0038
1260.00                  .0168                    .0044
1300.00                  .0182                    .0052

(Output from t = 1340 to 3500 deleted from this listing)

3500.00                  .3067                    .5972
3510.00                  .3167                    .8466
3520.00                  .3267                    .9511
3530.00                  .3368                    .8940
3540.00                  .3471                    .7883
3550.00                  .3575                    .7445
3560.00                  .3680                    .9106
3570.00                  .3787                   1.0941
3580.00                  .3895                   1.2325
3590.00                  .4004                   1.0154
3500.00                  .4116                    .9212
3610.00                  .4133                   1.3787
3620.00                  .4147                   1.0800
3630.00                  .4163                    .7665
```

Figure A-5 (Continued)

```
3640.00                .4179                1.0779
3650.00                .4197                1.0749
3660.00                .4216                 .8026
3670.00                .4238                 .7534
3680.00                .4265                 .8000
3690.00                .4299                 .7712
3700.00                .4344                 .7093
3710.00                .4402                 .6794
3720.00                .4475                 .6482
3730.00                .4560                 .6159
3740.00                .4656                 .5904
3750.00                .4759                 .5707
3760.00                .4855                 .5472
3770.00                .4947                 .5239
3780.00                .5033                 .5010
3790.00                .5107                 .4789
3800.00                .5169                 .4578

(Output from t = 3810 to 4500 deleted from this listing)

4500.00                .2155                 .1387
4510.00                .2135                 .1379
4520.00                .2115                 .1369
4530.00                .2094                 .1359
4540.00                .2074                 .1348
4550.00                .2054                 .1335

MAX FLOW AT BASE = .526569 CFS/FT
MAX FLOW, TOP SLOPE = 1.41945 CFS/FT
```

Figure A-5 (Continued)

Trench Failure

The input file for this case differs from the benchmark embankment example in that the horizontal slope for the first and third quadrant must now be specified as SX1 = 0.01, and the horizontal breakpoint must be set to B1 = 6 to represent the width of the failed trench. Timesteps are as in the 1/2% slump example above. The revised input file is shown in Figure A-5c with the changes highlighted. The peak flows for this case were computed to be 1.42 ft^3/sec/ft from the top slope and 0.53 ft^3/sec/ft from the side slope. An oscillation of the flowrate from the top slope is evident. It is not known whether this is a real phenomenon or a computational artifact. If the latter is the case, the peak flow from the top slope would be considerably smaller, representing a time-averaged value.

A listing of program SLOPE2D is given in Figure A-6.

```
      PROGRAM SLOPE2D
C     USNRC 12/12/86 SLOPE2DI FORTRAN VERSION
C     R CODELL
C     2D RUNOFF FROM SLOPES
C
C       INPUT VARIABLES
CXXXXXXXXXXXXXXXXXXXXXXXXXXXXXXXXXXXXXXXXXXXXXXXXXXXXXX
C       DX = GRID SPACING, FT
C       N1 = EFFECTIVE POROSITY OF ROCK LAYERS
C       D51 = D50 FOR TOP SLOPE, FT
C       D52 = D50 FOR SIDE SLOPE, FT
C       THICK1 = THICKNESS OF TOP SLOPE ROCK
C       THICK2 = THICKNESS OF SIDE SLOPE ROCK, FT
C       SX1 = X SLOPE ON TOP
C       SX2 = X SLOPE ON SIDE
C       SY1 = Y SLOPE ON TOP
C       SY2 = Y SLOPE ON SIDE
C       A1 = POSITON OF BREAK IN SLOPE DOWN THE HILL
C       B1 = POSITION OF BREAK ACROSS HILL
C       DT = INITIAL TIME STEP, SECONDS
C       NT = TOTAL NUMBER OF TIME STEPS
C       KP = NO. OF STEPS BETWEEN PRINTS OR PLOT POINTS
C       TR = TIME ORDINATE FOR RAINFALL TABLE, SECONDS
C       FR = FRACTION OF 1 HOUR PMP FOR RAINFALL TABLE
C       TSTART = STARTING TIME FOR SIMULATION, SECONDS
C       TCH = TIME AT WHICH SMALLER TIMESTEP BECOMES EFFECTIVE, SECONDS
C       DTCH = SMALLER TIMESTEP, SECONDS
C       K = FRICTIONAL INDEX FOR ROCK, E.G., 1 FOR SMOOTH ROCK,
C       2 FOR ROUNDED, 4 FOR ANGULAR
C       R8 = RAINFALL AMOUNT IN 1 HOUR PMP, INCHES
C       D81 = D84 ROCK DIAMETER FOR TOP SLOPE, FEET
C       D82 = D84 ROCK DIAMETER FOR SIDE SLOPE, FEET
C       NCOL = NUMBER OF COLUMNS
C       NROW = NUMBER OF ROWS
C       ISTART = LEFT GRID BLOCK IN A ROW
C       IEND = RIGHT GRID BLOCK IN A ROW
C       JSTART = TOP GRID BLOCK IN A COLUMN
C       JEND = BOTTOM GRID BLOCK IN A COLUMN
C
C               OUTPUT VARIABLES
CXXXXXXXXXXXXXXXXXXXXXXXXXXXXXXXXXXXXXXXXXXXXXXXXXXXXXX
C  QBRK = FLOWRATE AT SLOPE BREAK ALOMG CENTERLINE, CFS/FT
C  QCCENT = FLOWRATE AT BOTTOM OF SIDE SLOPE ALONG CENTERLINE
         INTEGER   A1,B1
       COMMON HY(40),D50(40),SX(35),SY(40),FR(20),TR(20),H(40),
     1 D8(40),N1,K,T9,ITIME,R8,R,DT,DX,D52,SY2,CON1,
     2 CON2,CON3,CON4,CON5,A1,D51,THICK1,D81,SY1,D82,
     3 THICK2,NROW,NCOL,B1,SX1,SX2,YBAR,KFAC
       DIMENSION SE(35,40),SEP(35,40),U(35,40),UP(35,40),
     1 V(35,40),VP(35,40),ISTART(40),IEND(40),JSTART(40),
     2 QC(40),JEND(40),QST(500),QSTB(500),TST(500)
       REAL N1,K,KFAC,KF2
       CHARACTER*80 TITLE
```

Figure A-6 Listing of program SLOPE2D

```
      CHARACTER*15 PTIT
      READ(5,'(A)') TITLE
      WRITE(6,111) TITLE
111   FORMAT(10X  ,'PROGRAM SLOPE2D - RUNOFF FROM SLOPES',/
     1 5X,A)
C
C     READ IN THE RAINFALL TABLE
C
      READ(5,*) NRAIN
      do 1 i=1,nrain
    1 READ(5,*) TR(I),FR(I)
      READ(5,*) DX,N1,D51,D52,THICK1,THICK2,SX1,SX2,SY1,SY2,A1,B1
      WRITE(6,99) DX,N1,D51,D52
99    FORMAT(10X,'GRID SIZE, DX = ',F10.1,'  FEET'/
     1 10X,'EFFECTIVE POROSITY, N1 = ',F10.3,/
     2 10X,'D50 ROCK DIAMETER ON TOP, D51 = ',F10.4, '  FEET',/
     3 10X,'D50 ROCK DIAMETER ON SIDE SLOPE, D52 = ',F10.4,
     4 ' FEET')
      WRITE(6,100) THICK1,THICK2
100   FORMAT(10X,'THICKNESS OF TOP LAYER, THICK1 = ',
     1 F10.2,'  FEET',/10X,'THICKNESS OF SIDE LAYER, THICK2 = ',
     1 F10.2,'  FEET')
      WRITE(6,101) SY1,SY2,SX1,SX2
      WRITE(6,106) A1,B1
106   FORMAT(10X,'POSITION OF SLOPE BREAK DOWN SLOPE, A1 ='
     1 ,I10,/10X,
     2 'POSITION OF SLOPE BREAK IN Y DIRECTION, B1 = ',I10)
101   FORMAT(10X,'Y SLOPE ON TOP, SY1 = ',F10.3,/
     1 10X,'Y SLOPE ON SIDE, SY2 = ',F10.3,/
     2 10X, 'X SLOPE ON TOP, SX1 = ',F10.3,/
     3 10X,'X SLOPE ON SIDE, SX2 = ',F10.3)
      READ(5,*) DT,NT,KP,TSTART
      WRITE (6 ,102) DT,NT,KP,TSTART
102   FORMAT(10X,'DT = ',F10.2,'  SECONDS',/10X,
     1 'NUMBER OF STEPS, NT = ',I10,/
     1 10X,'PRINT INTERVAL KP = ', I10,/
     2 10X,'TIME AT WHICH COMPUTATIONS COMMENCE, TSTART = ',
     3 F10.2,'  SECONDS')
      READ(5,*) TCH,DTCH
      WRITE(6,103) TCH,DTCH
103   FORMAT(10X,'TIME AT WHICH TIMESTEP CHANGES, TCH = ',
     1 F10.1,'  SECONDS',/10X,'NEW TIMESTEP, DTCH = ',
     2 F10.3,' SECONDS')
      KTCH=0
      READ(5,*)  K,R8,D81,D82
      WRITE(6,104) K,R8,D81,D82
104   FORMAT(10X,'FRICTION FACTOR INDEX, K = ',F10.1,/
     1 10X,'1 HOUR RAINFALL AMOUNT, R8 = ',F10.2,'  INCHES',/
     2 10X,'D84 DIAMETER FOR TOP SLOPE, D81 = ',F10.3,'  FEET',/
     3 10X,'D84 DIAMETER FOR SIDE SLOPE, D82 = ',F10.3, '  FEET',/
     4 )
```

Figure A-6 (Continued)

```
C      INPUT GRID DEFINITION
C
       READ(5,*) NCOL,NROW
       DO 3 I=2,NCOL
     3 READ(5,*) JSTART(I),JEND(I)
       DO 4 J=2,NROW
     4 READ(5,*) ISTART(J),IEND(J)
       R8=R8/(3600*12)
       CALL SETUP
       CALL SETCON
                 data kk,npl,kkk/3*0/
                 data qmax,qbrmax/2*0.0/
        itime=0
        r=0
C       INITIALIZE GRID
       DO 5 I=1,NCOL
       DO 5 J=1,NROW
       SE(I,J)=0
       SEP(I,J)=0
       U(I,J)=0
       V(I,J)=0
       UP(I,J)=0
       VP(I,J)=0
     5 CONTINUE
C
C      BEGIN NUMERICAL SOLUTION
C
       T9=TSTART
         R=0
       WRITE(6,6)
     6 FORMAT(10X,'TIME-SECONDS',8X, 'QCCENT - CFS/FT',8X,
      1 'QBREAK - CFS/FT')
         DO 77 LO=1,NT
       IF (T9.LT.TCH) GOTO 800
       IF(KTCH.EQ.1) GOTO 800
       KTCH=1
       DT=DTCH
       CALL SETCON
   800 CONTINUE
C        GET RAINFALL RATE ONTO SLOPE
       CALL RAIN
C      GET START AND FINISH OF EACH COLUMN VECTOR
       DO 7 I=2,NCOL
          IM1=I-1
          IP1=I+1
       JS=JSTART(I)
       JE=JEND(I)
C      CALCULATE SEP AT EACH WET POINT
       DO 8 J=JS,JE-1
          JM1=J-1
```

Figure A-6 (Continued)

```
      DIFX=(SE(IM1,J)+SE(I,J))*U(IM1,J)-(SE(IP1,J)+SE(I,J))*U(I,J)
      DIFY=(SE(I,JM1)+SE(I,J))*V(I,JM1)-(SE(I,J+1)+SE(I,J))*V(I,J)
      SEP(I,J)=SE(I,J)+R*CON2+CON1*(DIFX+DIFY)
    8 CONTINUE
    7 CONTINUE
C       NORMAL FLOW BOUNDARY CONDITION AT COLUMN BOTTOMS
        DO 9 I=2,NCOL
         IM1=I-1
         IP1=I+1
      JE=JEND(I)
      QC(I)=0
      KFAC=1
      YBAR=SE(I,JE)
      J=JE
C       CHANGE FLOW RESISTANCE WHEN ROCK TOP OVERFLOWS
      IF (YBAR.GT.H(JE))  CALL SKFAC(J)
      IF(SE(I,JE).GT.0) QC(I)=SE(I,JE)*SQRT(CON5/KFAC)
      DIFX=(SE(IM1,JE)+SE(I,JE))*U(IM1,JE)-(SE(IP1,JE)+SE(I,JE))*U(I,JE)
      DIFY=(SE(I,JE-1)+SE(I,JE))*V(I,JE-1)
      SEP(I,JE)=SE(I,JE)+R*CON2+CON1*(DIFX+DIFY)-QC(I)*CON3
    9 CONTINUE
C       CALCULATE VELOCITY
        DO 10 I=2,NCOL
      im1=i-1
      JS=JSTART(I)
      JE=JEND(I)
        DO 11 J=JS,JE-1
         JM1=J-1
         JP1=J+1
      UBRBR=(U(I,JP1)+U(I,J)+U(IM1,J)+U(IM1,JM1))/4
      VABS=V(I,J)**2+UBRBR**2
      KF2=1
      KFAC=1
      YBAR=(SEP(I,J)+SEP(I,JP1))/2
      IF(YBAR.GT.H(J)) CALL SKFAC(J)
      Y1=SEP(I,J)
C       CALCULATE VIRTUAL DEPTH
      IF(Y1.GT.HY(J).AND.KFAC.LT.1) Y1=HY(J)+(Y1-HY(J))*N1
      Y2=SEP(I,JP1)
      IF(Y2.GT.HY(JP1).AND.KFAC.LT.1) Y2=HY(JP1)+(Y2-HY(JP1))*N1
      IF (VABS.GT.0.0)  KF2=SQRT(1+UBRBR**2/VABS)*KFAC
      ARG=SY(J)-(Y2-Y1)/DX
      VP(I,J)=SQRT(CON4/KF2*D50(J)*ABS(ARG))*SIGN(1.0,ARG)
   11 CONTINUE
      VP(I,JE)=VP(I,JE-1)
   10 CONTINUE
      DO 12 J=2,NROW
         jm1=j-1
         jp1=j+1
      VP(1,J)=VP(2,J)
C       GET START AND FINISH OF EACH ROW VECTOR
      IS=ISTART(J)
      IE=IEND(J)
```

Figure A-6 (Continued)

```
      DO 13 I=IS,IE-1
               IP1=I+1
         IM1=I-1
      KFAC=1
      YBAR=(SEP(I,J)+SEP(IP1,J))/2
C       REDUCE FRICTION IF OVERTOPPING OCCURS
      IF (YBAR.GT.H(J)) CALL SKFAC(J)
C       CALCULATE VIRTUAL DEPTH
      Y3=SEP(I,J)
      IF(Y3.GT.HY(J).AND.KFAC.LT.1.0)  Y3=HY(J)+(Y3-HY(J))*N1
      Y4=SEP(IP1,J)
      IF(Y4.GT.HY(J).AND.KFAC.LT.1.0)  Y4=HY(J)+(Y4-HY(J))*N1
      ARG=SX(I)-(Y4-Y3)/DX
        vbrbr=(vp(i,j)+vp(ip1,j)+vp(i,jm1)+vp(im1,jm1))/4
        vab=sqrt(vbrbr**2+u(i,j)**2)
        up(i,j)=arg*con4/kfac*d50(j)/vab
   13 continue
   12 continue
        do 14 i=1,ncol
        do 15 j=1 ,nrow
        u(i,j)=up(i,j)
        SE(I,J)=SEP(I,J)
        V(I,J)=VP(I,J)
   15 CONTINUE
   14 CONTINUE
        T9=T9+DT
C       FLOWRATE AT BREAK BETWEEN TOP AND SIDE SLOPE
        QBRK=(.5625*(SE(2,A1)+SE(2,A1+1)) -.0625*(SE(3,A1)+
     1   SE(3,A1+1)))*(1.125*V(2,A1)-.125* V(3,A1))
        QCCENT=1.125*QC(2)-.125*QC(3)
        IF(QMAX.LT.QCCENT) QMAX=QCCENT
        IF(QBRMAX.LT.QBRK) QBRMAX=QBRK
        KKK=KKK+1
        IF(KKK.LT.KP) GOTO 16
        WRITE(6,90) T9,QCCENT,QBRK
   90 FORMAT(12X,F8.2,10X,F8.4,14X,F8.4,2F8.4)
C       STORE VALUES OF RUNOFF TO BE PLOTTED LATER
        NPL=NPL+1
        TST(NPL)=T9
        QST(NPL)=QCCENT
        QSTB(NPL)=QBRK
        KKK=0
   16 CONTINUE
77      CONTINUE
         WRITE(6,*) '    MAX FLOW AT BASE = ',QMAX,' CFS/FT'
         WRITE(6,*)'   MAX FLOW, TOP SLOPE = ',QBRMAX,' CFS/FT'
        STOP
        END
C
        SUBROUTINE SKFAC(J)
          INTEGER   A1,B1
        COMMON HY(40),D50(40),SX(35),SY(40),FR(20),TR(20),H(40),
```

Figure A-6 (Continued)

```
     1 D8(40),N1,K,T9,ITIME,R8,R,DT,DX,D52,SY2,CON1,
     2 CON2,CON3,CON4,CON5,A1,D51,THICK1,D81,SY1,D82,
     3 THICK2,NROW,NCOL,B1,SX1,SX2,YBAR,KFAC
        REAL N1,K,KFAC
C       CALCULATE REDUCTION IN K FOR OVERTOPPING
C       DARCY-WEISBACH FLOW ASSUMED
C       HIGH REYNOLDS NUMBER ASSUMED
        DH=(YBAR-H(J))*N1
        DWF=.00001
        DH3=3.85*DH
        IF(DH3.GT.D3(J)) DWF=0.881*ALOG(DH3/D8(J))
        ALPHA=H(J)*SQRT(D50(J)/K)+DH/N1*SQRT(8*DH)*DWF
        KFAC=D50(J)*(YBAR/ALPHA)**2/K
        IF(KFAC.GT.1.0) KFAC=1
        RETURN
        END
C
        SUBROUTINE RAIN
          INTEGER   A1,B1
        COMMON HY(40),D50(40),SX(35),SY(40),FR(20),TR(20),H(40),
     1 D8(40),N1,K,T9,ITIME,R8,R,DT,DX,D52,SY2,CON1,
     2 CON2,CON3,CON4,CON5,A1,D51,THICK1,D81,SY1,D82,
     3 THICK2,NROW,NCOL,B1,SX1,SX2,YBAR,KFAC
C
C       GENERATE RAINFALL RATE
C
        IF(T9.LT.TR(ITIME+1)) RETURN
        ITIME=ITIME+1
        R=R8*FR(ITIME)
        RETURN
        END
C
        SUBROUTINE SETCON
C
C       SET UP CONSTANTS WHICH ARE TIMESTEP DEPENDENT
C
          INTEGER   A1,B1
        COMMON HY(40),D50(40),SX(35),SY(40),FR(20),TR(20),H(40),
     1 D8(40),N1,K,T9,ITIME,R8,R,DT,DX,D52,SY2,CON1,
     2 CON2,CON3,CON4,CON5,A1,D51,THICK1,D81,SY1,D82,
     3 THICK2,NROW,NCOL,B1,SX1,SX2,YBAR,KFAC
        REAL N1,K
        CON1=DT/(2*N1*DX)
        CON2=DT/N1
        CON3=DT/(DX*N1)
        CON4=32.2*N1*N1/K
        CON5=32.2*D52*N1*N1*SY2/K
        RETURN
        END
        SUBROUTINE SETUP
```

Figure A-6 (Continued)

```
C
C       SETUP GRID, SET SLOPES, ROCK DIA AND THICKNESS
C
          INTEGER   A1,B1
        COMMON HY(40),D50(40),SX(35),SY(40),FR(20),TR(20),H(40),
     1 D8(40),N1,K,T9,ITIME,R8,R,DT,DX,D52,SY2,CON1,
     2 CON2,CON3,CON4,CON5,A1,D51,THICK1,D81,SY1,D82,
     3 THICK2,NROW,NCOL,B1,SX1,SX2,YBAR,KFAC
        REAL N1,K
c       correct layer thickness to match through and under flow
        RH1=D51
        DO 7 I=1,10
        RH1=(3.5*D81/13.486)*EXP(SQRT(D51/(8*RH1*K))*N1/0.881)
7       CONTINUE
        RH2=D52
        DO 8 I=1,10
        RH2=(3.5*D82/13.486)*EXP(SQRT(D52/(8*RH2*K))*N1/0.881)

8       CONTINUE
        THICK1=THICK1-RH1
        THICK2=THICK2-RH2
        DO 1 J=1,A1-1
        D50(J)=D51
        H(J)=THICK1
        D8(J)=D81
        SY(J)=SY1
    1 CONTINUE
        D50(A1)=(D51+D52)/2
        D8(A1)=(D81+D82)/2
        H(A1)=(THICK1+THICK2)/2
        SY(A1)=(SY1+SY2)/2

        DO 2 J=A1+1,NROW
        D50(J)=D52
        H(J)=THICK2
        D8(J)=D82
        SY(J)=SY2
    2 CONTINUE
        DO 3 I=1,B1-1
        SX(I)=SX1
    3 CONTINUE
        SX(B1)=(SX1+SX2)/2
        DO 4 I=B1+1,NCOL
        SX(I)=SX2
    4 CONTINUE
        DO 5 I=1,NROW-1
    5 HY(I)=(H(I)+H(IP1))/2
        RETURN
        END
```

Figure A-6 (Continued)

APPENDIX B

PROGRAM ROCKSIZE

Program ROCKSIZE is a BASIC language computer code to aid in the evaluation of the stable rock sizes for the hydrologic protection of tailings embankments from the effects of runoff. Maximum runoff rates predicted from program SLOPE2D or elsewhere are input to program ROCKSIZE, along with the physical attributes of the riprap and the slope of the embankment. The stable rock diameter is determined from the safety factor method and the Stephenson method, as discussed in Chapter 3.

The water level above the top of the rock layer surface, necessary for calculating of the safety factor method, is determined iteratively by evaluating the formula:

$$y^{i+1} = \left[\frac{2q_3}{0.881 \log\left(\frac{3.85y^i}{d_{84}}\right)\sqrt{8gS}}\right]^{2/3} a + (1 - a)y^i \qquad \text{(B-1)}$$

where a is the convergence factor less than unity (typically 0.2) and q_3 is the flow over the top of the rock.

If the water level is not higher than the surface of the rock layer, then the safety factor method is not used.

The stable rock diameter determined by the safety factor method includes the design safety factor specified in the input. The diameter determined by the Stephenson method must be scaled up manually for the desired factor of safety.

Program ROCKSIZE is listed in Figure B-1. The program is interactive and requests the following information:

K	friction index k for flow through rock layer; i.e., K = 1 for smooth marbles, K =2 for smooth gravel, K = 4 for crushed, angular rock
DBAR	average rock diameter, usually the harmonic mean, ft
D84	84% finer rock diameter, ft
Y1	thickness of rock layer, ft
S	slope of embankment
N1	effective porosity of rock
Q	peak downhill runoff to which rock is subjected, $ft^3/sec/ft$
SF	safety factor for SF method only
PH	angle of repose, degrees, from Figure 3-1
C	smoothness factor for Stephenson method only

```
10 REM PROGRAM ROCKSIZE
20 REM TO DETERMINE THE STABLE ROCK DIAMETER FOR A GIVEN FLOWRATE
30 REM DOWN AN ARMOR-COVERED SLOPE
40 REM USING STEPENSON AND SAFETY FACTOR FORMULAS
50 REM REFERENCE NUREG-1263, AUGUST 1988                    SEPTEMBER ?
60 REM R CODELL, US NUCLEAR REGULATORY COMMISSION
70 REM WASHINGTON DC 20555
80 REM
90 PRINT"     PROGRAM ROCKSIZE"
100 PRINT"     DETERMINE THE STABLE DIAMETER FOR RIPRAP ON ARMORED SLOPES"
110 PRINT"     BY STEPHENSON AND SAFETY FACTOR METHOD"
120 PRINT"     U.S. NUCLEAR REGULATORY COMMISSION, WASHINGTON D.C."
130 REM          INPUT DATA
140 REM          K = FRICTION INDEX FOR ROCK
150 REM        DBAR = MEDIAN ROCK DIAMETER, FT
160 REM         D84 = 84 PERCENTILE FINER ROCK DIAMETER, FT
170 REM          N1 = EFFECTIVE POROSITY
180 REM          H1 = RIPRAP LAYER THICKNESS, FT
190 REM           S = SLOPE
200 REM          PH = ANGLE OF REPOSE
210 REM          SS = SPECIFIC GRAVITY OF THE ROCK
220 REM           C = STEPHENSON CONSTANT = 0.22 FOR SMOOTH ROCK
230 REM                                    0.27 FOR CRUSHED ROCK
240 REM
250 PRINT"INPUT FRICTION INDEX, K  ";
260 INPUT K
270 PRINT"ENTER DBAR, D84, FT  ";
280 INPUT DBAR,D84
290 PRINT"ENTER LAYER THICKNESS, FT  ";
300 INPUT H1
310 PRINT"ENTER SLOPE  ";
320 INPUT S
330 PRINT"ENTER EFFECTIVE POROSITY  ";
340 INPUT N1
350 REM
360 REM CORRECT ROCK LAYER THICKNESS FOR AGREEMENT OF THROUGH AND OVERFLOW"
370 REM
380 RH=DBAR
390 FOR I=1 TO 10
400 RH=(3.5*D84/13.46)*EXP(SQR(DBAR/(8*RH*K))*N1/.881)
410 NEXT I
420 PRINT "CORRECTION TO LAYER THICKNESS = ";RH;" FEET"
430 H1=H1-RH
440 PRINT"ENTER PEAK RUNOFF, CFS/FT  ";
450 INPUT Q
460 V=SQR(S*32.2*N1^2*DBAR/K)
470 Q0=H1*V
480 IF Q<=Q0 THEN 490 ELSE 520
490 PRINT"FLOW IS BELOW ROCK SURFACE - SAFETY FACTOR METHOD DOES NOT APPLY"
500 GOTO 710
510 REM
520 REM CALCULATE STAGE ABOVE ROCK SURFACE
```

Figure B-1 Listing of program ROCKSIZE

```
530 REM
540 DQ=Q-Q0
550 Y=D84
560 C1=8*32.2*S
570 C2=SQR(C1)
580 REM A1 = CONVERGENCE FACTOR FOR CALCULATION OF STAGE ABOVE ROCK
590 A1=.2
600 FOR J=1 TO 100
610 DWF=.881*LOG(3.85*Y/D84)
620 YP=((DQ/(DWF*C2))^.66667 *A1)+(1-A1)*Y
630 IF YP>D84/3.85 THEN
640 Y=YP
650 GOTO 670
660 ELSE Y=1.01*D84/3.85
670 REM CONTINUE
680 NEXT J
690 PRINT
700 PRINT "STAGE ABOVE ROCK SURFACE = ";Y;"  FT"
710 REM CONTINUE
720 REM
730 REM SAFETY FACTOR METHOD
740 REM
750 ELSE
760 PRINT"ENTER ANGLE OF REPOSE, DEGREES";
770 INPUT PH
780 PRINT"ENTER SPECIFIC GRAVITY OF ROCK, GM/CC  ";
790 INPUT SS
800 IF Q<=Q0 THEN 910
810 TS=62.4*Y*S
820 AL=ATN(S)
825 PRINT"ENTER SAFETY FACTOR ";
827 INPUT SF
830 ET=COS(AL)*(1/SF-S/TAN(PH/57.3))
840 D1=21*TS/((SS-1)*62.4*ET)
850 PRINT
860 PRINT
870 PRINT"STABLE ROCK DIAMETER BY SAFETY FACTOR METHOD = ";D1;" FEET"
880 PRINT
890 REM CONTINUE
900 REM
910 REM STEPHENSON METHOD
920 REM ROCK DIAMETER FOR INCIPIENT MOTION
930 C1=Q*S^(7/6)*N1^.166667
940 PRINT"ENTER SMOOTHNESS FACTOR, C IN STEPHENSON FORMULA"
950 PRINT"(0.22 FOR SMOOTH ROCK AND 0.27 FOR ANGULAR CRUSHED ROCK)"
960 INPUT C
970 C2=  C*SQR(32.2)*((1-N1)*(SS-1)*COS(AL)*(TAN(PH/57.3)-SY))^1.66667
980 D2=(C1/(1.2*C2))^.66667
990 PRINT
1000 PRINT
1010 PRINT "STABLE ROCK DIAMETER BY STEPHENSON METHOD = ";D2;" FEET "
1020 END
```

Figure B-1 (Continued)

NRC FORM 336 (2-84) NRCM 1102, 3201, 3202

U.S. NUCLEAR REGULATORY COMMISSION

BIBLIOGRAPHIC DATA SHEET

SEE INSTRUCTIONS ON THE REVERSE

1. REPORT NUMBER (Assigned by TIDC, add Vol. No., if any)

NUREG-1263

2. TITLE AND SUBTITLE

Hydrologic Design for Riprap on Embankment Slopes

3. LEAVE BLANK

4. DATE REPORT COMPLETED

MONTH	YEAR
May	1988

5. AUTHOR(S)

R.B. Codell

6. DATE REPORT ISSUED

MONTH	YEAR
September	1988

7. PERFORMING ORGANIZATION NAME AND MAILING ADDRESS (Include Zip Code)

Division of High-Level Waste Management
Office of Nuclear Material Safety and Safeguards
U.S. Nuclear Regulatory Commission
Washington, DC 20555

8. PROJECT/TASK/WORK UNIT NUMBER

9. FIN OR GRANT NUMBER

10. SPONSORING ORGANIZATION NAME AND MAILING ADDRESS (Include Zip Code)

Same as box 7

11a. TYPE OF REPORT

Technical

b. PERIOD COVERED (Inclusive dates)

12. SUPPLEMENTARY NOTES

13. ABSTRACT (200 words or less)

Waste impoundments for uranium tailings and other hazardous substances are often protected by compacted earth and clay, covered with a layer of loose rock (riprap). The report outlines procedures that could be followed to design riprap to withstand forces caused by runoff resulting from extreme rainfall directly on the embankment. The Probable Maximum Precipitation for very small areas is developed from considerations of severe storms of short duration at mid-latitudes. A two-dimensional finite difference model is then used to calculate the runoff from severe rainfall events. The procedure takes into account flow both beneath and above the rock layer and approximates the concentration in flow which could be caused by a non-level or slumped embankment. The sensitivity to various assumptions, such as the shape and size of the rock, the thickness of the layer, and the shape of the embankment, suggests that peak runoff from an armored slope could be attenuated with proper design. Frictional relationships for complex flow regimes are developed on the basis of flow through rock-filled dams and in mountain streams. These relationships are tested against experimental data collected in laboratory flumes; the tests provide excellent results. The resulting runoff is then used in either the Stephenson or safety factor method to find the stable rock diameter. The rock sizes determined by this procedure for a given flow have been compared with data on the failure of rock layers in experimental flumes, again with excellent results. Computer programs are included for implementing the method.

14. DOCUMENT ANALYSIS - a. KEYWORDS/DESCRIPTORS

mine tailings, riprap, embankments, hydrologic models, Probable Maximum Precipitation (PMP), Mathematical Models

b. IDENTIFIERS/OPEN-ENDED TERMS

15. AVAILABILITY STATEMENT

Unlimited

16. SECURITY CLASSIFICATION

(This page)
Unclassified

(This report)
Unclassified

17. NUMBER OF PAGES

18. PRICE